THE STRESS-CORROSION CRACKING OF MILD STEEL IN NITRATE SOLUTIONS

being a thesis submitted as a requirement for the
degree of Doctor of Philosophy in the
University of Newcastle upon Tyne.

M. Henthorne, B.Sc., Dunelm
Department of Metallurgy,
University of Newcastle upon Tyne.

August 1965

Email: mh@michaelhenthorne.com

Contents

SYNOPSIS

The stress-corrosion cracking of 0.08% C and 0.30% C steels in boiling nitrate solution has been investigated. The principal aim has been to assess the role of stress in stress-corrosion cracking.

Tensile tests in boiling nitrate solution have enabled the stress required to initiate stress-corrosion cracks to be measured and compared with data from tensile tests in the absence of nitrate solution. Constant strain stress-corrosion tests in a hard-beam tensometer have been used in addition to conventional static stress-corrosion tests. The dependence of stress-corrosion propensity on grain size, strain rate and pre-strain has been studied.

Thin film electron microscopy has been used to compare the dislocation arrangements in a steel susceptible to stress-corrosion cracking with those in a more resistant steel. Initial stages in the corrosion of mild steel in nitrate solutions have been studied by examination of thin foils in the electron microscope, both before and after their immersion in nitrate solution.

The investigation has revealed no evidence for purely mechanical stages in stress-corrosion cracking and previous evidence for such stages has been shown to be capable of alternative interpretation. A cracking mechanism is proposed, by which failure occurs as a result of continuous electrochemical corrosion. The role of stress is attributed to that of opening up corrosion fissures, so as to make the corrodent available at the fissure tip.

INTRODUCTION

The main aim of this investigation was to assess the role of stress in stress corrosion cracking. The action of stress in stress-corrosion cracking has previously been attributed to one or more of the following four functions:-

(1) The opening up of corrosion fissures to allow fresh corrodent to reach the fissure tip. This explanation for the action of stress is generally thought to over simplify the problem, since it does not explain why such large stresses are required in certain cases, nor why the stress necessary for cracking is dependent upon both the chemical composition and the heat treatment of a material susceptible to cracking.
(2) The fracture of corrosion products which would otherwise protect the underlying material.
(3) The operation of short bursts of purely brittle fracture ahead of corrosion fissures. This explanation accounts for the fact that crack propagation rates are high compared with normal corrosion processes, but it is difficult to explain the occurrence of brittle fracture in normally ductile materials.
(4) The production of a chemically active structure at the tip of a corrosion fissure. The chemically active structure may be either mechanical defects (e.g. dislocation pile-ups, stacking faults, etc.) produced by the applied stress, or continuously deforming material at the tip of a propagating crack.

The latter of these four possibilities has received slightly more support than the others, possibly because it is less specific. Recent work on the effect of grain size on the stress-corrosion cracking of stainless steel (1), magnesium-7% aluminium (1) and copper alloys (2), has revived interest in the brittle fracture mechanism for cracking, since in all these stress-corrosion systems, the stress to cause cracking has been found to bear a linear relationship with $(\text{grain diameter})^{-1/2}$. In all cases this behaviour has been interpreted as providing evidence in support of a brittle fracture stage in cracking because in the Petch brittle fracture equation, fracture stress is proportional to $(\text{grain diameter})^{-1/2}$. This interpretation is not necessarily correct, since a Petch relationship exists for processes other than brittle fracture.

It was therefore decided to commence the present investigation with a more thorough examination of the extent to which the mechanisms, which operate in producing fracture in the absence of a corrosive environment, are effective in producing stress-corrosion fracture. The system chosen for this study was mild steel in boiling nitrate solutions. There were three reasons for this choice –

(a) Considerable work had previously been carried out on this system in these laboratories.
(b) The mechanical properties of mild steel have received a great deal of attention during recent years.
(c) If stress-corrosion cracking did involve a stage of brittle fracture then such a stage would be expected to be dominant in a material known to be susceptible to brittle fracture.

1. REVIEW OF LITERATURE

Stress-corrosion cracking has recently been reviewed (3), therefore only the stress-corrosion of mild steel in nitrate solutions is dealt with here. Since the main aim of this work has been to investigate the stress aspect the relevant physical metallurgy of mild steel is reviewed. The latter includes deformation and fracture, strain ageing, thin film electron microscopy and properties of grain boundaries.

1.1 Stress-corrosion cracking of mild steel in nitrate solutions

There is general agreement that cracking is

(a) intergranular,
(b) capable of electrochemical control,
(c) dependent on stress,
(d) not found in pure iron,
(e) most severe when the corrodent is at or near its boiling temperature.

The majority of the early investigators confined their attention to the problem of why cracking is intergranular. The anodic character of grain boundaries has usually been attributed to grain boundary precipitation. Waber and McDonald (4) suggested that Fe_4N is the grain boundary phase responsible for cracking. Fe_4N is anodic to ferrite, but since it is not present in sufficient quantity to form a continuous grain boundary film, the authors proposed that Fe_4N is formed by strain induced precipitation just ahead of a corrosion fissure. Even if this were true it does not explain why cracking is intergranular. If grain boundary precipitates are important in the stress-corrosion cracking of mild steel then the majority of experimental evidence seems to suggest that iron carbide is the phase most likely to be present in mild steel grain boundaries. Parkins (5) has proposed a cracking mechanism based on distortion at grain boundaries, and has attributed the major cause of this distortion to the precipitation of Fe_3C. The Fe_3C is not attacked by the nitrate solution since it is cathodic to ferrite, but the carbide particles distort adjacent ferrite and it is the distorted ferrite that forms an anodic path. Parkins proposed this mechanism as a result of a study into the effect of carbon content on stress-corrosion susceptibility. He found that steels containing about 0.1% C, were more susceptible than lower and higher carbon steels. He observed that in the 0.1% C steel the carbon was in the form of discrete Fe_3C particles, whereas in the higher carbon steels the carbon was in the form of lamellar pearlite. In support of his interpretation, Parkins showed it was possible to make a resistant 0.22 C steel susceptible to cracking, by subcritically annealing so as to convert the pearlite to spheroidised carbide particles. It is thought that a mechanism dependent upon electrochemical attack of regions adjacent to grain boundary carbide particles fails to answer two questions:-

(1) Why do cracks remain intergranular between the carbide particles?
(2) Bearing in mind the fact that crack propagation can be electrochemically controlled, why, as reported by Parkins, do cracks propagate in resistant pearlitic steels after being initiated in a decarburized surface layer?

There seems to be no doubt that subcritically annealing does increase susceptibility but it is thought that this may be due to causes additional to enhanced ferrite attack adjacent to carbide particles.

The preference for certain grain boundaries to be attacked has been investigated by Logan (6) and Flis et al (7). Both groups of workers agreed in their observation that the difference in orientation between two grains determines the rate of attack at the boundary between them. Logan found that 69% of stress-corrosion cracks formed at boundaries where the difference in orientation was greater than 10^0. Logan gives no information regarding the percentage of the grain boundaries that would be expected, on purely statistical grounds to have an orientation difference greater than 10^0. As a result of their observations, Flis et al suggested that intergranular cracking is not due to impurities at grain boundaries, but to differences in energy between iron atoms situated in differently oriented faces and grain boundaries. They give no consideration to the possibility that impurity segregation might also be dependent upon grain boundary "mismatch". The immunity of pure iron to stress-corrosion cracking (5, 19) is also difficult to explain by this theory.

The most systematic approach to the electrochemical aspect has been that of Parkins and Usher (8, 9), who determined the effectiveness of different nitrate solutions in producing cracking. For a given chemical strength the nitrates varied in their ability to cause cracking. The order of decreasing potency was NH_4NO_3, $Ca(NO_3)_2$, $LiNO_3$, KNO_3 and $NaNO_3$. It was noted that the most potent nitrates were those with the lowest pH. The authors pointed out that this would be expected from a knowledge of the chemistry of the nitrates. For example, NH_4NO_3, being a salt of a weak base and strong acid, would dissociate in solution to give an acid reaction, whereas $NaNO_3$, being a salt of a strong base and strong acid would give a solution of higher pH. To demonstrate the validity of their interpretation that potency was directly related to pH, they showed that lowering the pH of $NaNO_3$ with a little nitric acid, produced a solution similar in potency to an NH_4NO_3 solution of the same pH. Parkins and Usher also found that $Fe(NO_3)_3$ produced a high rate of general corrosion on mild steel and point out that since this salt is a product of the anodic corrosion reaction in a grain boundary fissure, the solution at the tip of the fissure is more acidic than the bulk solution. Assuming an anodic path to exist at grain boundaries, the authors proposed a mechanism of electrochemical attack dependent upon an autocatalytic reaction producing acid conditions at the crack tip.

Crack propagation has been investigated by Engell and Baumel (10) with the aid of electrode potential and specimen extension measurements during a static stress-corrosion test. They give no experimental details concerning the type of test or the method of detecting the increase in specimen length. The results of a typical test are shown in Fig. 1.1. The potential measurements of Engell and Baumel have been confirmed by Van Rooyen (11) and are shown in Fig. 1.2. Both sets of workers attribute the discontinuities in specimen extension and electrode potential to discontinuous crack propagation. Engell and Baumel propose that the majority of crack propagation is a purely mechanical process and that stress-corrosion cracks are a series of brittle cracks initiated from corrosion fissures. The objection to this theory is that mild steel fails by transgranular rupture at the temperature of boiling nitrate solutions. From data given by Engell and Baumel it is estimated that each purely mechanical stage would require crack propagation over a distance of twenty grain diameters. It does not seem feasible that crack propagation could involve such large jumps and remain intergranular. It is thought that the assumption (also made by workers in other stress-corrosion systems) that discontinuous specimen extension proves discontinuous crack propagation is not valid. The assignment of the potential deflections to the exposure of unfilmed material at the tip of a crack is also questionable. Since the area exposed at the tip of a crack would be a very small fraction

of the total specimen area, it seems unlikely that the potential change would be as large as that recorded by Engell and Baumel and Van Rooyen.

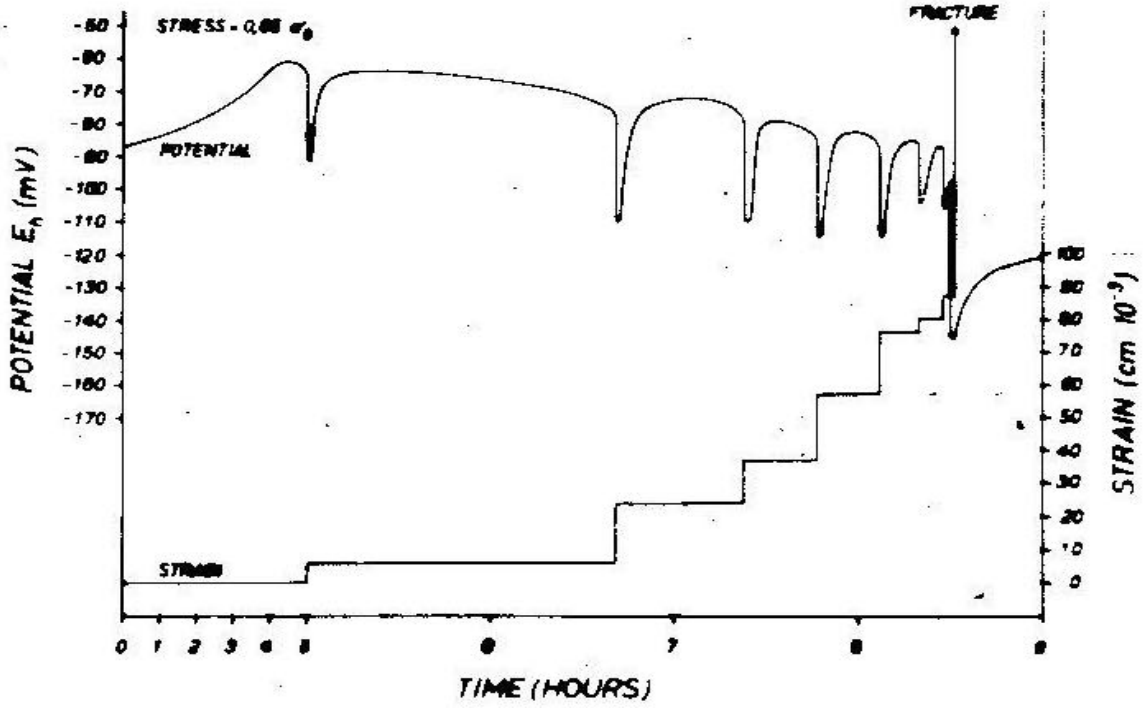

Fig. 1.1 Electrode potential and specimen extension changes in mild steel stressed to 65% of its U.T.S. in boiling 55% $Ca(NO_3)_2$ solution. (Engell and Baumel (10)

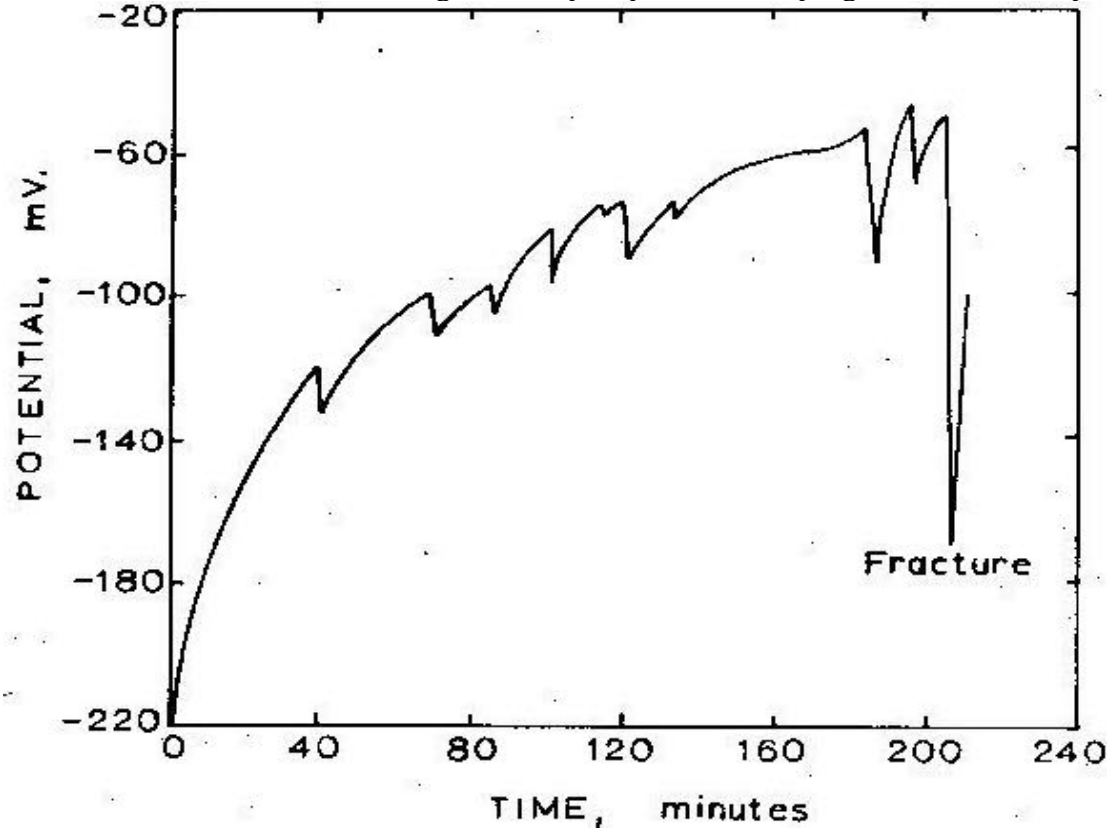

Fig. 1.2 Potential deflections during stress-corrosion cracking of mild steel in boiling nitrate solutions. (Van Rooyen (11))

Several investigators (12–15) have suggested that strain-ageing is the cause of cracking. This suggestion is usually based on the following observations:-

(1) Cracking does not occur at room temperature, when strain-ageing effects are small,
(2) Both stress-corrosion cracking and strain-ageing may be eliminated by aluminium additions.

The basic fault with strain-ageing theories is that they fail to explain why cracking is intergranular. It is possible to explain the resistance of steels with aluminium additions on a basis other than strain-ageing, since Parkins and Brown (16), in an investigation into the effect of alloy additions on stress-corrosion susceptibility, have shown that during a stress-corrosion test an aluminium steel is much more noble than a plain carbon steel.

The effect of prestrain on stress-corrosion cracking has aroused considerable controversy, probably because investigators studying this problem have used different methods of applying the strain. There is general agreement (5,17,18) that material which has been deformed by rolling is less susceptible to stress-corrosion cracking than annealed material. The resistance of rolled material to cracking is probably due to residual compressive stresses in the surface of the material. In support of this interpretation are the findings of Parkins (5), that rolled material can be made susceptible by pre-straining (beyond the yield strain) in tension. Parkins also found that increasing amounts of plastic strain further increased the susceptibility but the effect was small compared with the difference between as rolled material and material strained just beyond the yield strain (about 2%). It seems doubtful whether the increase in susceptibility with increasing plastic strain is significant, since the results were obtained using constant strain bend tests and it is almost certain that some stress relaxation occurred during the test. This relaxation (due to plastic deformation in the test specimen) would be expected to be less marked in the severely pre-strained material, with the result that the applied stress during the tests would increase with prestrain.

Logan, (6) has proposed a stress-corrosion theory for several systems including mild steel in nitrate solutions. The cracking mechanism is dependent upon the rupturing of oxide films at the tip of a crack, as a result of local strain at that point. The film-free metal is preferentially dissolved since it is anodic to the film-covered crack sides. This theory fails to explain why cracking remains intergranular.

Uhlig (20) has proposed a general theory for stress-corrosion cracking, based on the chemisorption of selected ions, which, by reducing the surface energy of the material at the apex of a crack, facilitate short bursts of brittle fracture. In the application of this theory to the stress-corrosion of mild steel in nitrate solutions, Uhlig and Sava (18) investigated the effect of heat treatment on stress-corrosion susceptibility of commercial mild steel, pure carbon steel, pure nitrogen steel and electrolytically pure iron. They found that mild steel quenched from 950^0C was susceptible to cracking but became resistant after ½ hour at 100-250^0C. Longer heat treatments at temperatures of 450-550^0C induced susceptibility. They proposed that the susceptibility of quenched steel indicates the importance of C and N atoms rather than carbides and nitrides. Low temperature (100-250^0C) heat treatments promote the formation of carbides and nitrides thus removing C and N atoms from grain boundary positions. At a temperature of 450-550^0C these carbides and nitrides re-dissolve in ferrite and the C and N atoms segregate to grain boundaries. It is difficult to understand how quenched steel may be distinguished from steel heat treated at 100^0C for ½ hour since the stress-corrosion test itself takes place at 115^0C and lasts for several hours. Probably the most significant result obtained by Uhlig and Sava was

the fact that both pure C steel and pure N steel were susceptible to cracking. To explain why segregation of C and N atoms at grain boundaries causes cracking, Uhlig and Sava propose that chemisorption would occur preferentially at defect sites, and that the purpose of the C and N atoms is to lock imperfections produced ahead of the crack. In view of the fact that chemisorption is dependent upon chemical variables such as pH, it is difficult to prove or disprove the chemisorption mechanism of cracking. It is thought that the heat treatments used by Uhlig and Sava might have had effects additional to those considered by the authors.

In the work published during the last fifteen years there appears to be general agreement on the following points:-

(1) C or N are necessary for cracking.
(2) Pearlitic steels are more resistant to cracking than spheroidised carbide steels.
(3) The selection of certain grain boundaries for cracking is dependent upon the relative orientation of the grains adjacent to the boundary.

There is disagreement on the answers to the following questions:-

(1) Why is cracking intergranular?
(2) What is the role of stress?
(3) Is crack propagation continuous or discontinuous?
(4) What is the effect of prior deformation on cracking susceptibility?
(5) Is strain-ageing necessary before cracking can occur?

It is thought that much of this disagreement is due to the following factors:-

(1) Materials with different mechanical properties have been compared directly. This includes experiments in which materials have been compared after receiving different heat treatments.
(2) Failure times obtained from constant strain and constant load tests have been compared without sufficient attention to the fact that cracking occurs under increasing stress in a constant load test and decreasing stress in a constant strain test.
(3) With the exception of Smialowski and his co-workers no effort has been made to supply a solution of constant composition throughout a test even though the majority of tests last for several hours and often several days. Smialowski and Szklarska-Smialowska (21) have shown that the pH of an ammonium nitrate solution in contact with iron changes considerably as a result of general corrosion, as shown in Fig. 1.3. This observation is significant if it is remembered that Parkins and Usher (8, 9) found susceptibility to cracking to be dependent upon pH. The failure to supply a solution of constant composition might cause considerable error in a long term test, especially in tests which involve large, mild steel straining jigs being in contact with the corrodent.

1.2. Deformation and fracture of mild steel

During the past fifteen years, a large amount of work has been carried out in an attempt to understand the deformation and fracture behaviour of mild steel. The majority of this work has been concerned with the ductile to brittle transition and has involved testing at room temperature and below with strain rates higher than 1×10^{-4} sec^{-1}.

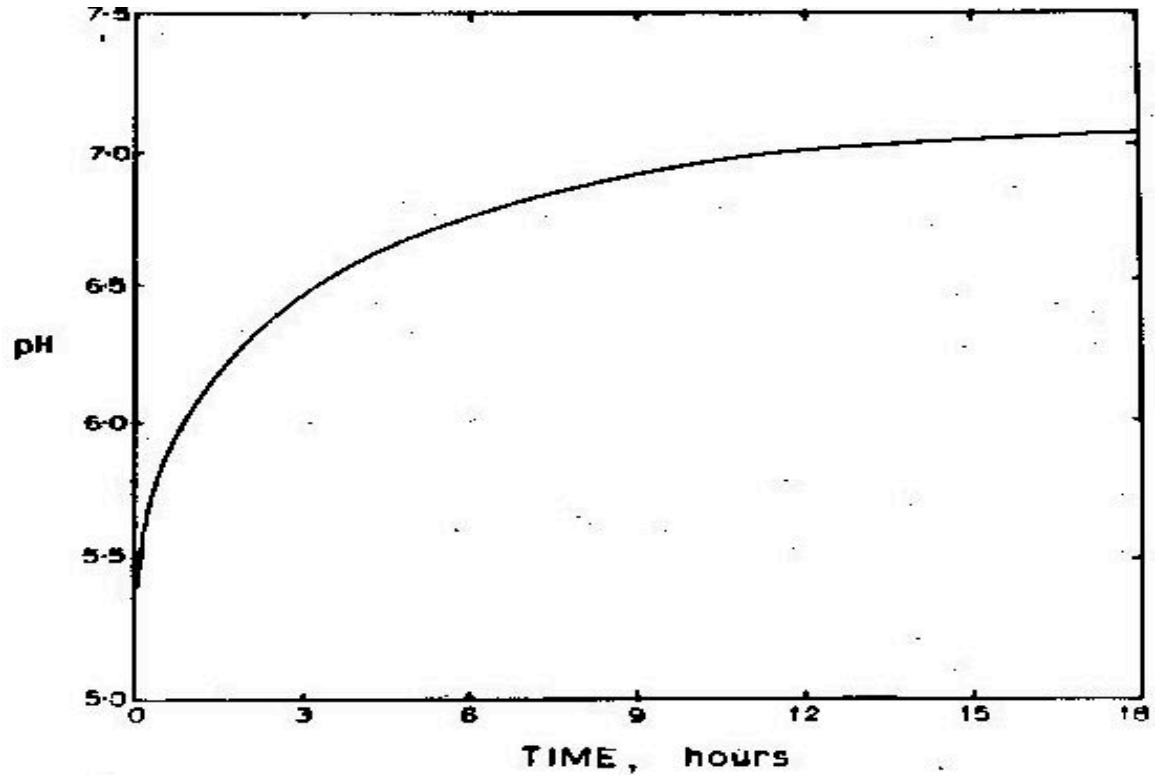

Fig. 1.3 Variation of pH with time during the general corrosion of iron in ammonium nitrate solution. (Smialowski and Szklarska-Smialowska (21))

The basis of most deformation and fracture work has been the Petch relationship $\sigma = \sigma_0 + k\, l^{-1/2}$ where l is the average grain diameter, σ_0 and k are constants and σ may denote lower yield stress, proportional limit, proof stress, cleavage stress or ductile fracture stress. The equation was derived (22) by consideration of the interaction of dislocations with grain boundaries and although thin film electron microscopy observations have made it necessary to revise the original ideas of this interaction, there is no doubt as to the validity of the relationship. It is generally accepted that σ_0 is a measure of the stress opposing the motion of a free dislocation through a single crystal whilst k is a measure of the stress required ahead of an array of dislocations for the propagation of yielding or fracture.

The two main problems in deformation fracture theories have been to decide firstly how slip is propagated across grain boundaries and secondly whether the terms σ_0 and k describe the same mechanism in the different processes for which the Petch relationship applies. The three possible mechanisms for this propagation of slip across a grain boundary are:-

(1) Dislocations exert sufficient pressure on one side of a grain boundary to allow them to burst through into the adjacent grain.

(2) The pressure at a grain boundary due to dislocation arrays on one side of it is sufficient to operate dislocation sources on the other side.

(3) Grain boundaries are sources of free dislocations which are locked by interstitial atoms until a stress of sufficient magnitude to unlock them is applied.

It is probable that the propagation of slip involves mechanism (2) possibly coupled with mechanism (3). The problem as to whether σ_0 and k describe the same mechanism in all the

processes for which the Petch equation applies is apparently more simple since it is possible to compare the values of these constants for the different processes. It is probable that σ_0 has the same meaning in all processes. The value of k is not the same for all processes but it probably does describe the same mechanism in yielding and the early stages of plastic flow (23). The importance of interstitials on the value of k is shown in Fig. 1.4.

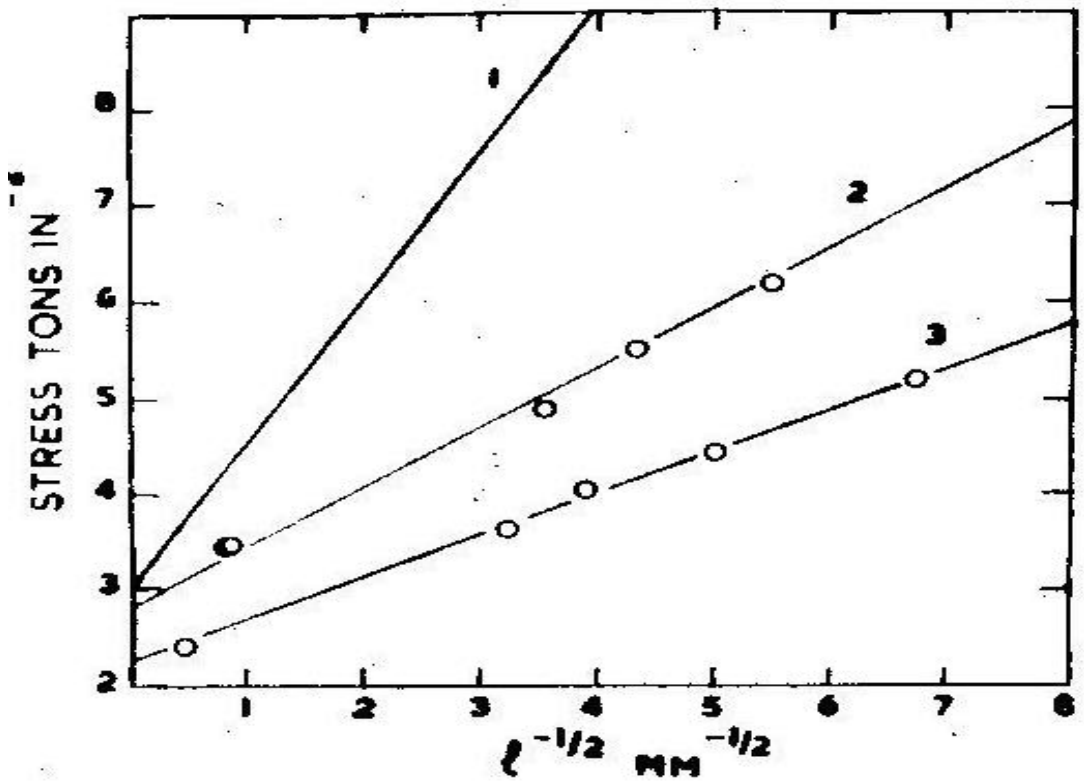

Fig. 1.4 The effect of C and N removal from Swedish iron on the yield stress/grain size relationship at room temperature. 1. Annealed iron, lower yield point. 2. Partial yield point suppression. 3. Proportional limit after yield point suppressed. (Armstrong et al (23))

The dependence of k on interstitials led Cottrell (24) to propose that k is a measure of the stress required to unlock a dislocation from interstitial elements. This explanation has received considerable support but the temperature independence (below room temperature) of k has suggested that k describes a more complicated process than solely unlocking. The true meaning of k has not yet been determined and for the purpose of this work k will be considered to be a measure of the resistance of a grain boundary to yielding, flow, etc.

No grain size data has been reported at the temperatures and strain rates at which mild steel fails by stress-corrosion cracking in nitrate solutions.

1.3 Strain- Ageing

The return of a yield point in a tensile test after prior plastic strain and ageing is one result of the phenomenon of strain-ageing. During a slow strain rate tensile test there is sufficient time for strain-ageing to occur during the test and the repeated yielding that occurs is called jerky flow. The minimum temperature at which jerky flow will occur in a tensile test at a strain rate $\dot{\varepsilon}$, has been shown by Cottrell (25) to be given by the relationship $\dot{\varepsilon} = Ce^{-Q/RT}$

where C = 10^{-7} sec.$^{-1}$ and the activation energy Q, is similar to that (18,200 cal/mole) for the diffusion of N in α iron. The minimum temperatures for jerky flow to occur are given for three strain rates in Table 1.1.

TABLE 1.1
Criteria for jerky flow in α iron

Strain rate, sec.$^{-1}$	1.4 x 10^{-5}	8.3 x 10^{-3}	5.0
Temperature °C	57	137	347

Jerky flow has been attributed by Cottrell to the locking of moving dislocations by interstitial atoms. The locking raises the work hardening rate until sufficient stress is attained to allow a wave of plastic deformation to run through the specimen. This interpretation has been quite well received, but there has been considerable controversy regarding the problem as to whether plastic deformation occurs by unlocking of dislocations, or whether new dislocations are formed. In support of the latter are the results (26) from a study of vanadium (which shows similar strain-ageing behaviour to α iron), in which it was observed by thin film electron microscopy that the density of dislocations increases more rapidly during jerky flow than during normal work hardening. It seems likely that the plastic strain results from both unpinning of existing dislocations and the operation of new sources.

1.4 Thin film electron microscopy

The dislocation arrangements in thin foils of α iron have been studied by several investigators during the past five years. The two aspects which have received the most attention are the dislocation arrangements in plastically deformed iron, and the importance of dislocations in strain and quench ageing.

The dislocation arrangements in plastically deformed iron have been studied by Brandon and Nutting (27), Keh (28, 29) and Weissmann (29). They agree in their findings that after the yield point, dislocations are arranged in loose networks. The dislocations are jogged and non-uniformly distributed. As the amount of plastic deformation is increased, a cell structure develops until a limiting cell size is reached at a strain of about 8%. Further strain causes thickening of the cell walls and the density of dislocations within the cells is very low. None of these observations revealed any evidence of regular dislocation pile-ups.

Quench-ageing has been studied by Hale and McLean (30), Leslie (31) and Keh and Wriedt (32). The three groups of workers agree in their findings that precipitation of carbides and nitrides does occur on dislocations during the ageing after quenching. In a study of strain-ageing Leslie and Keh (33) found that carbide or nitride precipitation was not necessary for the process of strain-ageing.

One of the most significant factors arising from the thin film investigations has been their reliability and in several cases independent investigations have revealed almost identical results. This reliability has almost certainly resulted in the increased use of thin foil electron microscopy in the study of mechanical properties, but iron is probably one of the more difficult of the common metals to study for two reasons:-

(1) Good quality foils of α iron are more difficult to prepare than foils of most other common metals.
(2) The magnetic properties of α iron can cause complications in the operation of the electron microscope.

1.5 Grain boundaries in mild steel

There is considerable evidence that C and N atoms segregate at grain boundaries in mild steel. The evidence for this segregation has come from two sources - (1) Internal friction experiments, (2) Thin foil electron microscopy.

Lagerberg and Josefsson (34) found that the smaller the grain size of a material the lower its internal friction. This must be due to either the formation of more carbides and nitrides in the small grain size material or to the grain boundary segregation of C and N. The authors show that in favour of the latter is the fact that the maximum solubility of C in iron is greater in the small grain size material than in the large, as shown in Fig. 1.5.

Further evidence for the segregation of interstitials at grain boundaries is the cathodic nature of the grain boundaries in several electrolytes. Phillips (35) has investigated this effect with the aid of thin film microscopy. He found no evidence of precipitation in the cathodic grain boundaries and proposed that their resistance to thinning, shown in Fig, 1.6, is due to interstitial segregation.

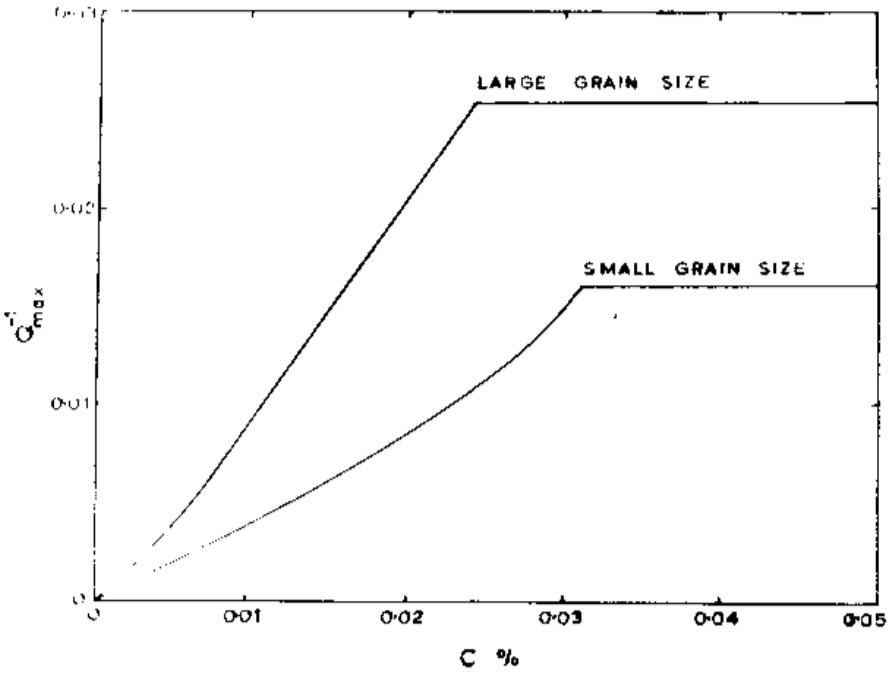

Fig. 1.5 The effect of grain size on the relationship between internal friction and C content. (Lagerberg and Josefsson (34))

Fig. 1.6. Evidence that grain boundaries are cathodic to adjacent ferrite. Thin film. (Phillips (35))

In an attempt to justify this claim, Phillips showed that the resistance to thinning was maximal in material slow cooled from 690°C, only slight in material quenched from 690°C and absent after decarburization. He was unable to identify any grain boundary phase other than α iron in contradiction to the claims of Tsou et al (36) regarding the existence of austenitic films at grain boundaries. Phillips also noticed a tendency for preferential thinning in zones adjacent to grain boundaries.

Brandon and Nutting (37) also found evidence of grain boundary segregation in thin foils of α iron. They observed regions adjacent to grain boundaries which were more transparent to electrons than the bulk of the grain. The effect was not due to preferential thinning (although this was sometimes found to occur) and was thought to be evidence of impurity free zones resulting from grain boundary segregation. The high intensity of the transmitted beam in these regions was attributed to the lack of non coherent scattering normally associated with impurities.

2 EXPERIMENTAL PROCEDURE

2.1 Materials

A 0.08 C and a 0.30 C steel have been used. The 0.08 C steel was known to be susceptible to stress-corrosion cracking and had the following analysis:-

Element	C	N	Mn	S	Si	P
Weight %	0.08	0.002	0.35	0.03	0.01	0.02

The 0.30 C steel was thought likely, on the basis of previous work (5), to be resistant to stress-corrosion cracking when the carbon was in the form of lamellar pearlite and susceptible when the carbon was in the form of discrete spheroidal carbide particles. The 0.30 C steel had the following analysis:-

Element	C	N	Mn	S	Si	P
Weight %	0.30	0.004	0.64	0.04	0.15	0.02

Both steels were in the form of 3/16" diameter rod. All material was given an appropriate heat treatment before testing.

2.2 Heat Treatment

Heat treatments were carried out in a vacuum of 1×10^{-5} mm. Hg. Two horizontal tube furnaces were constructed for this purpose. Silica furnace tubes were wound with Kanthal "A" wire so as to give constant temperature hot zones of at least 3" at all temperatures. Fig. 2.1 shows the temperature distribution at three different temperatures. The two furnaces were operated from the same vacuum system as shown in Fig. 2.2.

Electrical power was supplied to these furnaces by motorised Variacs. The rate of heating, time at temperature, and rate of cooling were programmed with the aid of two short interval switches and a 24 hour dial time switch as shown in Fig. 2.3. The Ether set control pointer, which was driven together with the Variacs was pre-set to operate micro-switch A on reaching an annealing temperature and micro-switch B on returning to room temperature. Temperature control was achieved with a thermocouple adjacent to the furnace windings. A thermocouple situated inside the furnace tube, at the centre of the hot zone, enabled the actual temperature during any heat treatment to be measured.

2.3 Grain size measurement

Grain size determinations were carried out on either small samples, included in each heat treatment specifically for this purpose, or on samples taken from just beyond the gauge length of tensile specimens. Since the constant temperature zones in the heat treatment furnaces (see Fig. 2.1) were three times the gauge length of the tensile specimens, either method yielded the same result.

Grain diameters were measured by an intercept method on a projection microscope. The microscope stage was fitted with vernier scales reading to $\pm$ 0.01 mm. A minimum of 600 grains were counted in each grain size determination.

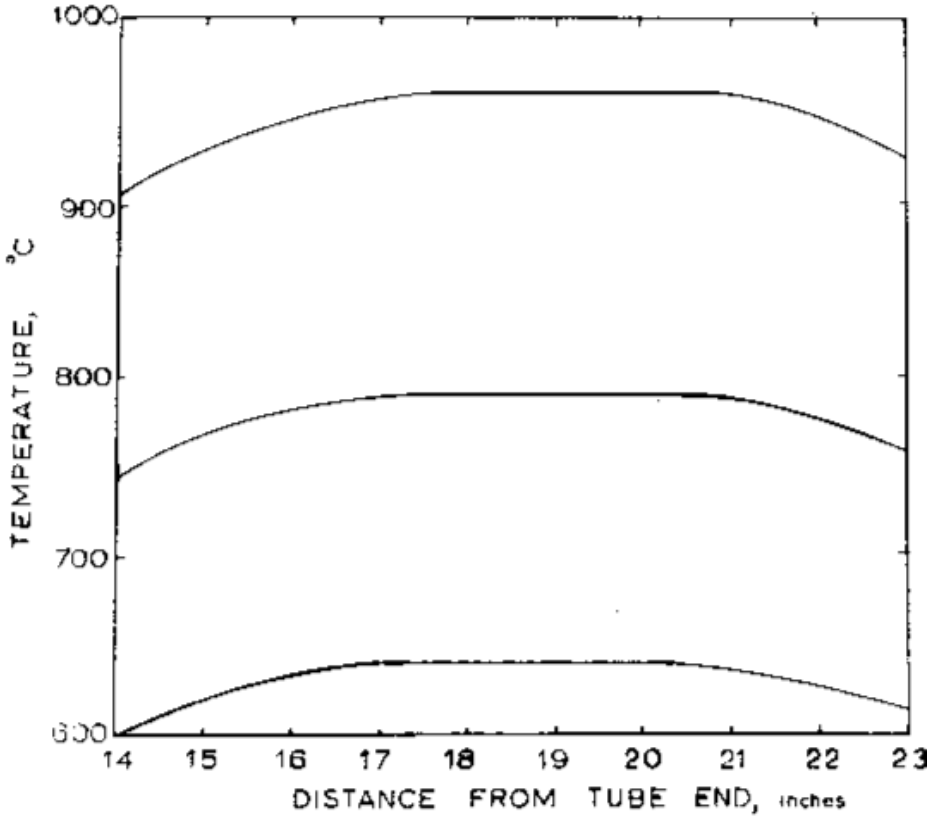

Fig. 2.1 Temperature distribution in vacuum furnace.

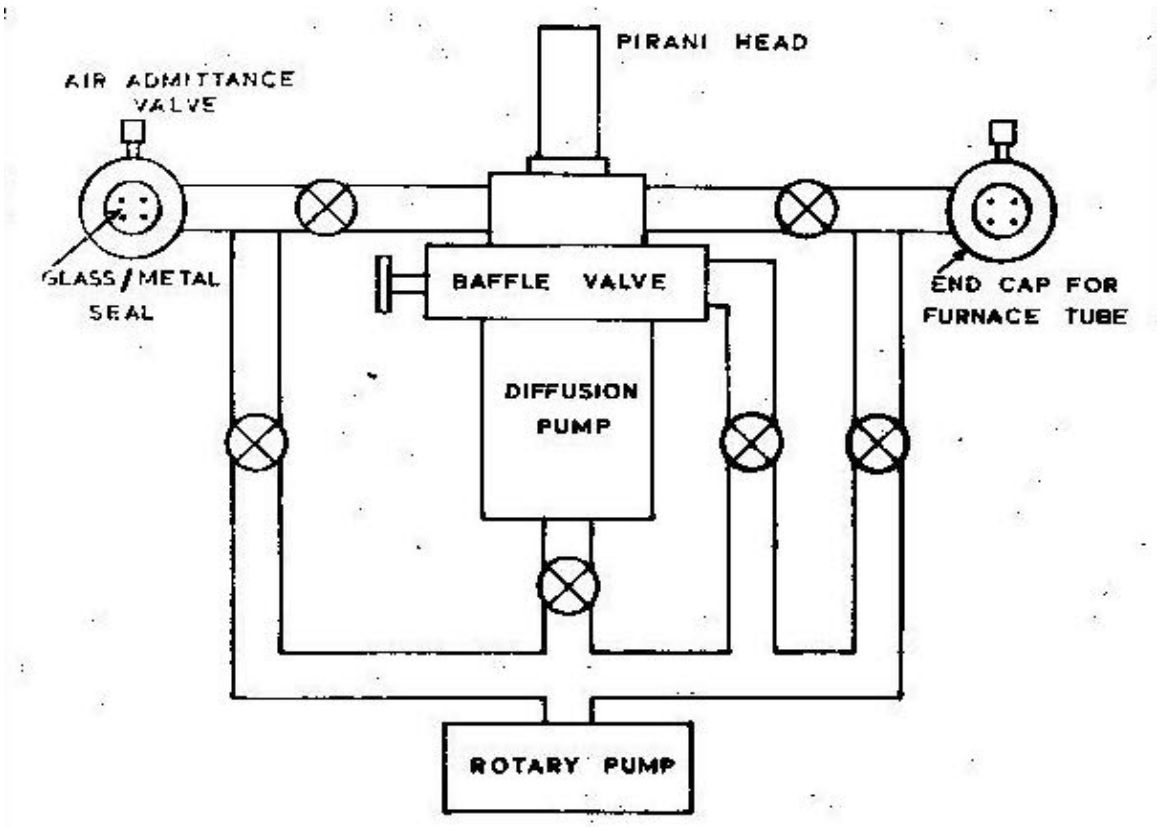

Fig. 2.2 Vacuum system.

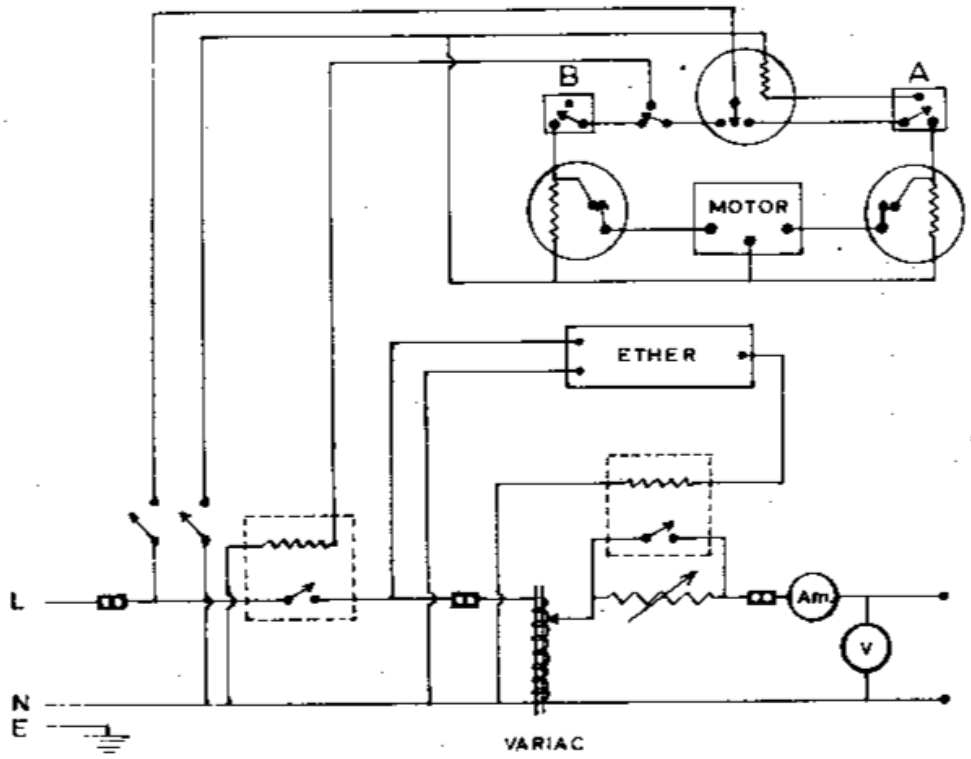

Fig. 2.3 Circuit diagram for furnace control.

2.4 Corrosion solutions

All solutions were made up with distilled water. All solutions were used at their boiling temperature and except where stated otherwise an 8N $Ca(NO_3)_2$ solution was used. The calcium nitrate was in the form $Ca(NO_3)_2.4H_2O$ and had a minimum purity of 98%. This solution boiled at 115°C. For some experiments a more potent solution was obtained by adding ammonium nitrate to the 8N $Ca(NO_3)_2$ solution. The ammonium nitrate was in the form NH_4NO_3 and had a minimum purity of 99%.

2.5 Mechanical testing

Two basically different types of test were used:-

(1) Constant strain static stress-corrosion tests.
(2) Continuous tensile tests, both in the presence of boiling nitrate solution and in oil at 115°C.

2.5.1 Constant strain tests

One series of constant strain tests were carried out using an identical technique to that previously used by Parkins and Usher (9). Specimens of length 12" and diameter 3/16" were restrained in rectangular jigs consisting of two 3" x 1" a 5/8" beams held parallel by two 11" lengths of ½" diameter steel rod bolted to the beams as shown in Fig. 2.4 (a). The beams

contained a central hole through which the specimen passed and strains were maintained on the specimen by locking nuts threaded onto the ends of the specimen. The dimensions of the jig were such that a glass cell containing the corrodent could be placed round the specimen and inside the jig. The corrosion cell, shown in Fig. 2.4 (b) consisted of a thick walled Pyrex glass tube, surrounded, over its mid portion, by a glass jacket. The glass jacket contained an electric heating coil and was filled with glycerol to ensure uniform heat transfer to the corrodent in the inner tube. A condenser was attached to the inner tube by means of a side arm near the end of the tube. The specimens were subjected to known stresses by loading them in a Hounsfield tensometer. The test procedure was as follows:-

(a) The specimen was inserted in the cell so that a threaded portion, 2" long, protruded from each end of the cell.
(b) The cell was placed in the jig by removing one of the end plates.
(c) The complete unit (jig plus cell) was transferred to the tensometer.
(d) The nitrate solution was added and boiled for half an hour.
(e) The required stress was applied to the specimen.
(f) The locking nuts on the specimen were tightened and the load transferred from the tensometer to the jig.
(g) The unit was connected in series with other units in a heating rig.
(h) The time to total failure (i.e. locking nuts slack) was found by inspection.

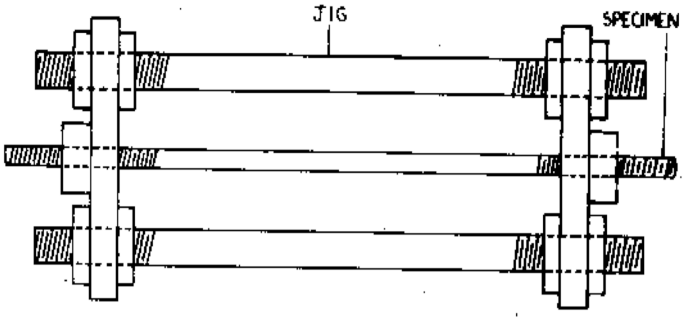

(a)

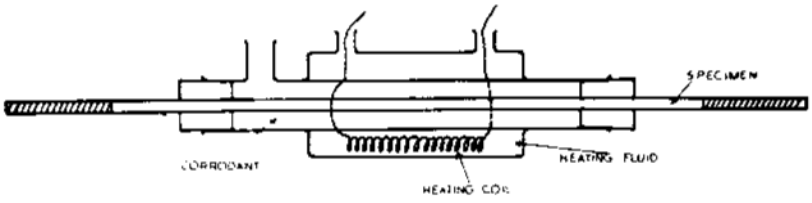

(b)

Fig. 2.4 (a) Straining jig. (b) Corrosion cell.

All other constant strain stress-corrosion tests were carried out in a hard-beam tensometer fitted with a Langham-Thompson load cell as shown in Fig. 2.5. The specimen type and corrosion cell, used in all hard-beam static tests and all the continuous tensile tests described in section 2.5.2 are shown in Figs. 2,6 and 2.7. The corrosion cell consisted of a simple glass tube – rubber bung assembly heated by an electric coil AA , and connected to a water cooled condenser at B. The air admittance valve C allowed solution to be added after the specimen was in position. The upper bung fitted loosely round the specimen so as to permit extension of the specimen during a tensile test.

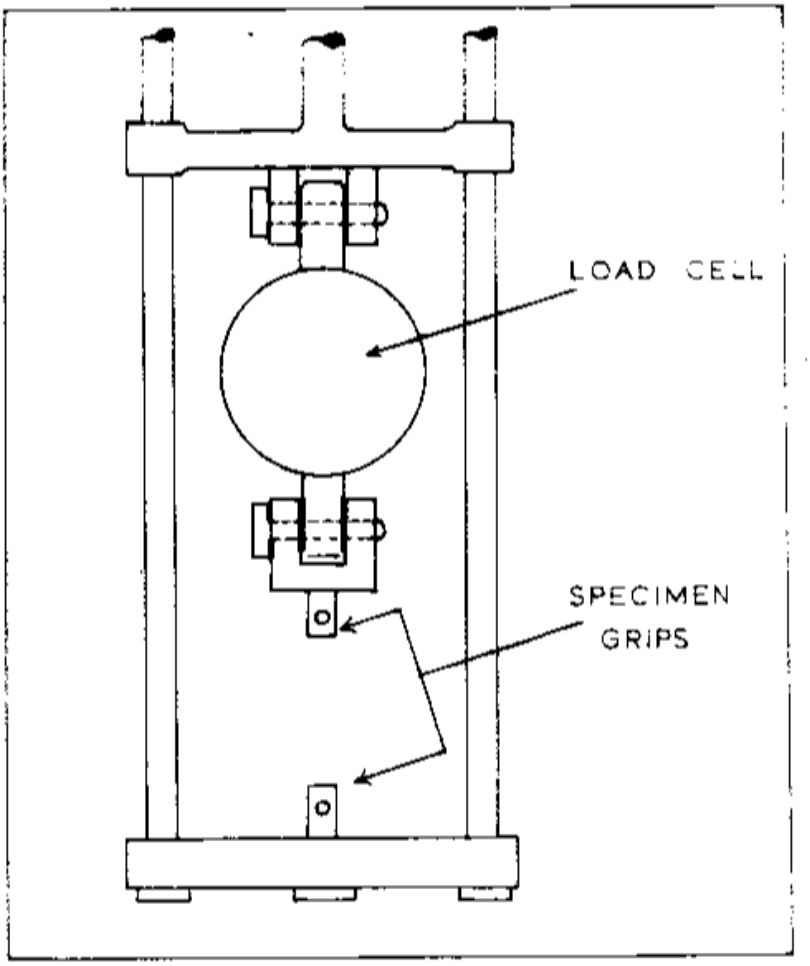

Fig. 2.5 Position of load cell in hard-beam tensometer.

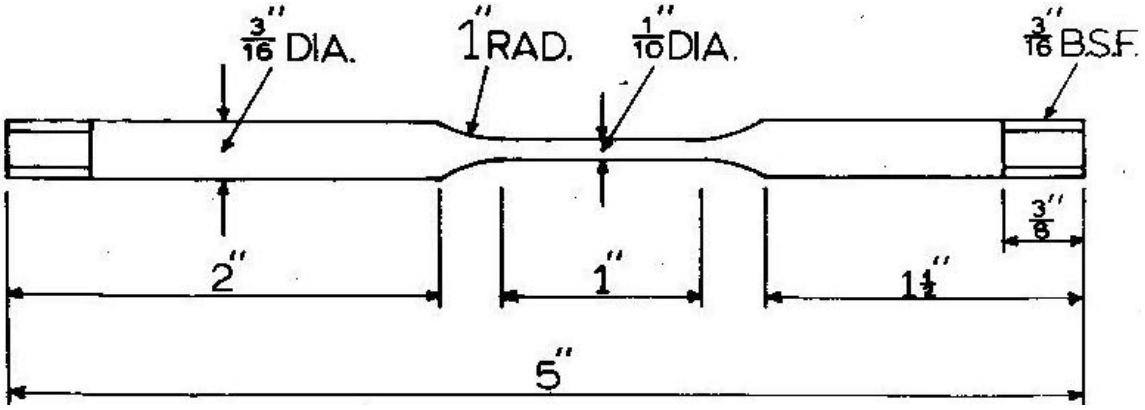

Fig. 2.6 Tensile specimen

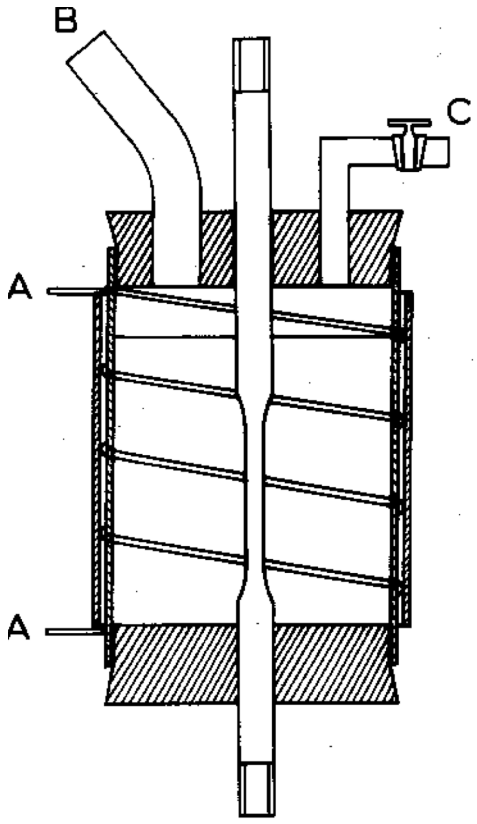

Fig. 2.7 Corrosion cell

The testing procedure for a constant strain stress-corrosion test in a hard-beam tensometer was as follows:-

(a) The corrosion cell, specimen and self aligning grips were positioned in the tensometer.
(b) The nitrate solution was added and boiled for half an hour.
(c) The specimen was strained at a rate of 4.8×10^{-4}/sec. until the required load was reached.
(d) After ten minutes, the load (which had dropped slightly due to specimen extension) was re-adjusted to its original value by slightly increasing the strain.

(e) The load was continuously recorded until complete failure occurred (at which point the load was equal to zero). In addition to the time to total failure, the time to open crack formation (i.e., the first load drop) could be measured.

Three recorders were used during the course of the work:-

(1) A Houston X-Y recorder fitted with a time base on the X-axis. The time base gave pen sweeps in the range 1"/sec. to 1"/min. In the Y direction the maximum pen speed was 15"/sec. and the maximum pen acceleration was 600"/sec^2.
This recorder was used to investigate crack propagation.
(2) A Phillips X-Y recorder fitted with a time base to give chart speeds in the range 0.4"/hour to 20"/hour.
(3) A Forster recorder with a chart speed of 2 ½ "/hour.

The latter two recorders were used for measuring time to total failure (i.e. zero load) and time for open crack initiation (i.e., time before first load drop).

2.5.2 Continuous tensile tests

Tensile tests were carried out in either a motorized Hounsfield tensometer with facilities for measuring the maximum load during a test and the total time, or in a hard-beam tensometer with facilities for plotting load-extension curves on an X-Y recorder. In any series of tests, the same tensometer was used for the series.

It was intended to measure the stress required to initiate stress-corrosion cracks during a continuous tensile test in the presence of boiling nitrate solution. Coleman et al (1) had previously determined stress-corrosion crack initiation stresses for stainless steel in $MgCl_2$ and Mg-7% Al in a $NaCl/K_2CrO_4$ solution. The method used by these workers, to determine the crack initiation stress was to remove specimens from the test at intervals and examine for surface cracks at a magnification of 20x. The objection to this method is that many tests have to be carried out in order to obtain one accurate value of the crack initiation stress. It was therefore decided to develop a testing procedure which would give a crack initiation stress from one test. It was not possible to detect when cracking commenced by examination of the load-extension curve for discontinuities (which would be expected at the onset of cracking) because at 115°C the curve is discontinuous due to jerky flow. Fig. 2.8 shows typical stress-strain curves for the 0.08 C steel at room temperature and at 115°C. It was therefore decided to use a strain rate sufficiently slow to make the load required to initiate the cracking equal to the maximum load recorded during the tensile test. This meant that once cracking had commenced, the extension of the specimen due to the crack opening up, relaxed the load more rapidly than it was being applied by the tensile machine.

Fig. 2.9 shows the load extension curves obtained during tensile tests, (a) in oil at 115°C and (b) in boiling nitrate solution. In (b) open stress-corrosion crack formation has occurred at B. Both curves are identical during the stage AB. The definition of cracking used in this work was a crack visible by surface examination at a magnification of 100x. A preliminary investigation during which specimens were removed at intervals during stage AB (Fig. 2.9(b)) and examined for surface cracks, at a magnification of 100x, showed that a strain rate of 1×10^{-5} sec^{-1} complied with the condition that the maximum load recorded during the test was the load

at which surface cracks first became visible. Test times at a strain rate of 1 x 10^{-5} sec^{-1} were of the order of two hours.

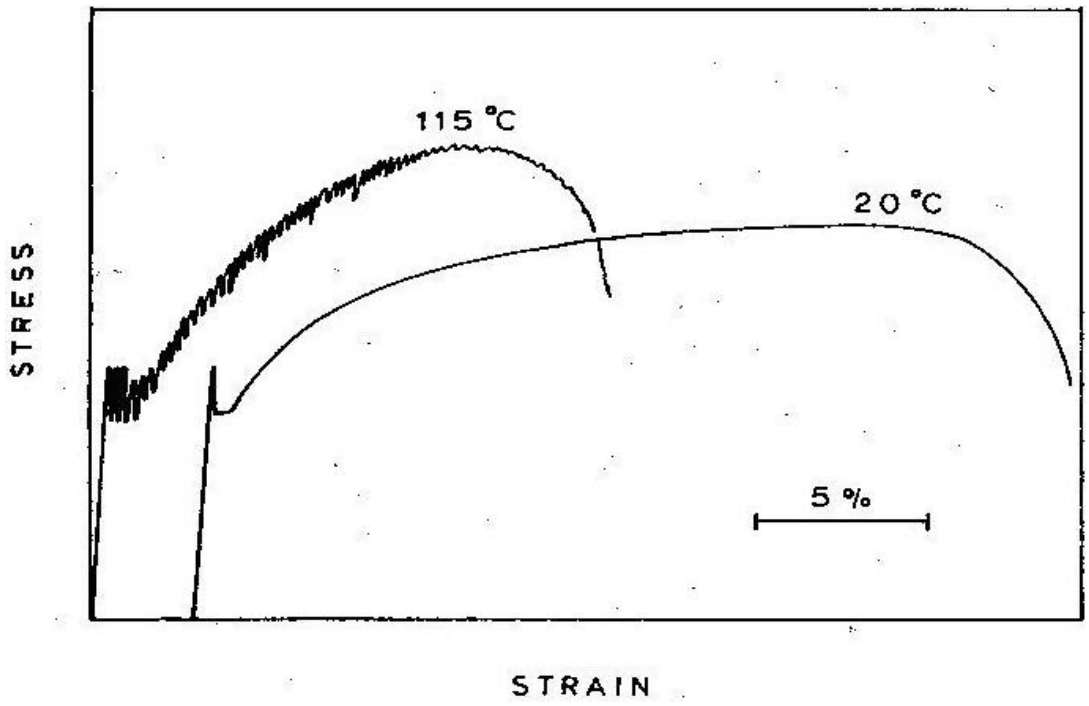

Fig. 2.8 Stress/Strain curves for 0.08 C steel. $\dot{\epsilon}$ = 1 x 10^{-5}/sec^{-1}

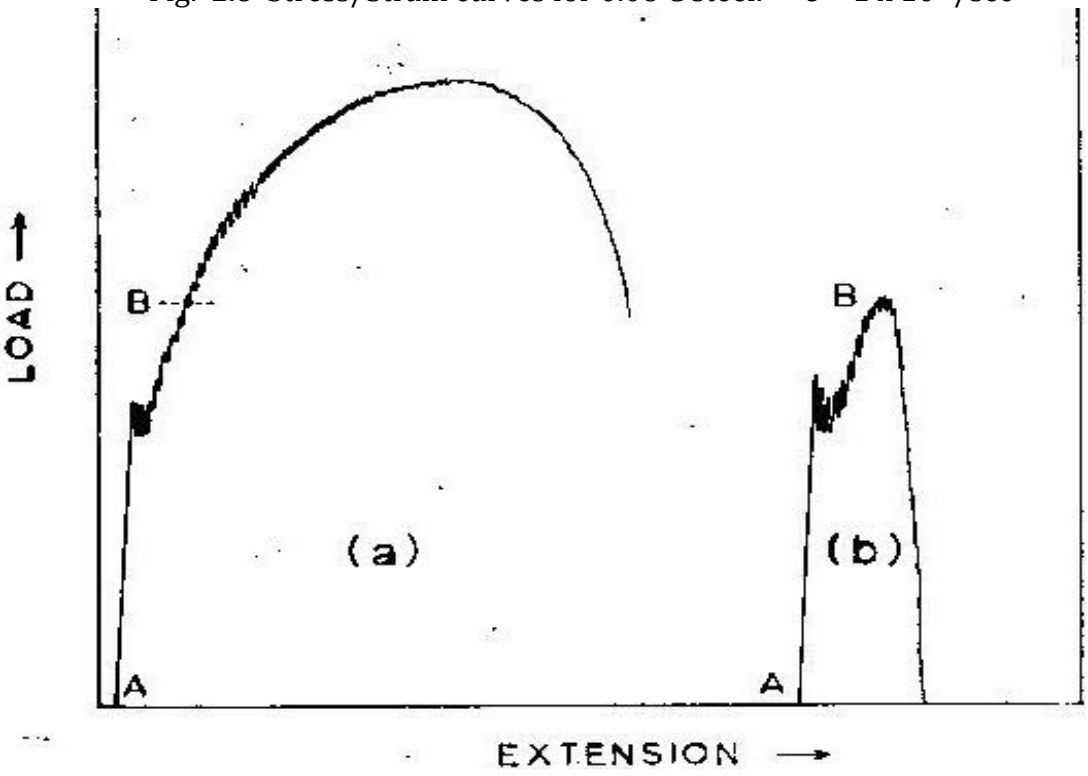

Fig 2.9 Continuous tensile tests at a strain rate of 1 x 10^{-5} sec^{-1}.
(a) In oil at 115°C (b) In boiling nitrate solution

The testing procedure was as follows:-

(a) The corrosion cell, specimen and self aligning grips were positioned in the tensometer.
(b) The nitrate solution was added and boiled for half an hour.
(c) The tensile specimen was tested to complete failure. In the tests in a Hounsfield tensometer the maximum load during the test was recorded by a steel index in the mercury column. In tests in a hard-beam tensometer the load extension curves were plotted on an X-Y recorder throughout the test.

In order to compare the behaviour of a material in a stress-corrosion tensile test with that in the absence of a corrodent, tensile tests were carried out in oil heated to 115°C $\pm$ 1°C in a cell identical to the corrosion cell. The specimens tested in oil were identical to the stress-corrosion tensile specimens. All tests in oil were carried out on a hard-beam tensometer and load-extension plots were obtained during each test.

2.6 Thin film electron microscopy

The majority of the foils examined were prepared from cold rolled sheet, but some foils were prepared from tensile specimens in order to confirm that the dislocation arrangements formed during a stress-corrosion test were the same as those formed during cold rolling.

2.6.1 Preparation of thin foils from cold rolled sheet

The procedure was as follows:-

(a) Steel strips, 3" x 1" x 0.008" were prepared from bulk material by cold rolling and vacuum annealing.
(b) The steel strips were electropolished until 0.001" thick. The edges of the sheet were protected by lacquer during this stage.
The electropolishing conditions were:-

electrolyte - 10% perchloric acid, 90% acetic acid
cathode - stainless steel
voltage - 18 volts
current density - 0.2 amps/cm^2

The specimen was rotated at 30 revs/minute, about the axis of the cylindrical cathode. Foils were washed in methyl alcohol and dried in warm air.
(c) A disc 1/8" diameter was punched out of the sheet with a hardened steel punch.
(d) The disc was transferred to the platinum holder shown in Fig. 2.10. In this holder, the disc was sandwiched between the platinum plates. Holes in the plates exposed circular areas 1/16" diameter at the centre of the disc. The inside faces of the plates were recessed in the region of the holes to prevent the disc moving. One plate was fastened rigidly to the bulk of the holder and the other was hinged so as to fit tightly onto the rigid plate when in the closed position. The hinged plate assisted rapid removal of the foil for washing and drying. While in use the plates were clamped together by a mild steel clip. This clip had a dual function since it was partially lacquered to leave an exposed area, which was polished together with the actual specimen. The unlacquered area of the clip was calculated to give the correct overall current density for the cell used.

(e) Using the same conditions as in (b) the disc was electropolished until perforated. The perforation time (always less than three minutes) was found by trial and error. Once this time had been found then up to thirty foils could be prepared from the same sheet in a known time of less than three minutes each.

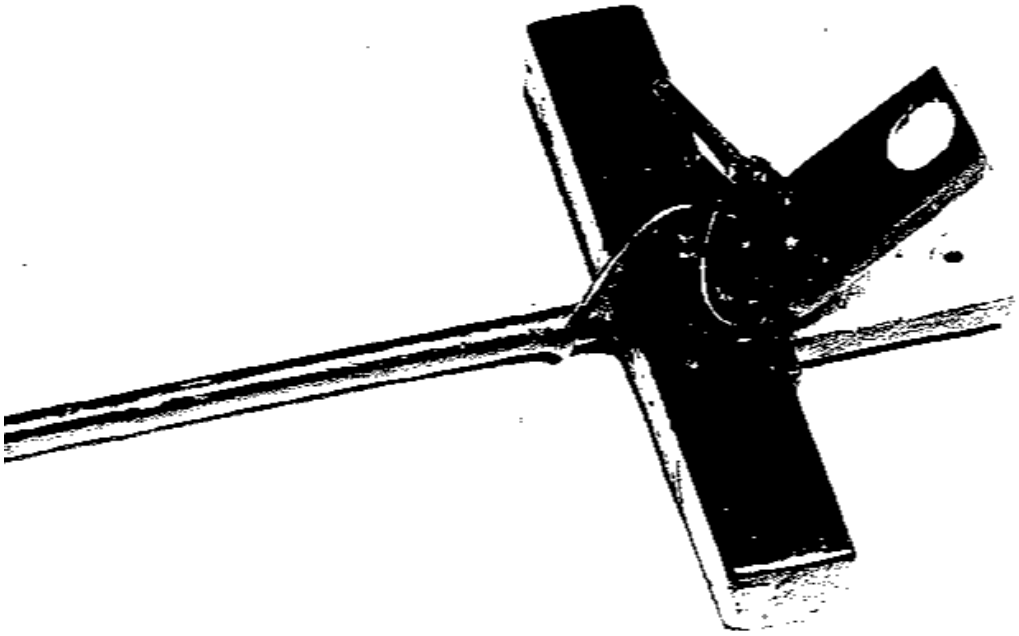

Fig. 2.10 Specimen holder for electropolishing thin foils.

2.6.2. Preparation of thin foils from bulk specimens

(a) Discs approximately 1 mm. thick were cut from 3 mm. diameter rod.
(b) The faces of the discs were emeried until the faces were flat and approximately parallel.
(c) Using a stainless steel holder to protect the disc periphery it was electromachined from both sides until the central portion was approximately 0.005" thick. The electromachining electrolyte was 50% HCl and the operating voltage was 50 volts.
(d) The disc was transferred to the platinum holder described in 2.6.1 (d) and with the conditions stated in 2.6.1 (b) was electropolished until perforated. Since the perforation time could not be readily estimated the electropolishing unit was positioned on an optical bench so that the disc prevented light from a point source from reaching a telescope. Continual observation through the telescope enabled the disc to be removed immediately after perforation. The time taken for perforation to occur was 15 to 30 minutes.

2.6.3 Discussion of preparation techniques

The advantage of these two methods over the more conventional window techniques was that the disc periphery was protected during the final thinning and so gave the foil rigidity. This was particularly important in the tests involving corrosion of thin foils, since considerable handling of the foil was necessary.

Method (1) was more satisfactory than method (2) for two reasons:-

(a) Once the thin sheet had been polished to a thickness of 0.001", a large number of foils could be easily prepared in less than three minutes each.
(b) Since the starting material for the final thinning was thinner than in the electromachined discs, the areas thinned sufficiently for electron penetration were larger.

To justify the use of method (1) it was necessary to ensure that the properties of the thin sheet were representative of the bulk material and that no severe deformation occurred during the mechanical punching operation. A preliminary study of the dislocation structure in cold worked low carbon steel showed the dislocation arrangements and density to be independent of whether method (1) or (2) was used to prepare the foil. Foils prepared from sheet material without using a punch (i.e., final foil cut with a razor blade) were found to be identical to those punched out.

3 RESULTS AND DISCUSSION

3.1 A comparison between stress-corrosion cracking and tensile behaviour in the absence of a corrodent

The parameters normally varied in the study of a fracture process are grain size, strain rate and temperature. In this case the temperature range over which cracking readily occurs is small, and therefore only the effects of grain size and strain rate have been investigated.

3.1.1 The influence of grain size on stress-corrosion cracking

In the initial investigation, constant strain tests in jigs of the type shown in Fig. 2.4, page 17 were used. The applied stress necessary to cause complete failure in 24 hours $\pm$ 1 ½ hours was determined. The results are shown in Fig. 3.1. Although there is considerable scatter in these results it is clear that there is a grain size effect. The increasing scatter with decreasing grain size is probably due to the fact that several large cracks were usually observed in the small grain size material, whereas the larger grain sized material normally contained only one large crack. Any variation in the number of large cracks leads to scatter in the time to total failure measurements because the open cracks relax the stress on the specimen and so increase the time to total failure.

It was thought that in order to study the grain size effect quantitatively it was necessary to use a test which –

(a) provided a result with more physical meaning than the static test.
(b) Gave less scatter.
(c) Was short in duration.

It was decided to carry out continuous tensile tests in boiling nitrate solution, with the intention of measuring the stress at which cracking was initiated. As stated previously (section 2.5.2), a stress-corrosion crack was defined as a crack visible by surface examination at a magnification of 100x. Stress-corrosion tensile tests were carried out at a strain rate of 1×10^{-5} sec^{-1}. Duplicate tests in oil at 115°C enabled yield stress and flow stress to be calculated. Fig. 3.2 shows the variation of yield stress, 5% flow stress and stress-corrosion fracture initiation stress with grain size.

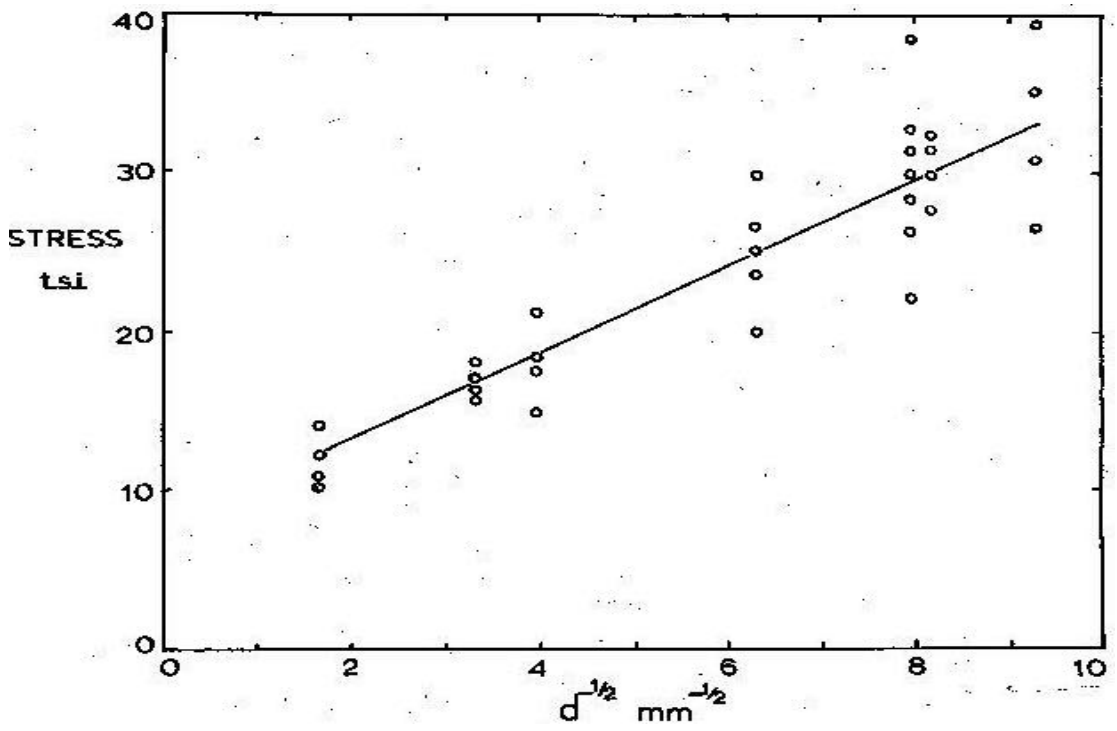

Fig. 3.1 Influence of grain size on the applied stress required to cause failure in 24 hours in a static stress-corrosion test.

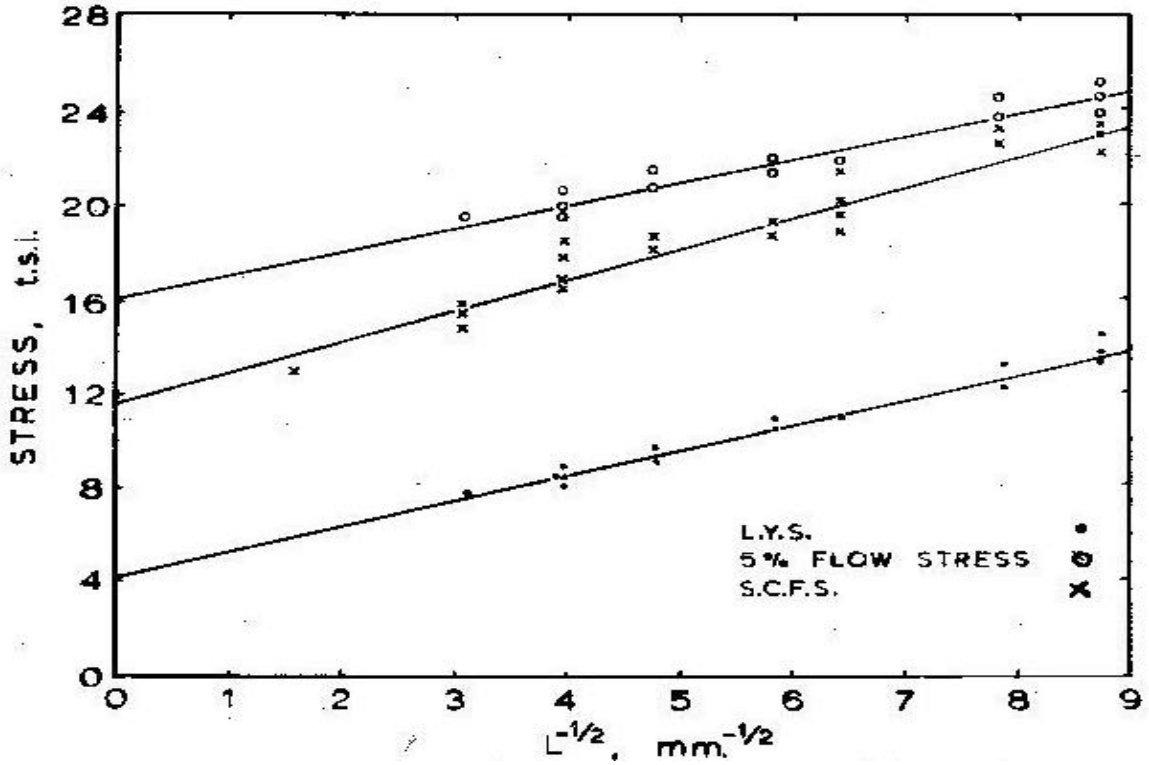

Fig. 3.2 Effect of grain size on yield stress, 5% flow stress and stress-corrosion fracture stress (S.C.F.S).

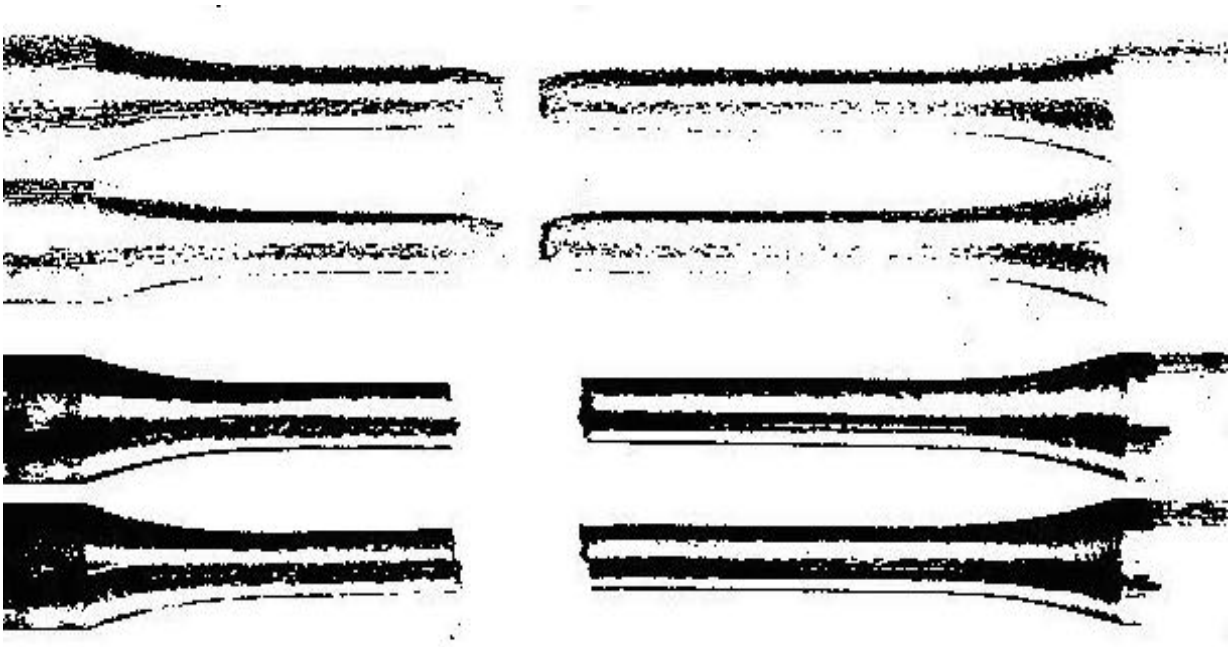

Fig. 3.3 Failed specimens photographed on a mirror.
Top - Tensile specimen pulled to fracture in oil at 115°C.
Bottom - Specimen pulled to fracture in boiling nitrate solution at 115°C.

Fig. 3.3 shows the fracture in the stress-corrosion tensile specimens to be macroscopically brittle compared with the fractures in oil. These results are discussed together with the strain rate results in section 3.1.2.

3.1.2 The influence of strain rate on stress-corrosion cracking

Material of grain size $l^{-1/2} = 4.0\ mm^{-1/2}$ was used throughout this part of the work. The effect of strain rate on stress-corrosion fracture initiation stress, yield stress, etc. is shown in Fig 3.4. At strain rates faster than $5 \times 10^{-5}\ sec^{-1}$, the criterion (i.e., maximum load recorded is equal to the load required to initiate a crack visible by surface examination at a magnification of 100x) being used to measure fracture stress, was not valid since the propagating cracks were unable to relax the load more rapidly than it was being applied by the tensile machine. Therefore the determination of the open crack initiation stress at strain rates higher than $5 \times 10^{-5}\ sec^{-1}$ required the use of several specimens because specimens had to be removed from the test at predetermined intervals and examined for surface cracking. At strain rates faster than $5 \times 10^{-4}\ sec^{-1}$, no cracking was detectable by surface examination at a magnification of 100x, and the fracture appearance was identical to that obtained in a test in oil at 115°C (See Fig. 3.3 Top).

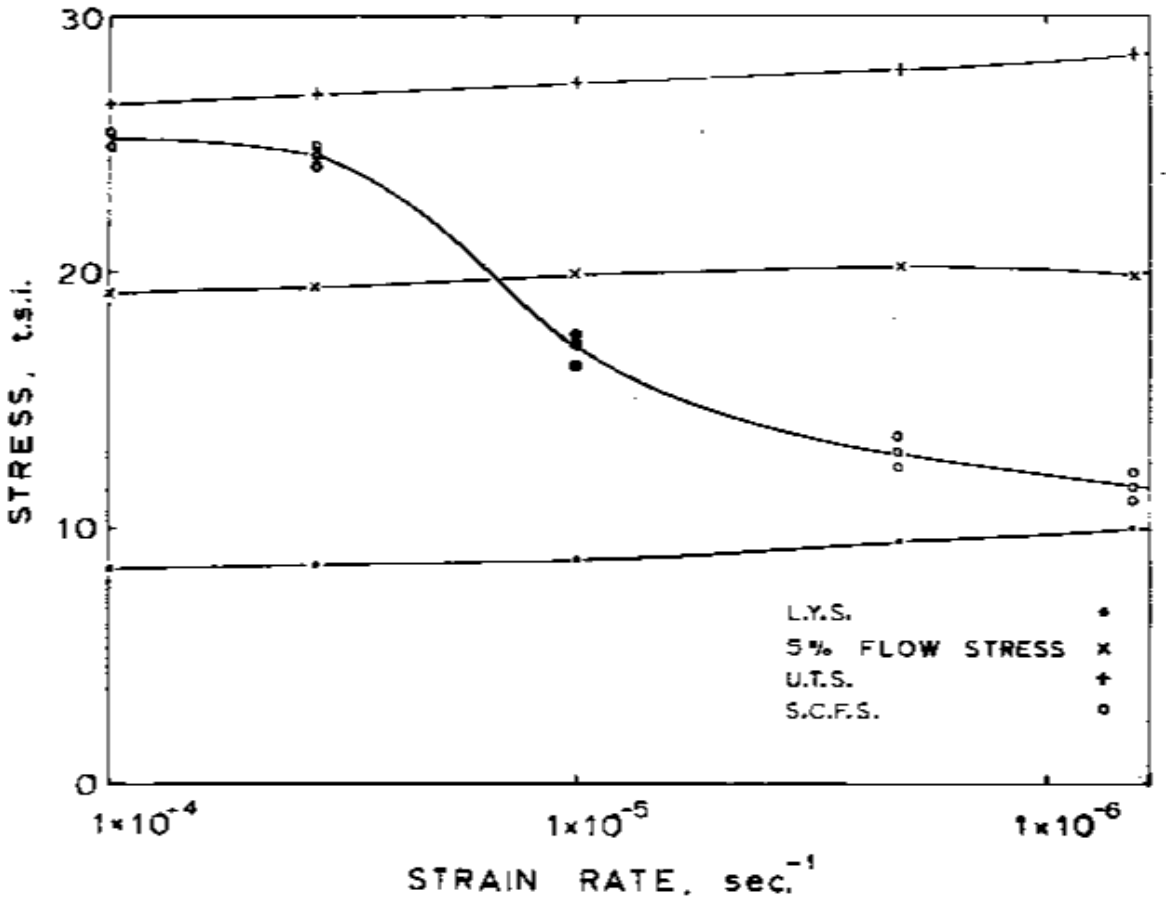

Fig. 3.4 Effect of strain rate on yield stress, 5% flow stress, U.T.S, and stress-corrosion fracture stress.

3.1.3 Discussion of grain size and strain rate results

The grain size results shown in Fig. 3.2, together with those obtained for the 0.30 C steel (Fig. 3.18 Page 41) suggested a similarity between stress-corrosion fracture initiation stress and flow stress. It was first thought that this similarity was an indication that a particular strain was required in a material before cracks were initiated in it. The load extension curves, Fig. 3.5, during stress-corrosion tests at different strain rates, show that this is not the case and the amount of plastic strain that has occurred at the onset of cracking decreases as the strain rate decreases.

The grain size and strain rate results were not fully understood until the completion of the investigation into the role of stress during a static test (Section 3.3) which showed that it is extremely important to distinguish between open and unopened cracks. In this work and in the other grain size investigations (1, 2), the criterion for cracking has been an open crack visible on the specimen surface.

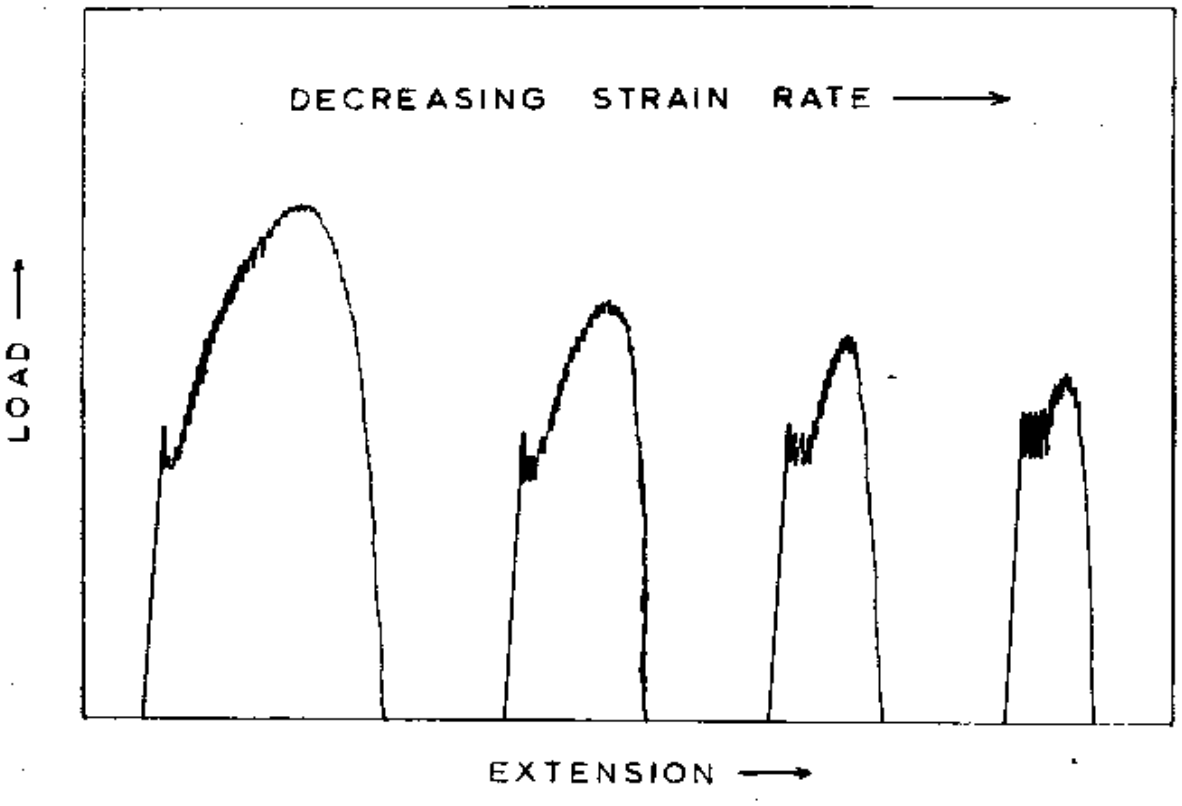

Fig. 3.5 Effect of strain rate on stress-corrosion cracking in continuous tensile tests.

In the static test investigation (Section 3.3), it was found that considerable penetration could occur before an open crack forms. This raised the question as to whether the stress-corrosion fracture stress measured in the tensile test was in fact the stress at which cracking commenced. This question was investigated by removing specimens from the stress-corrosion tensile tests at stresses lower than their so-called stress-corrosion fracture initiation stress. Metallographic examination of longitudinal sections from those specimens revealed considerable intergranular penetration, which in some instances reached a depth of 0.15 mm. Fig. 3.6 shows typical penetration in a specimen removed from the tensile test at a stress just below its so-called fracture initiation stress.

It appeared that the stress-corrosion fracture stress measured in this work, and quite possibly in other investigations into the effect of grain size on stress-corrosion cracking, was the stress required to form an open crack rather than a critical stress required to initiate the stress-corrosion process. The application of the findings of the static test investigation to a continuous tensile test is not straightforward, since theoretically, any crack formed after the upper yield point in a tensile test is an open crack because plastic deformation has occurred in the material beyond it. However, almost all grain boundaries exposed to the surface are initially attacked and the plastic deformation that occurs in the specimen during the early stages of the test is not localized in the material ahead of any particular crack, so that the cracks may be considered from a practical viewpoint, to be unopened.

Fig. 3.6 Intergranular penetration in a stress-corrosion tensile specimen prior to the formation of an open crack. x400

As the depth of penetration increases, some cracks (i.e. those which are between favourably oriented grain boundaries) penetrate more rapidly than the majority. Once a small number (often only one) of cracks have reached a critical depth (considerably deeper than the majority) then the resultant stress increase opposite these cracks localizes further plastic deformation in these areas and converts these to open cracks visible by surface examination at 100x. It is thought that the only significance of the stress-corrosion fracture stress measured in a continuous tensile test is that it is the stress on the specimen after the time required to attain this critical amount of penetration. Typical stress/time curves obtained during stress-corrosion tensile tests on materials of different grain size are shown in Fig. 3.7. E and E^1 represent the open crack initiation stress, D and D^1 represent any given flow stress. It is clear from Fig. 3.7, that the total times to open crack formation are different whereas one might have expected them to be the same if continuous penetration occurred throughout the test until it had reached a critical depth. This apparent anomaly can be explained on the basis of the results of the static test investigations (Section 3.3) from which it was concluded that the rate of penetration was greatly accelerated by deformation of the material ahead of the crack. It therefore seems likely that the amount of penetration during the elastic portion AB and A^1B^1 of the curves shown in Fig. 3.7, will be negligible compared with the penetration during the plastic stage.

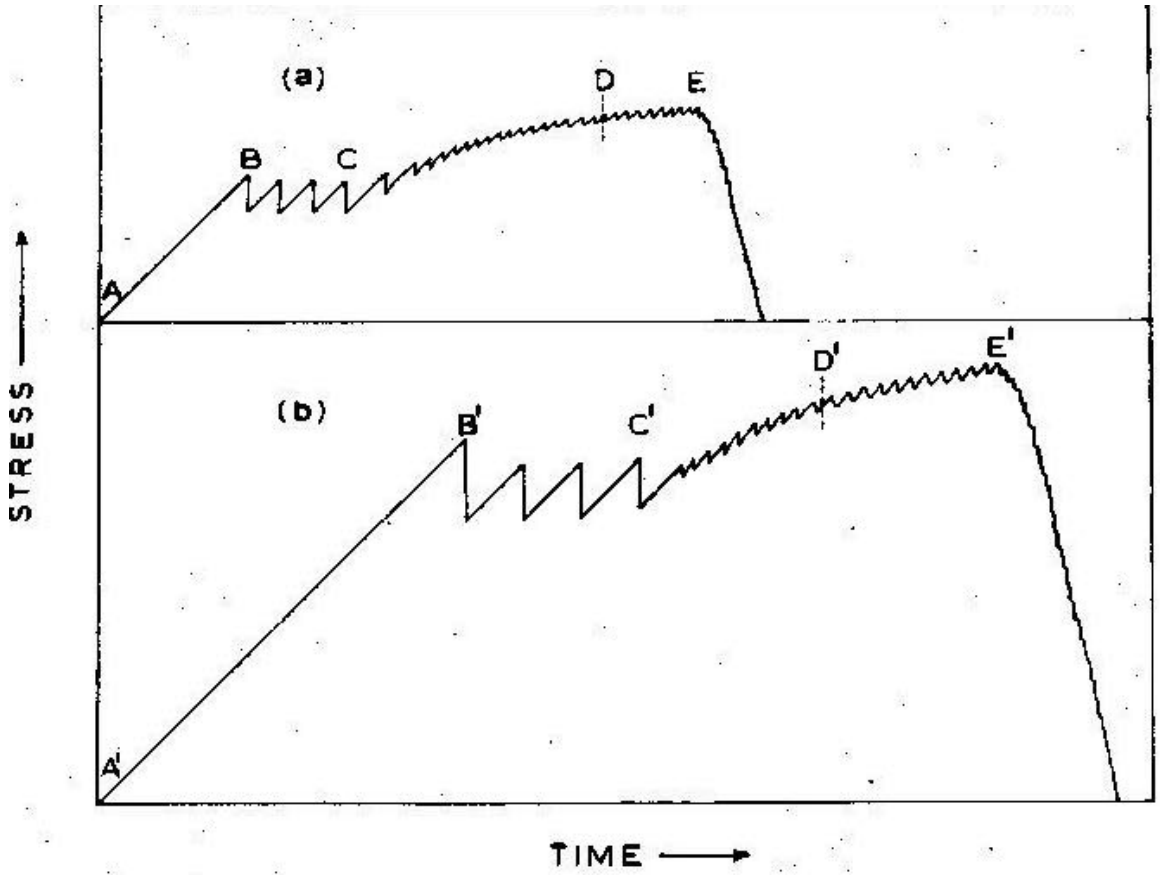

Fig. 3.7 Stress/time relationship during a continuous stress-corrosion tensile test.
(a) large grained material
(b) small grained material

If the crack initiation stress was the stress on the specimen at a certain time after the upper yield point, then the stress-corrosion fracture plot (Fig. 3.2, page 26) would have the same slope as the flow stress plot. It can be seen (Fig. 3.2) that this is almost the case. The fact that the stress-corrosion fracture stress plot is slightly steeper than the flow stress plot, means that the period B^1E^1 (Fig. 3.7) is greater than BE. This is thought to be due to the fact that the yield strain increases with decreasing grain size and the period B^1C^1 is greater than BC. In a slow strain rate test, serrated yielding occurs during this stage and although considerable deformation occurs, it occurs in a few large, rapid (a fraction of a second) steps. Since it was concluded from the static test investigation that continuous deformation is the factor that accelerates penetration, it seems likely that the amount of penetration that occurs during the stages BC and B^1C^1 is negligible compared with the penetration during an equal period of time in stage CE or C^1E^1. In support of this interpretation it can be seen (Fig. 3.7) that the times CE and C^1E^1 are equal.

Further evidence for the necessity of a certain period of time after yielding, before an open crack can form in a tensile test, was obtained from some tests in which the strain rate was changed from a high to a low strain rate during the test. Fig. 3.8 (a) shows the load-time curve for a stress-corrosion tensile test on material of grain size $l^{-1/2} = 3.1\ mm^{-1/2}$, at a strain rate of $2 \times 10^{-6}\ sec^{-1}$. Figs. 3.8 (b) and (c) show the effect of passing through the early stages of the curve

at a strain rate of 2 x 10^{-3} sec^{-1} (this stage lasted less than 10 seconds), before continuing the test at a strain rate of 2 x 10^{-6} sec^{-1}. Fig. 3.8 (c) shows that as the amount of pre-strain at the faster strain rate is increased the fracture stress also increases due to the fact that a certain period of plastic straining is required before an open crack can form.

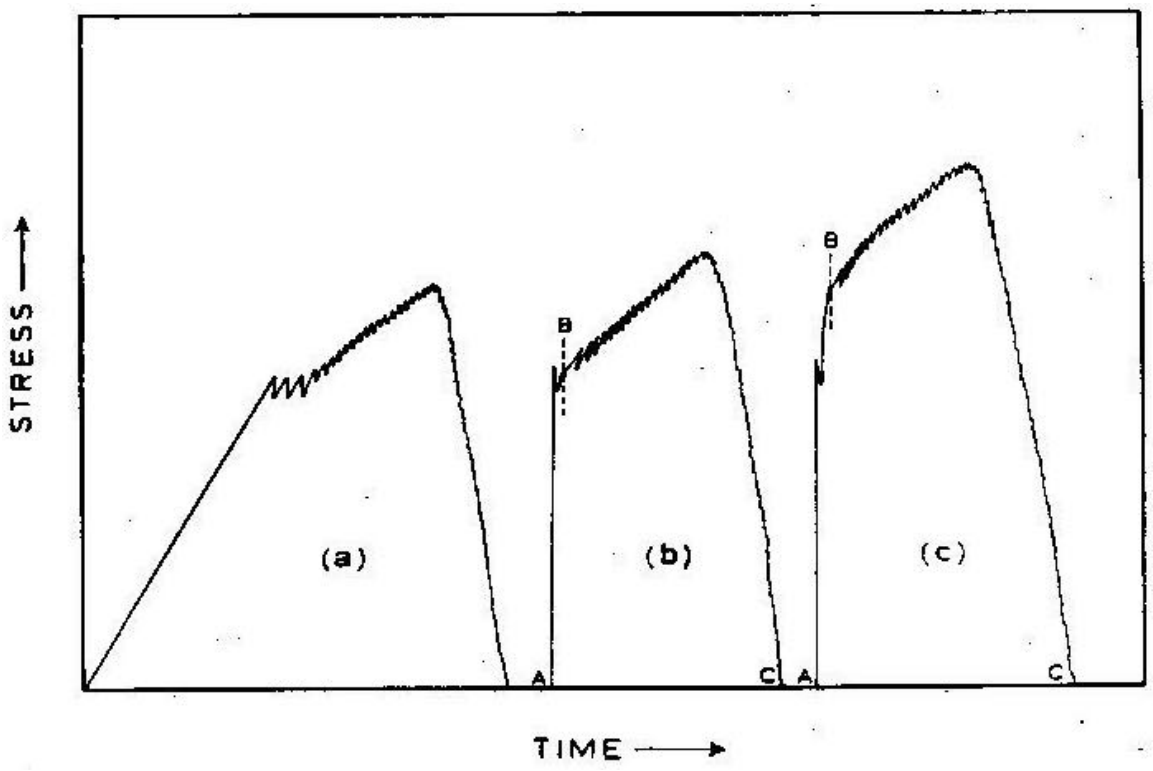

Fig. 3.8 Variation of strain rate during a continuous stress-corrosion tensile test.

(a) Rate throughout test = 2 x 10^{-6} sec^{-1}
(b) AB - $\dot{\epsilon}$ = 2 x 10^{-3} sec^{-1}, BC - $\dot{\epsilon}$ = 2 x 10^{-6} sec^{-1}
(c) AB - $\dot{\epsilon}$ = 2 x 10^{-3} sec^{-1}, BC - $\dot{\epsilon}$ = 2 x 10^{-6} sec^{-1}

If this interpretation of the stress-corrosion fracture stress is correct, then one would expect the open crack formation period, after elastic strain and serrated yielding to be independent of strain rate. The results in Table 3.1 show this to be the case.

Table 3.1
The effect of strain rate on the time to open crack formation.

Strain rate, sec^{-1}	5 x 10^{-5}	1 x 10^{-5}	3.8 x 10^{-6}	8 x 10^{-7}
Total time to open Crack formation (mins)	40	60	120	400
Time to open crack Formation after Serrated yielding (mins)	35	50	55	50

The experimental observation that no stress-corrosion cracking was detectable at strain rates faster than 5×10^{-4} sec^{-1} can also be explained by a cracking mechanism that involves continuous penetration during the test. It is thought that stress-corrosion does occur at strain rates higher than 5×10^{-4} sec^{-1} but that due to the relatively slow rate of the corrosion reactions, any cracks that form are too small for identification by surface examination at a magnification of 100x. The duration of a tensile test at a strain rate of 5×10^{-4} sec^{-1} is about 7 minutes, and the maximum depth of penetration is 0.03 mm. The fact that at a strain rate of 1×10^{-3} sec^{-1} (the next highest rate available) no cracks were detected, is quite feasible, since the crack depth expected in such a test would be about 0.015 mm. The aspect ratio for cracks in specimens tested at 5×10^{-4} sec^{-1} was about 10. Hence the mouth of a crack formed in a test at 1×10^{-3} sec^{-1} would be of the order of 1μ wide. Cracks of this size would not be distinguishable from surface machining marks and surface etching. The view that the limiting strain rate for cracking is a function of the crack size detectable was supported by the observation that when a stronger corrodent ($Ca(NO_3)_2 + NH_4NO_3$) was used, cracking was detected at a strain rate of 1×10^{-3} s^{-1}.

3.2 Stress-corrosion cracking in 0.30 C steel

The main aim of this investigation was to determine why 0.30 C steels are more resistant to stress-corrosion cracking when the carbon is in the form of lamellar pearlite, than when the steel has been subcritically annealed (one week at 650°C) to convert the pearlite to discrete carbide particles. The influence of grain size on the stress-corrosion cracking of 0.30 C steel has also been investigated so as to afford a comparison with the 0.08 C steel.

Since an $l^{-1/2}$ relationship had been shown to exist for the stress-corrosion cracking of 0.08 C steel, it seemed likely (at the time of this investigation) that dislocations were important in the cracking process. It was therefore decided to compare, with the aid of thin film microscopy, the dislocation arrangements in deformed 0.30 C pearlitic steel with those in deformed 0.30 C spheroidised carbide steel. Thin foils were prepared from steel sheet, which had been cold rolled 2, 4, 10, 15 and 20%. The grain size of all foils was $l^{-1/2} = 6.5$ $mm^{-1/2}$.

The dislocation arrangements in foils deformed 2, 4 and 15% are shown in Figs. 3.9 – 3.11. The dislocation arrangements in the susceptible 0.08 C steel are shown for comparison. The results for the 0.08 C steel are in agreement with those of previous investigators (27, 28, 29). In order to determine whether the dislocation arrangements in cold rolled material were typical of those formed during a stress-corrosion tensile test, thin foils were prepared from a 0.08 C test specimen which had failed by stress-corrosion after a deformation of 8%. Fig. 3.12 shows the dislocation arrangements in the stress-corrosion test specimen to be identical to those in the cold rolled sheet.

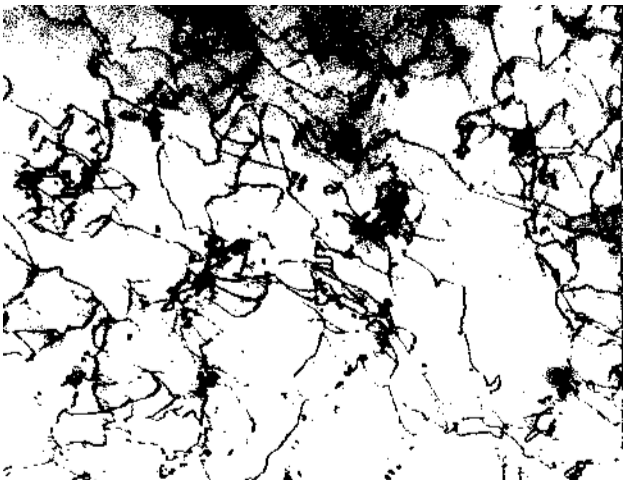

0.30 C Pearlitic

0.30 C Spheroidised

0.08 C

0.5 μ

Fig. 3.9 Dislocation arrangement in steels deformed 2%

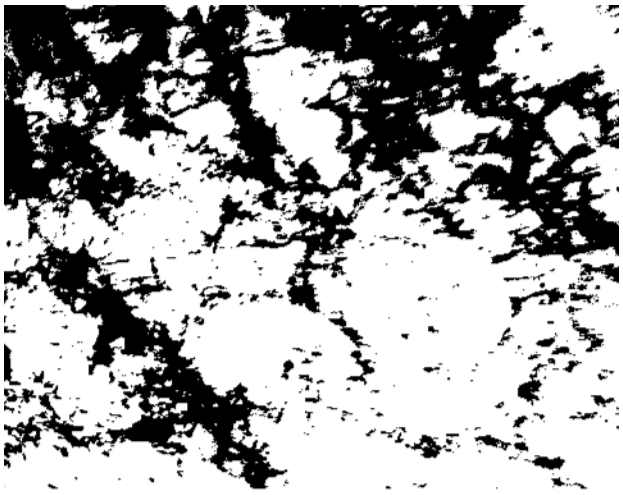

0.30 C Pearlitic

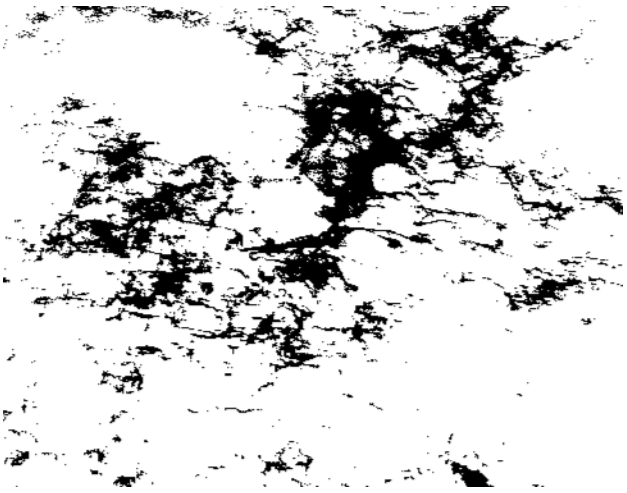

0.30 C Spheroidised

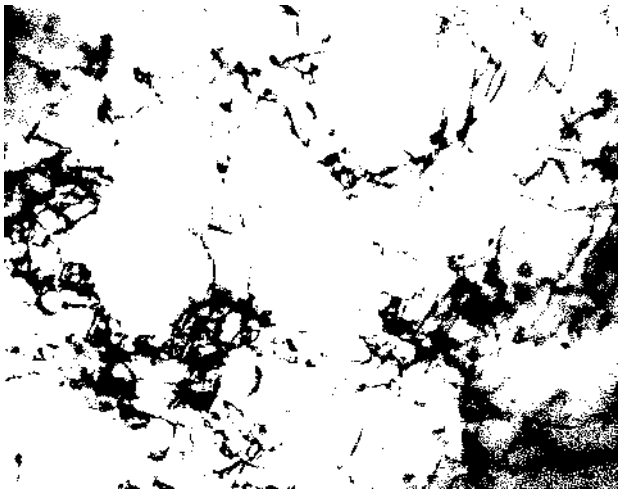

0.08 C

0.5 μ

Fig. 3.10 Dislocation arrangement in steels deformed 4%

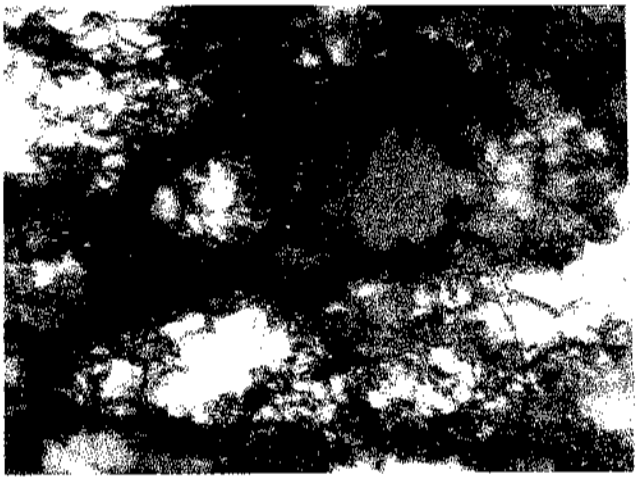

0.30 C Pearlitic

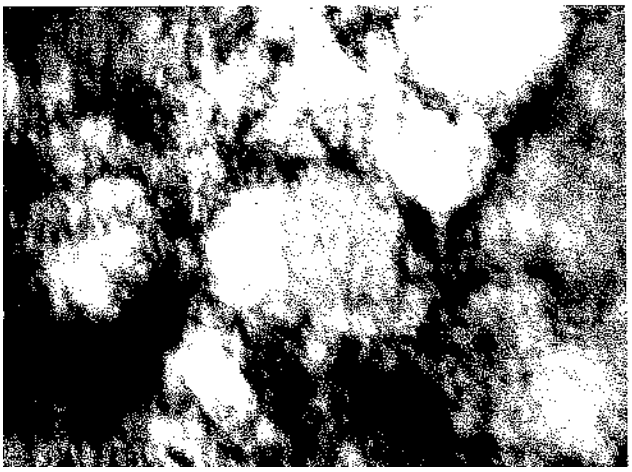

0.30 C Spheroidised

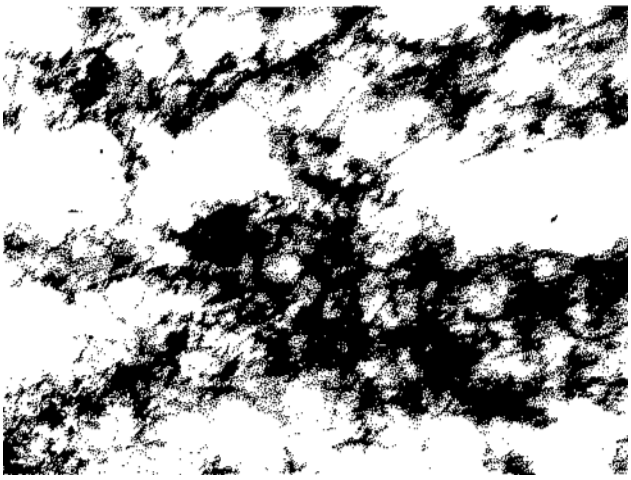

0.08 C

0.5 μ

Fig. 3.11 Dislocation arrangement in steels deformed 15%

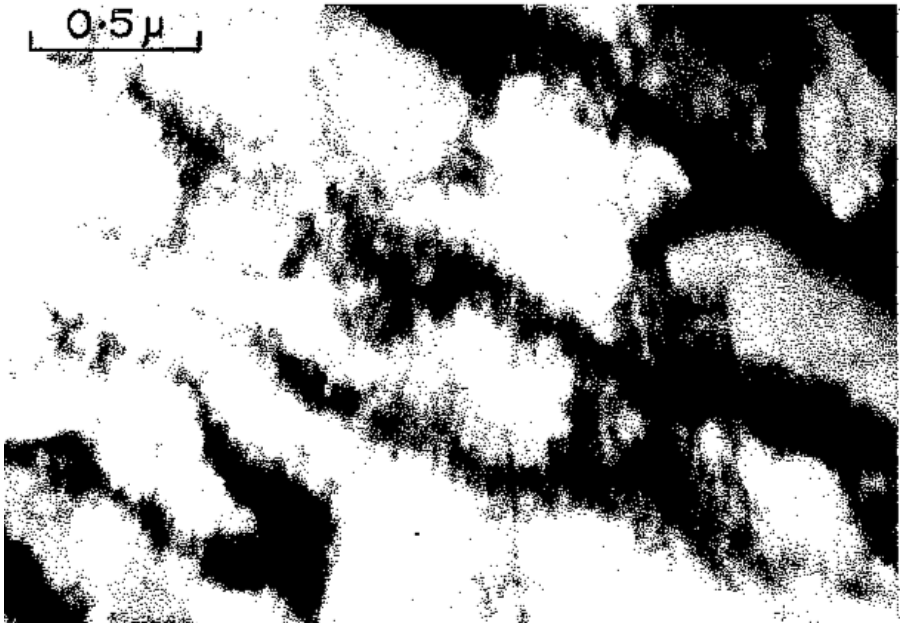

Fig. 3.12 Dislocation arrangements in a thin foil prepared from a tensile specimen.

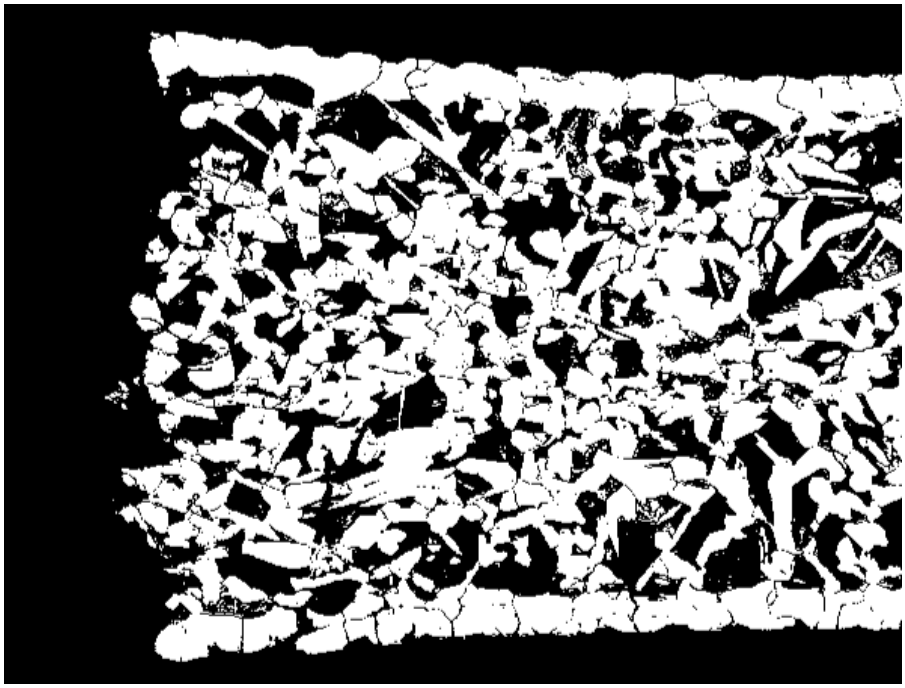

Fig. 3.13 Stress-corrosion fracture in surface decarburized 0.30 C pearlitic steel. X30

Figs. 3.9 – 3.11 show that the type of dislocation arrangement is identical in all three steels. The only difference between the steels is that for a given deformation, the dislocation

density in the pearlitic steel is higher than that in the spheroidised carbide steel. It appeared that if dislocations were important in the cracking process, then the pearlitic steel should fail by stress-corrosion in the same manner as the spheroidised carbide steel. The fact that this had been reported not to be the case (5) suggested that pearlitic steels were resistant for electrochemical, rather than structural reasons. However, the fact that cracks had been reported (5) to propagate through pearlite, once initiated in decarburized material was difficult to explain on an electrochemical basis. It was therefore decided to investigate the cracking of surface decarburized pearlitic steel to determine whether the cracking was true stress-corrosion. Stress-corrosion tests at a strain rate of 1×10^{-5} sec^{-1} were used to study the cracking of material of grain size $l^{-1/2} = 6.0$ $mm.^{-1/2}$, which had been surface decarburized to a depth of 7% of its diameter. These tests confirmed the observations of Parkins (5) that cracks will propagate through pearlite. The rate of crack propagation was typical of that expected for a stress-corrosion crack. Fig. 3.13 shows a typical fracture and Fig. 3.14 shows actual cracks in the pearlitic regions.

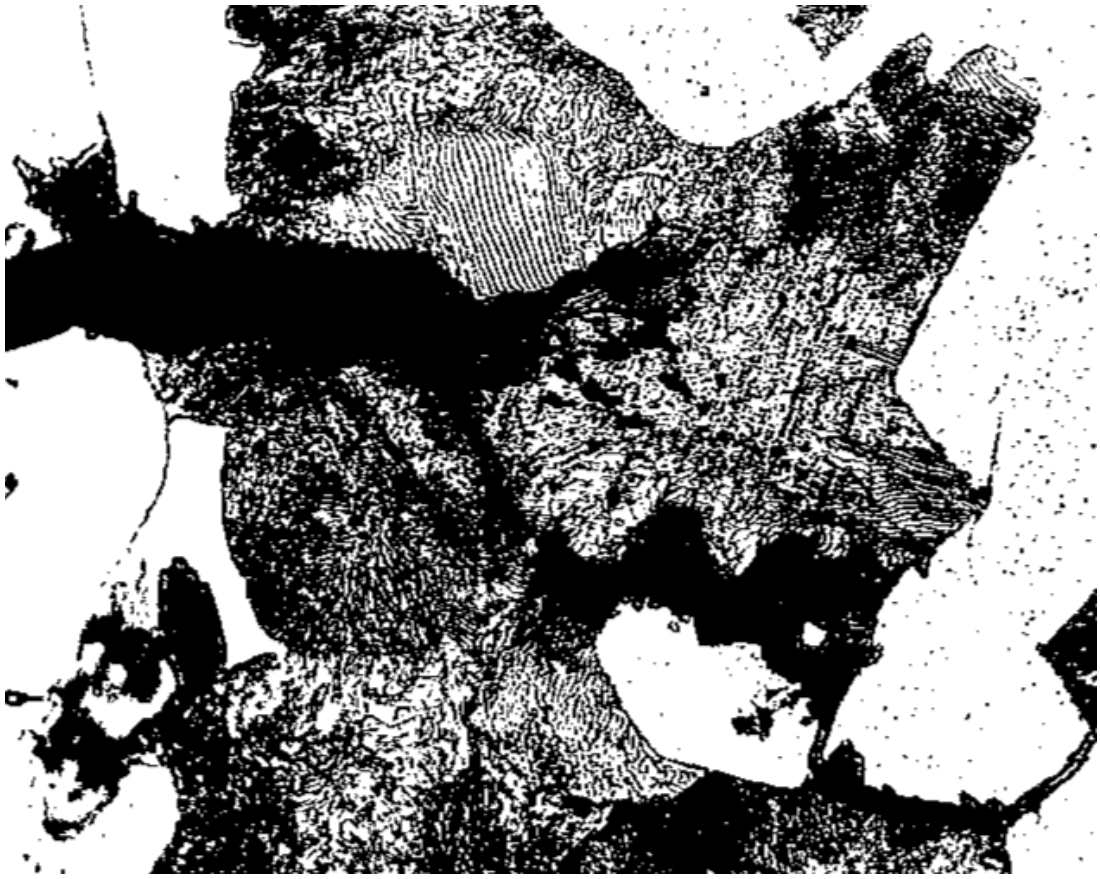

Fig. 3.14 Stress-corrosion cracks in 0.30 C pearlitic steel. X500

The most significant result in this investigation was the observation that if the decarburized later was removed (either by machining or electropolishing) from a specimen of the type shown in Fig. 3.13, the specimen was still susceptible to stress-corrosion cracking in

the stress-corrosion tensile test. A typical fracture is shown in Fig. 3.15. The 0.30 C pearlitic steel was also found to fail by stress-corrosion cracking in a static stress-corrosion test but the applied stress required to cause failure was much greater than for the spheroidised carbide steel of the same grain size.

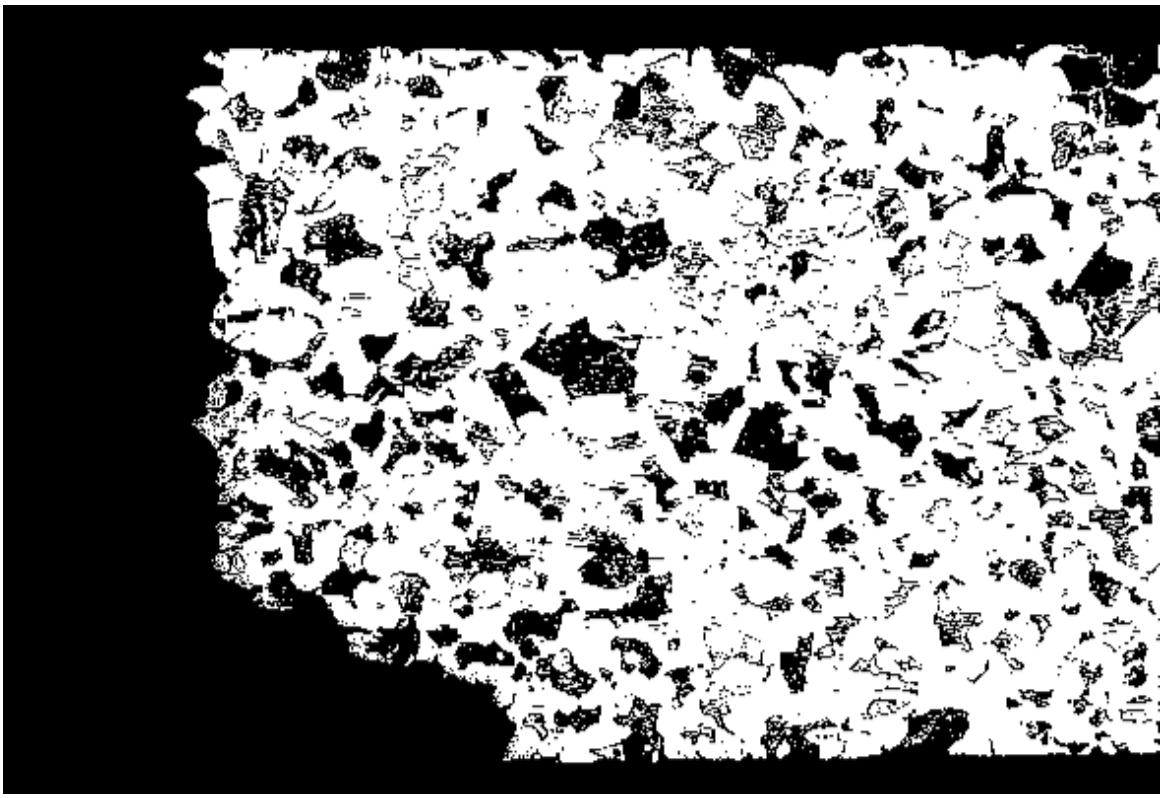

Fig. 3.15. Stress-corrosion fracture in 0.30 C pearlitic steel. X30

The observation that the 0.30 C pearlitic steel and the spheroidised carbide steel both failed by stress-corrosion cracking in a continuous tensile test, whereas they had widely differing susceptibilities in a static constant strain test, suggested that the subcritical annealing treatment (used to spheroidise the carbide) had an effect additional to that of increasing the corrosion susceptibility of the grain boundaries. It is thought that an important result of the subcritically annealing treatment is its effect on the deformation behaviour of the steel. Fig. 3.16 shows stress-strain curves for a pearlitic and a spheroidised carbide steel of the same grain size, tested at 115°C at a strain rate of 1×10^{-5} sec^{-1}. These curves show that in a static stress-corrosion test, an applied load which would give a stress approaching the U.T.S. in the spheroidised carbide steel would only just exceed the yield stress in the pearlitic steel. It is also clear, from Fig. 3.16, that the plastic deformation necessary for crack propagation can occur more easily in the spheroidised carbide steel than in a pearlitic steel at the same stress or strain.

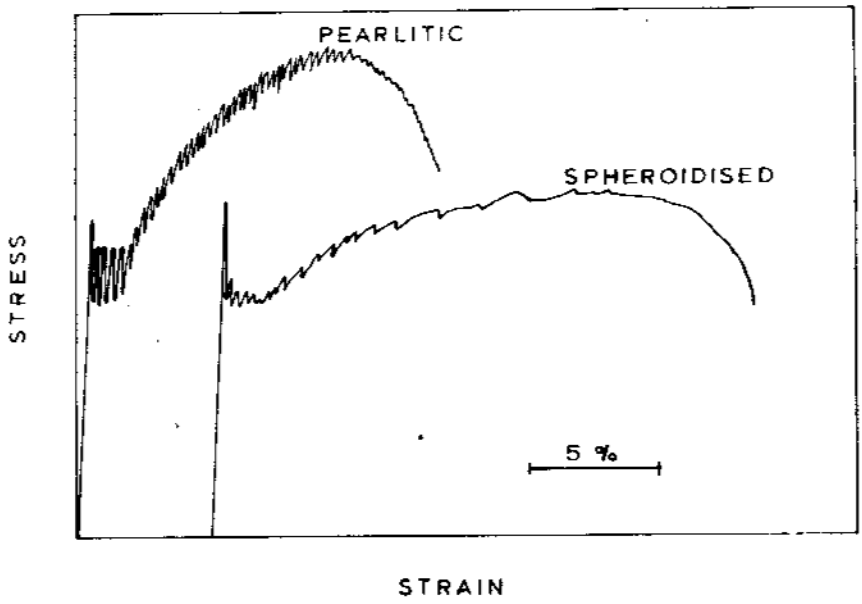

Fig. 3.16 Stress/strain curves for 0.30 C steel in the annealed (pearlitic) and subcritically annealed (spheroidised carbide) conditions.

The sub-critical annealing treatment may also affect stress-corrosion susceptibility by altering the electrochemical nature of the grain boundaries, either by increasing the interstitial segregation at grain boundaries or by the carbide particle effect proposed by Parkins (5). The fact that 0.30 C pearlitic steels have been found to fail by stress-corrosion cracking in this investigation does not in itself condemn the carbide particle mechanism because the thin film studies showed most pearlite colonies to be surrounded by an almost continuous string of carbide particles as shown in Fig. 3.17.

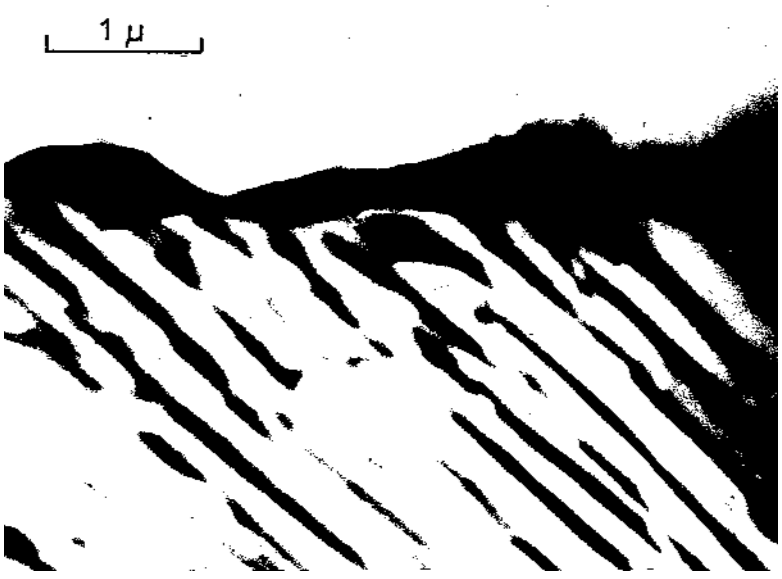

Fig. 3.17 Carbide particles bordering a pearlite colony. Thin film.

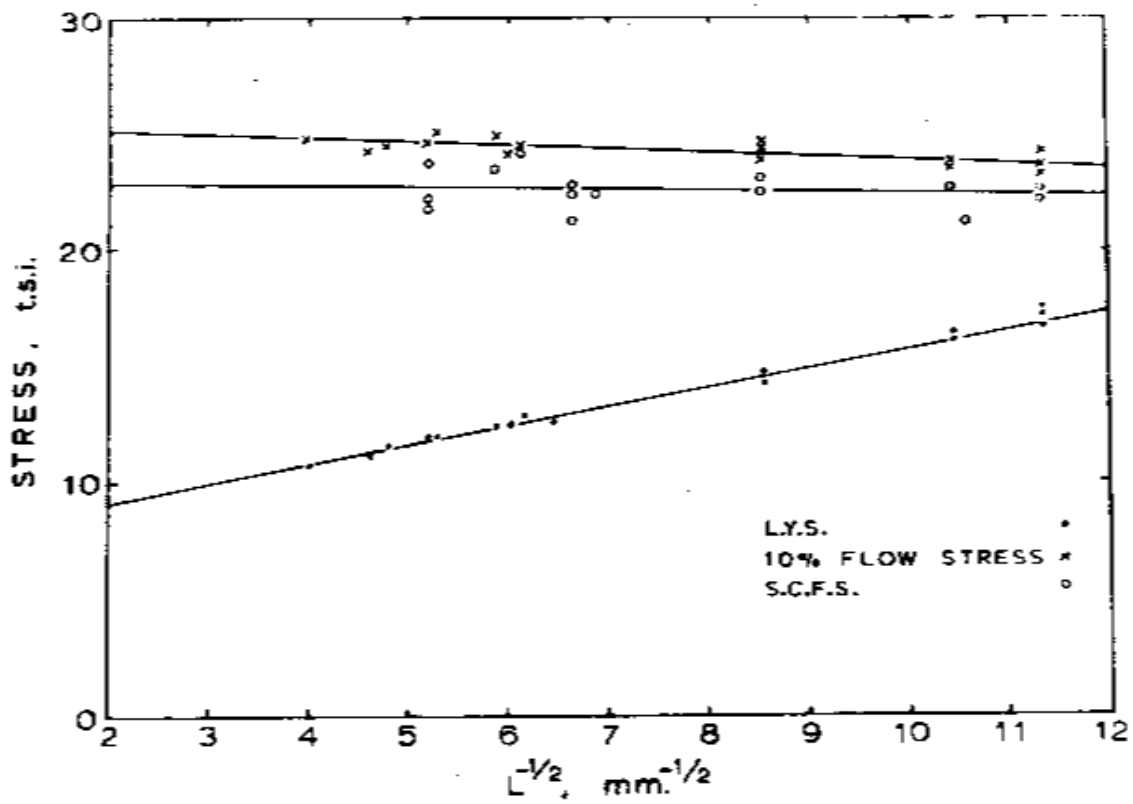

Fig. 3.18 The influence of grain size on the tensile properties of 0.30C spheroidised carbide steel.

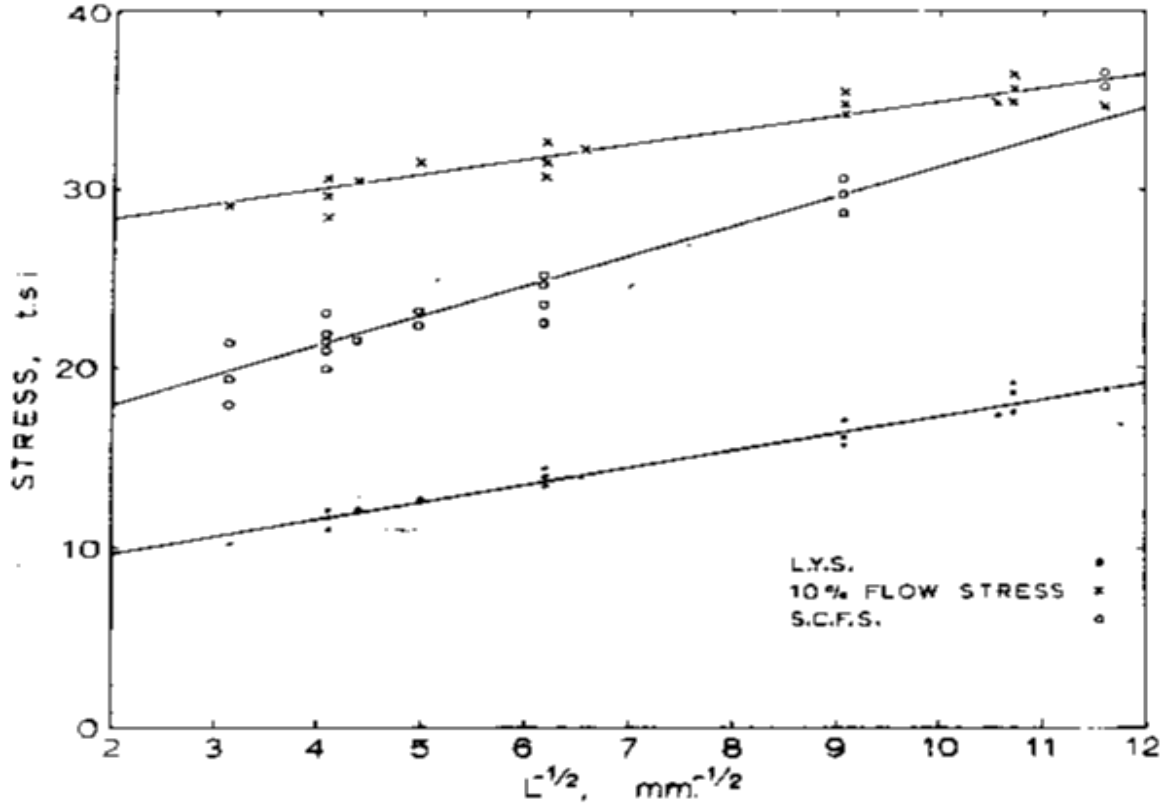

Fig. 3.19 The influence of grain size on the tensile properties of 0.30 C pearlitic steel.

Since a marked grain size effect had been observed in the stress-corrosion cracking of the 0.08 C steel (Section 3.1.1) it was decided that in order to satisfactorily compare the pearlitic and spheroidised carbide steels they should be compared over a range of grain size. Continuous stress-corrosion tensile tests at a strain rate of 1×10^{-5} sec^{-1} were used and tensile tests in oil at 115°C enabled stress-corrosion fracture stress to be compared with yield stress and flow stress, as shown in Figs. 3.18 and 3.19. The 0.30 C spheroidised carbide steel behaves similarly to the 0.08 C steel (see Fig. 3.2) in that its stress-corrosion fracture stress varies with grain size in the same manner as flow stress. The pearlitic steel appears to differ in this respect but this is thought to be due to the fact that the flow stress measurement is an average of the properties of ferrite and pearlite, whereas the formation of a stress-corrosion crack is dependent upon material in the vicinity of an incipient crack. In large grained material the pearlite is present in large colonies and it is possible for a crack to form in a ferrite area, without the restriction to deformation of the pearlite having as much influence as it has in the flow stress measurement.

It was concluded that pearlitic steels will fail by stress-corrosion cracking but in most commercial cases where the grain size is smaller than $l^{-1/2} = 8$ $mm^{-1/2}$, the spheroidised steel is much more susceptible. The difference in susceptibility between the two steels is thought to be mainly due to the greater work hardening capacity of the pearlitic steel which restricts the deformation required for stress-corrosion crack propagation.

3.3 The role of stress during a static stress-corrosion test

The behaviour of a material undergoing a static stress-corrosion test has previously been investigated (10, 40, 41)) by measurements of the specimen extension during the test. The behaviour normally obtained is shown in Fig. 3.20. It is usual to associate the period AB with

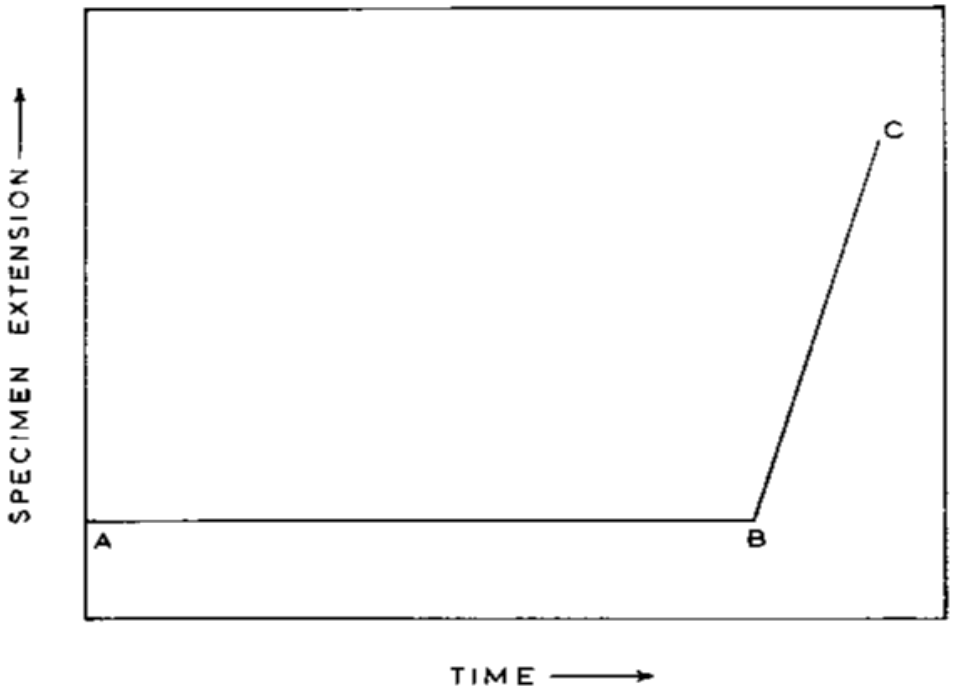

Fig. 3.20 Specimen extension during a static stress-corrosion test. (Schematic)

crack initiation and BC with crack propagation. The present work showed that changes in the applied stress or the corrodent strength have a greater influence on the period AB than on BC, as shown in Table 3.2.

TABLE 3.2

Effect of testing variables on initiation and propagation periods in the stress-corrosion cracking of 0.08 C steel

Applied stress t.s.i.	Solution (boiling)	Initiation time (hours)	Propagation time (hours)
18	4N $Ca(NO_3)_2$ + 50g NH_4NO_3 / litre	3 ¾	1 ¾
18	8N $Ca(NO_3)_2$ + 100g NH_4NO_3 /litre	1 $^1/_8$	1 ½
10	8N $Ca(NO_3)_2$ + 100g NH_4NO_3 /litre	6	1

The main aim of the present investigation was to determine:-

(a) Why an initiation period exists,
(b) Whether crack propagation involves continuous electrochemical attack or is assisted by purely mechanical rupture over small distances.

3.3.1 Crack initiation

The initial stages of chemical attack on 0.08 C steel in nitrate solutions were studied with the aid of thin film electron microscopy. The material used had a grain size of $l^{-1/2} = 6.5\ mm^{-1/2}$ and was in either the fully annealed (slow cooled from 1000°C) or 2% deformed condition. Each foil was examined in the electropolished condition before removing from the microscope and immersing in the corrodent. In all the foils examined, the grain boundaries were found to be cathodic to the grains when immersed in boiling nitrate solution. Although the grain boundaries were cathodic to the grains, a region immediately adjacent to the grain boundaries was anodic to both the grain boundaries and the grain interior. It appeared that the intergranular corrosion of mild steel in nitrate solutions was not, strictly speaking, intergranular. Fig. 3.21 shows typical corrosion adjacent to a grain boundary AA in annealed material which had been immersed in boiling nitrate solution for five seconds. In the material which had been deformed 2%, etch pits were observed in addition to attack adjacent to grain boundaries. Typical pits which have penetrated the foil are shown in Fig. 3.22 which also shows the high rate of attack in the region of grain boundary AA. No attempt was made to apply stress to the foils, shown in Figs, 3.21 and 3.22. during their immersion in the nitrate solution. The type of attack shown in Figs. 3.21 and 3,22 was also observed in foils immersed in nitrate solution at room temperature, but the extent of the attack (for a given period of immersion) was less than in a boiling solution.

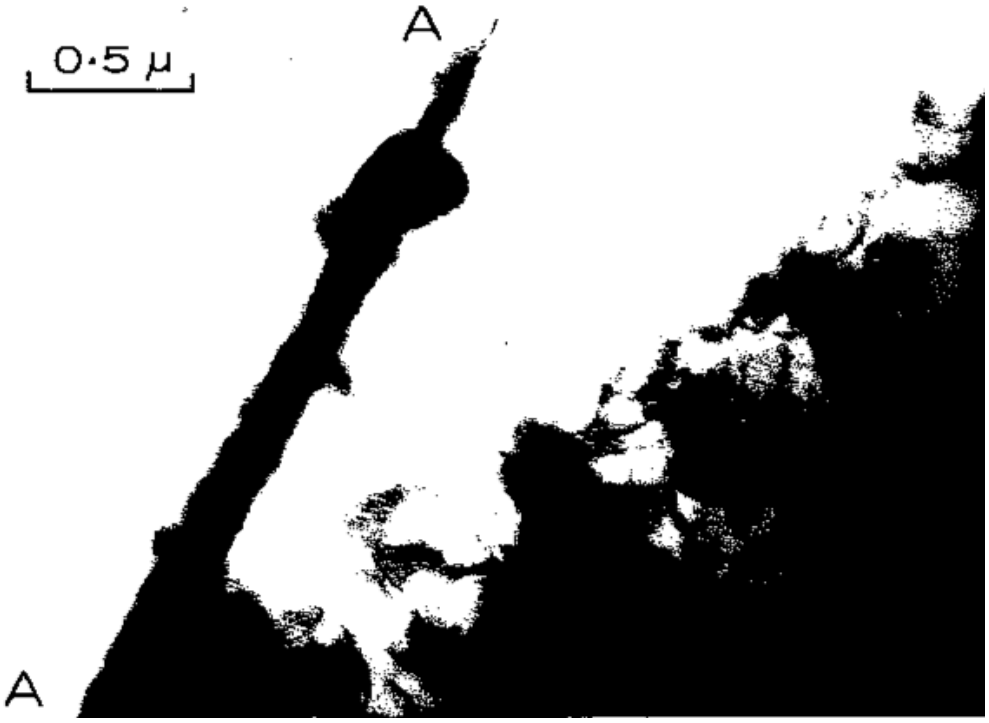

Fig. 3.21 Preferential attack adjacent to a grain boundary in annealed 0.08 C steel after immersion in boiling nitrate solution. Thin film.

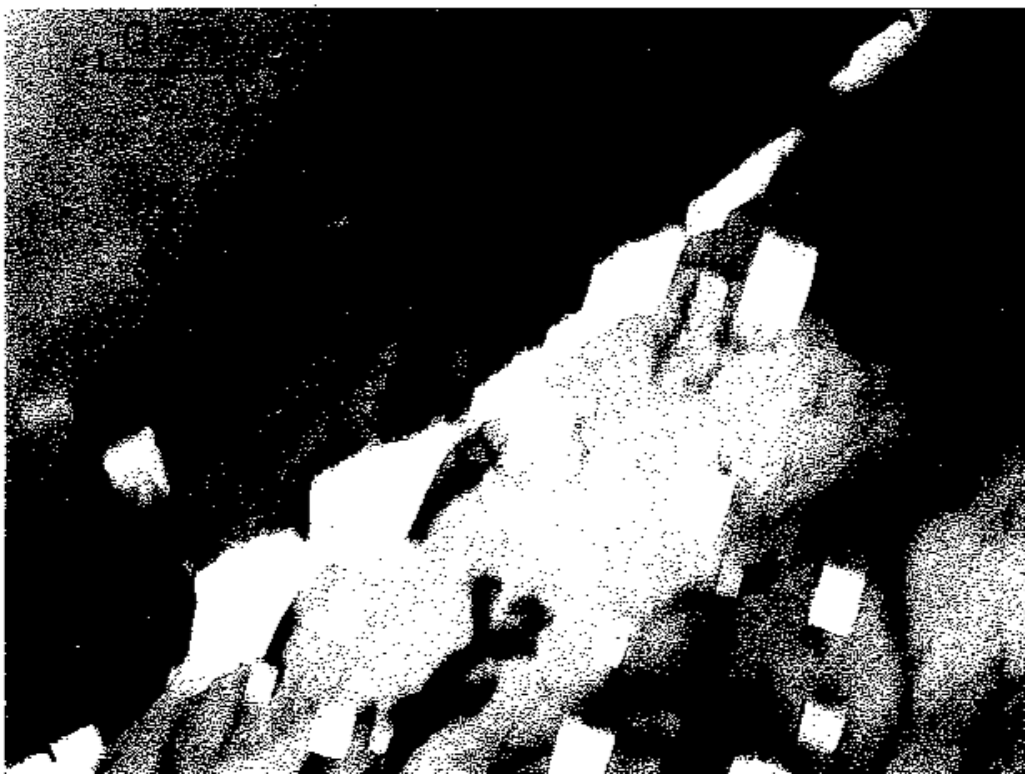

Fig. 3.22 Dislocation etch-pits in 0.08C steel deformed 2% and immersed in boiling nitrate solution. Thin film. Same scale as Fig. 3.21.

During the series of experiments involving the immersion of thin foils in boiling nitrate solutions, two observations were made which are relevant to previous stress-corrosion hypotheses. The main objection to the oxide film rupture theory proposed by Logan (6, 19) is that it does not explain why cracking is intergranular. This objection was substantiated by the present work. Thin foils immersed in boiling ammonium nitrate solution for 15 seconds, were found to be coated with a visible oxide film. Foils coated with this film were deformed (by bending) and examined in the electron microscope. Fig. 3.23 shows typical cracks in the oxide film. There is no tendency for preferential cracking at the boundary AA, even where it might be expected at B. The other observation of relevance to a cracking mechanism previously proposed (5), concerns preferential attack on the ferrite near grain boundary carbide particles. One of the objections to a cracking mechanism involving preferential attack in the region of grain boundary carbides is that each particle would have to distort a grain boundary over large distances to account for the fact that cracking is 100% intergranular. Fig. 3.24 shows preferential attack adjacent to a 0.30 C spheroidised carbide steel which had been deformed 5% before immersion in boiling nitrate solution.

Fig. 3.23 Cracks in oxide film. Thin film.
Dark areas – oxide film. Bright areas – underlying metal

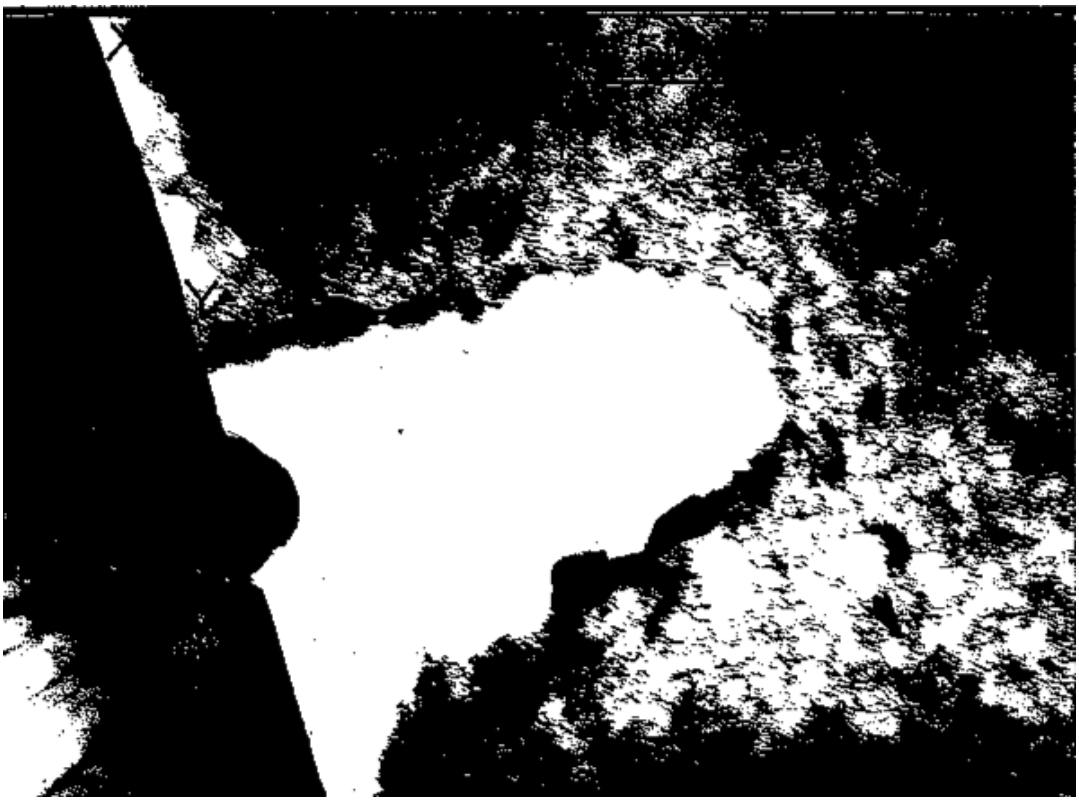

Fig. 3.24 Preferential attack at a grain boundary carbide particle. Thin film. Same scale as Fig. 3.21

There were no other carbide particles in the areas immediately adjacent to the area shown in Fig. 3.24. There is no doubt that preferential attack has occurred in the region of the carbide particle but the attack is local and does not appear to be related to the penetration XY adjacent to the grain boundary.

Since grain boundary attack had been found to occur readily even in the absence of applied stress it was necessary to explain why initiation periods are normally several hours and are often several days. This problem was investigated with the aid of constant strain tests in a hard beam tensometer fitted with a Langham-Thompson load cell. Material of grain size $l^{-1/2}$ = 4.0 $mm^{-1/2}$ was used throughout the investigation. The 8N $Ca(NO_3)_2$ solution was made more potent by the addition of 100g. NH_4NO_3 per litre. Static test conditions were chosen to give an initiation period in the order of 6 hours. An initial applied stress of 11.5 t.s.i. on material which had been prestressed to 22 t.s.i. was found (from five duplicate tests) to give an initiation period of 5 ½ hours $\pm$ ¾ hour. The change in applied load (directly related to specimen extension) during the static stress-corrosion test is shown in Fig. 3.25. It has recently (3, 7) been suggested that the initiation period, for the stress-corrosion cracking of stainless steel in chloride solutions, is the time required for a certain degree of strain-ageing to occur. The possibility that strain- ageing was the cause of the initiation period for the stress-corrosion of mild steel was investigated as follows. The static stress-corrosion tests which had been found to have an initiation period of 5 ½ hours were repeated but the specimens were stressed in air at 115°C, for periods of up to 24 hours prior to adding to the boiling nitrate solution. The addition of the

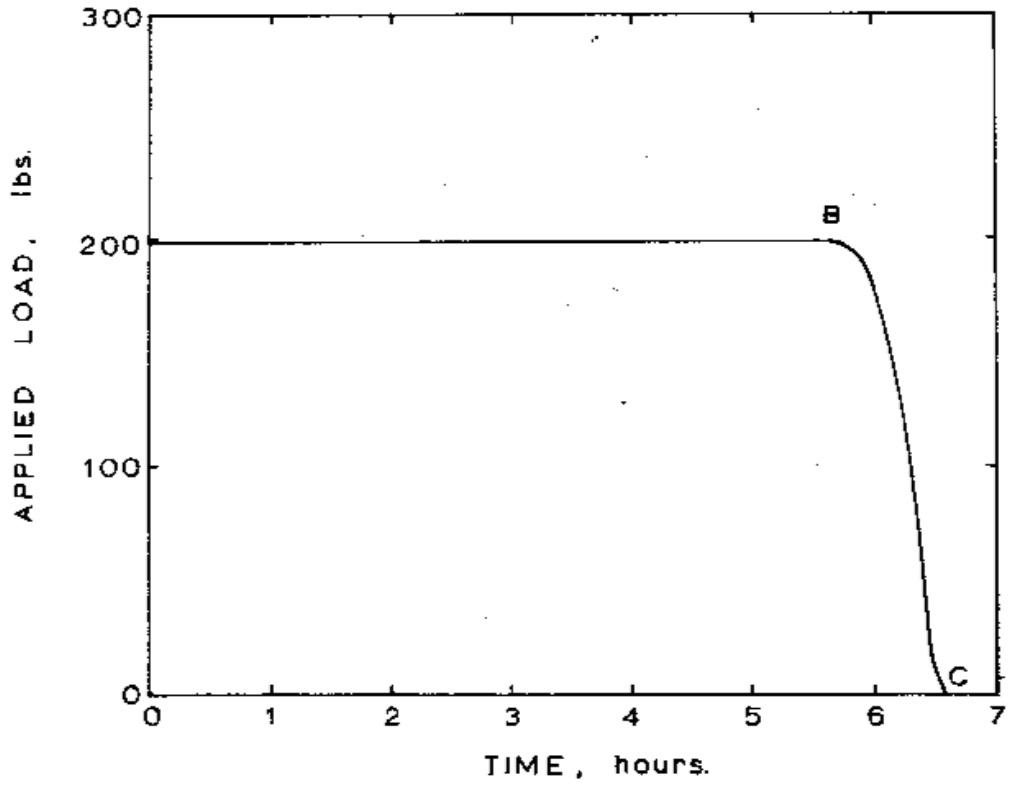

Fig. 3.25 Change in applied load during a constant strain stress-corrosion test. Note: The relaxation of load during the stage BC is not actually continuous – see Section 3.2.2.

nitrate solution caused a slight temperature change which resulted in extension of the specimen and slight relaxation of the applied load. It was therefore necessary, immediately after adding the solution to adjust the strain on the specimen so as to keep the load constant. The crack initiation period after adding the solution was measured. The initiation periods after several ageing treatments are shown in Table 3.3.

TABLE 3.3

Time at stress and temperature before adding corrodent. (hours)	Crack initiation period after addition of corrodent. (hours)
0	5 ½
1	6 ¼
3	6
6	5 ½
12	6
24	6 ¼

It was concluded that the initiation period was not a period required to give a certain degree of ageing and that the corrodent played an active part during crack initiation.

The fact that surface attack occurred within several seconds of immersion in nitrate solution tended to detract from the oxide film removal theories which have been suggested as a cause of the initiation period in other stress-corrosion systems. It seemed more likely that the initiation period involved a change in the corrodent such as a concentration effect in grain boundary fissures formed during the initial surface attack. The stress dependence of the initiation period (see Table 3.2) did not, however, support this possibility. It was then realized that the criterion (i.e. specimen extension) being used to determine the initiation period might not be valid. If cracks could form without opening up and causing specimen extension, then stress-corrosion cracking could be taking place during the so called initiation period. This possibility was investigated by unloading and removing specimens from the test before the completion of this period. After removal from the test the specimens were pulled to fracture in order to open up any stress-corrosion cracks. Specimens removed from the stress-corrosion test, just prior to the completion of the so called initiation period, were found to contain cracks covering areas of about 50% of the specimen cross-sectional area, as shown in Fig. 3.26 (a). The cracked area is represented diagrammatically in Fig. 3.26 (b).

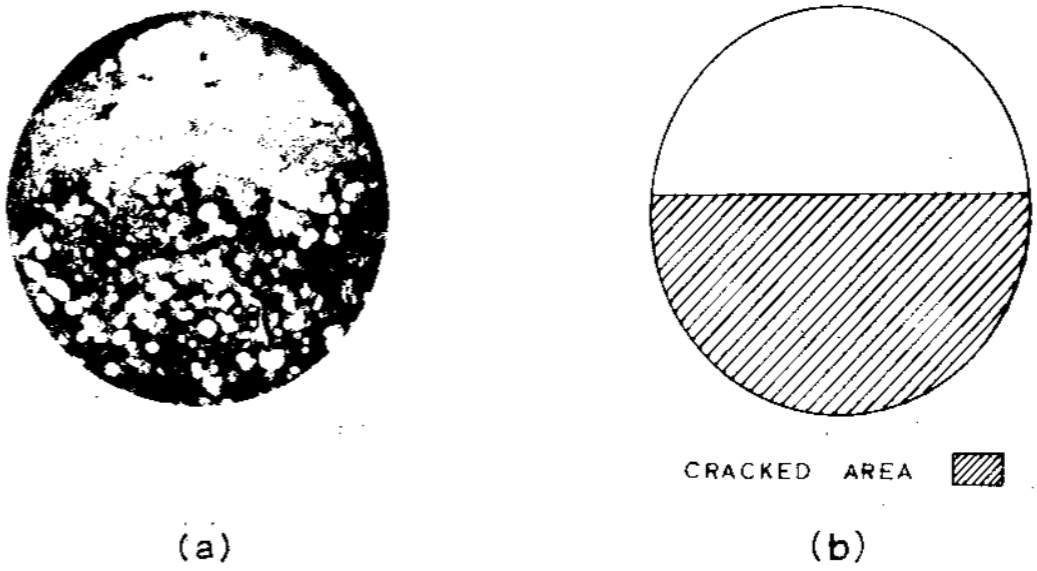

Fig. 3.26 Stress-corrosion crack formed during the open crack initiation period.

The initiation period measured in the constant strain test was clearly an open crack initiation period. The fact that penetration to the extent of 50% of the specimen cross-sectional area could occur without specimen extension and the formation of an open crack was attributed to the fact that the specimens had been pre-strained to a stress of 22 t.s.i., whereas the applied stress during the test was only 11.5 t.s.i. In order to form an open crack it is necessary to plastically deform the material beyond the crack which in this case would require a stress of 22 t.s.i. (actually a higher stress would be required because of strain ageing during the test). In order to obtain a stress of 22 t.s.i. with an applied stress of 11.5 t.s.i. the cross-sectional area must be reduced by approximately 50%. The stress-corrosion crack shown in Fig. 3.26 was clearly the largest crack in the specimen since fracture occurred opposite that crack when the

specimen was pulled to tension after removal from the test. In order to investigate any smaller cracks, longitudinal sections were prepared from specimens which had been removed from the stress-corrosion teat and pulled to their U.T.S. in air. Typical sections of specimens removed from the stress-corrosion test after periods of ½, 1, 3 and 5 hours are shown in Fig. 3.27. It appeared that intergranular penetration occurred continuously throughout the open crack initiation period. During the first ½ hour of the stress-corrosion test most grain boundaries were penetrated. This penetration did not generally exceed two grain diameters during the entire test but at a few (often only one and normally not more than three) points in each specimen, the penetration continued until a depth of about 1.2 mm. was reached and an open crack formed as a result of plastic deformation in the material beyond the crack. In order to measure the rate of penetration during the open crack initiation period, specimens were removed from the test after ¼, ½, 1, 2, 4, 5 and 5 ½ hours. Specimens were also removed at times of ¼, ½ and 1 hour after open crack formation.

Three specimens were obtained for each time. After their removal from the test the specimens were pulled to their U.T.S. in air, mounted longitudinally in bakelite and ground on a linishing machine. At grinding intervals of 0.005", the depth of the deepest crack was measured on a projection microscope. The shape of a typical crack, shown in Fig. 3.28 is such that the removal of 0.005" of material in between measurements allows a good assessment of maximum penetration to be made.

The relationship between the maximum depth of penetration and the time after which the specimen was removed from the stress-corrosion test is shown in Fig. 3.29. It was found that a crack did not have to move a distance equal to the specimen diameter to cause complete failure because once an open crack had formed penetration advanced from all points on the specimen perimeter. The cracked area during open crack propagation may be represented by the shaded area in Fig, 3.30.

The fact that significant penetration only occurred on one front (See Fig 3.26) during the open crack initiation period was attributed to the probability that elastic strain in the uncracked material ahead of a crack would not be uniform across the specimen. The band of material undergoing tensile elastic strain in excess of that in the surrounding material would be of the general shape shown in Fig. 3.31.

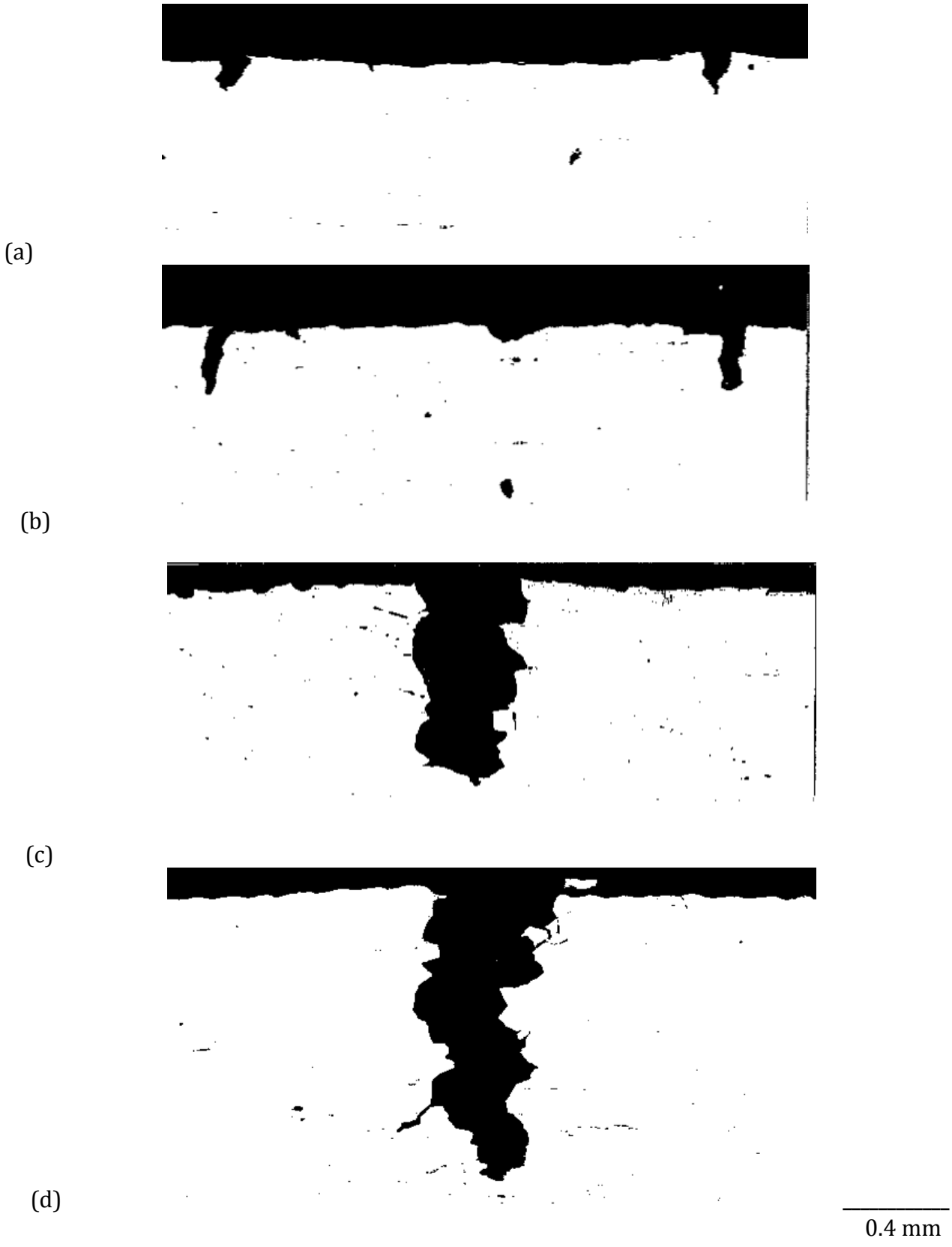

Fig. 3.27 Stress-corrosion cracks formed during the open crack initiation period, (a) ½ hour, (b) 1 hour (c) 3 hours (d) 5 hours. The cracks have been opened up by pulling the specimen in tension after removal from the stress-corrosion test.

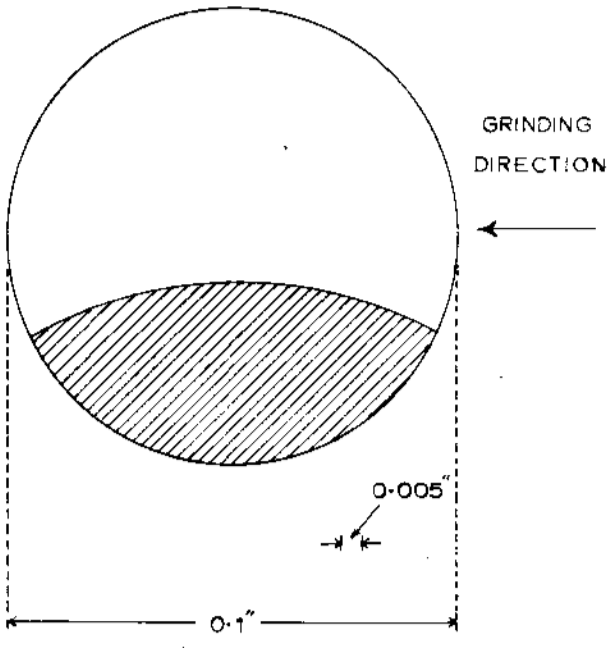

Fig. 3.28 To show that the maximum depth of penetration is approximately uniform for distances of 0.005" along the penetration front.

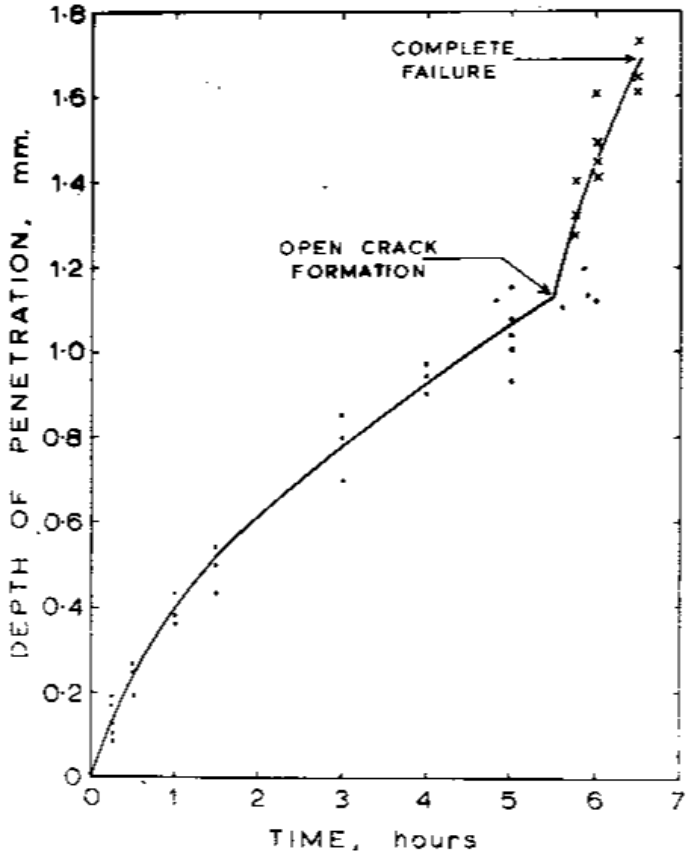

Fig. 3.29 Maximum crack depth during a constant strain stress-corrosion test.

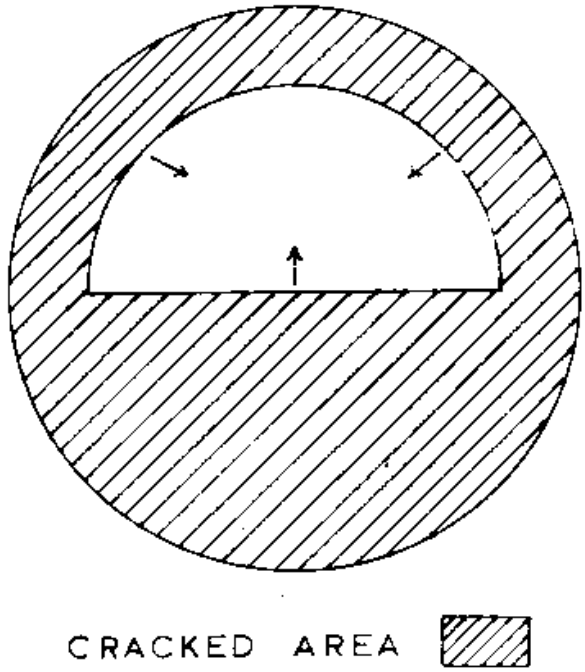

Fig. 3.30 Stress-corrosion crack propagation of an open crack.

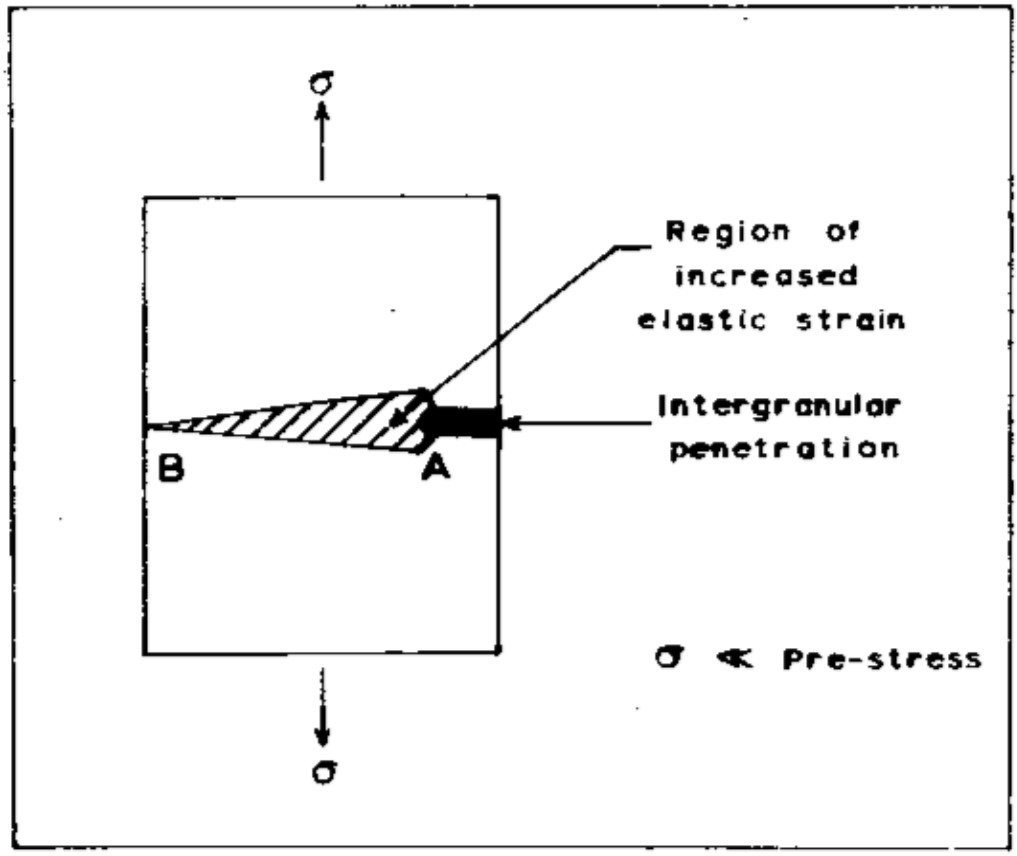

Fig. 3.31 Distribution of tensile elastic strain in material ahead of a stress-corrosion crack.

In effect the specimen is slightly bent opposite the penetration and the tendency to open up a deep crack at A is greater than the tendency to open up a shorter crack at B. When an open crack is formed, by the plastic deformation of the material between A and B, then cracks at both A and B are opened up.

It is proposed that the so called initiation period is a period during which intergranular penetration occurs until it has reduced the effective cross-sectional area of the specimen to such an extent that the resultant stress increase on the material beyond the penetration is sufficient to cause this material to plastically deform. Fig. 3.32 (a) shows the test history of the stress-corrosion test described in this section and Fig. 3.32 (b) shows the change in stress on the uncracked area as a result of continuous penetration during the test. The elastic strain associated with the increase in stress from P to Q (Fig. 3.32) microscopically opens up the crack during the open crack initiation stage and allows fresh corrodent to reach the penetration front. If this interpretation of the open crack initiation period is correct then initiation periods should increase with increasing prestrain and it should be possible, with a knowledge of the rate of propagation of unopened cracks, to calculate the initiation period for any given prestress. It was therefore decided to calculate the effect of prestrain on crack initiation periods and to compare the results with experimental data.

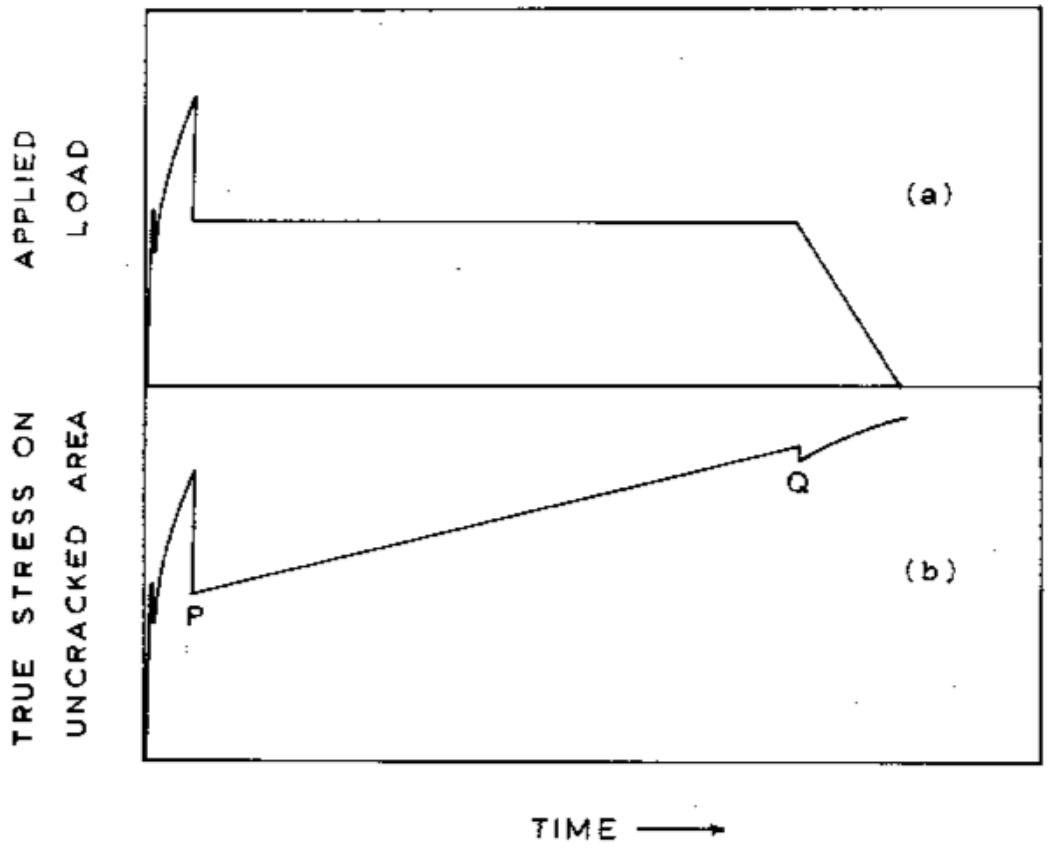

Fig. 3.32 Interpretation of the open crack initiation period.

An equation for the initiation period in a stress-corrosion test on pre-strained material was derived as follows:-

Let the cross sectional area of the specimen = A
Let the applied load during the stress-corrosion test = L
Let the pre-stress (this is a true stress) = σ_p
Let the area of an unopened crack at any instant = a

Any stress concentration at the tip of an unopened crack is ignored in this calculation because it would only cause local effects at the crack tip and would not influence the deformation behaviour of the bulk of the material beyond the crack.

The stress (σ_u) on the uncracked material ahead of an unopened crack is given by

$$\sigma_u = \frac{L}{A-a} \qquad \ldots\ldots\ldots\ldots\ldots\ldots\ldots\ldots \quad (1)$$

The initiation period is complete when

$$\sigma_u = \sigma_p + \sigma_a \qquad \ldots\ldots\ldots\ldots\ldots\ldots\ldots\ldots \quad (2)$$

where σ_a is the additional stress required to overcome the effects of strain-ageing during the test.
Combining (1) and (2), the initiation period is complete when

$$A - a = L / (\sigma_p + \sigma_a) \quad \ldots\ldots\ldots\ldots\ldots\ldots\ldots \quad (3)$$

Now the uncracked area, (A-a) at any instant is dependent upon the shape of the unopened crack and its rate of penetration. The shape of an unopened crack was found to change as the depth of penetration increased. During the early stages of penetration, the cracked area was, to a good approximation, equal to the segment of a circle with the initial point of attack at the centre of the circle as shown in Fig. 3.33 (a). Fig. 3.33 (b) shows an actual crack. As the penetration proceeds, the crack moves forward on a wider front and as the centre of the specimen is approached, the crack may be approximated to the shape shown in Fig. 3.34 (a). Fig. 3.34 (b) shows an actual crack. For a crack of the shape shown in Fig. 3.33 (a), the uncracked area, A-a, is given by

$$A\text{-}a \approx \pi r^2 - \pi d^2/2 + 2dr - d(r^2 - d^2)^{1/2} - r^2 \sin^{-1}(d/r) \quad \ldots\ldots \quad (4)$$

where r is the specimen radius and d is the maximum depth of penetration. The approximation is valid when d<r. Equation (4) may be further approximated to

$$A\text{-}a \approx \pi r^2 - \pi d^2/2 \quad \ldots\ldots\ldots\ldots\ldots\ldots\ldots \quad (5)$$

This approximation is valid when $d \to 0$. For a crack of the shape shown in Fig. 3.34 (a), the uncracked area is given by

$$A - a = \pi r^2/2 + (r - d)\,(2rd - d^2)^{1/2} + r^2 \sin^{-1}((r-d)/r) \quad \ldots\ldots\ (6)$$

The solution to equations (4), (5) and (6) are shown in Fig. 3.35.

The solution to the approximation given in equation (5) follows the more accurate solution for cracks of the shape shown in Fig. 3.35 during the early stages of penetration, and tends to move towards the solution for cracks of the shape shown in Fig. 3.34 as the depth of penetration increases. Since this is also the way in which the crack shape changes, equation (5) is a good assessment of the uncracked area for values of $d \leq r$. For values of $d > r$, the cracked area is given by the equation (6) which can be simplified to

$$A - a = 3.5r^2 - 2rd \quad \ldots\ldots\ (7)$$

when $0.3r < d < 1.7r$.

Hence when $d \leq r$, (3) and (5) give:-

$$d_c = (2r^2 - 2L/(\pi(\sigma_p + \sigma_a))\,)^{1/2} \quad \ldots\ldots\ (8)$$

where d_c is the depth of penetration required before an open crack can be formed.

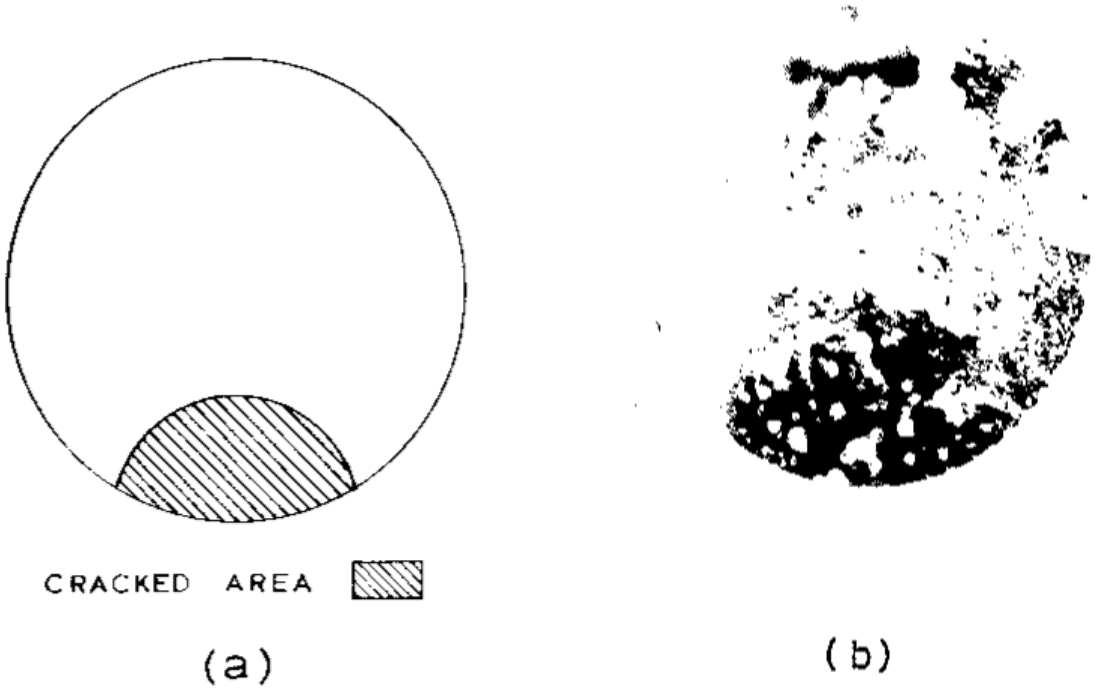

Fig. 3.33 (a) Estimated shape of stress-corrosion crack during the early stages of penetration. (b) Actual crack.

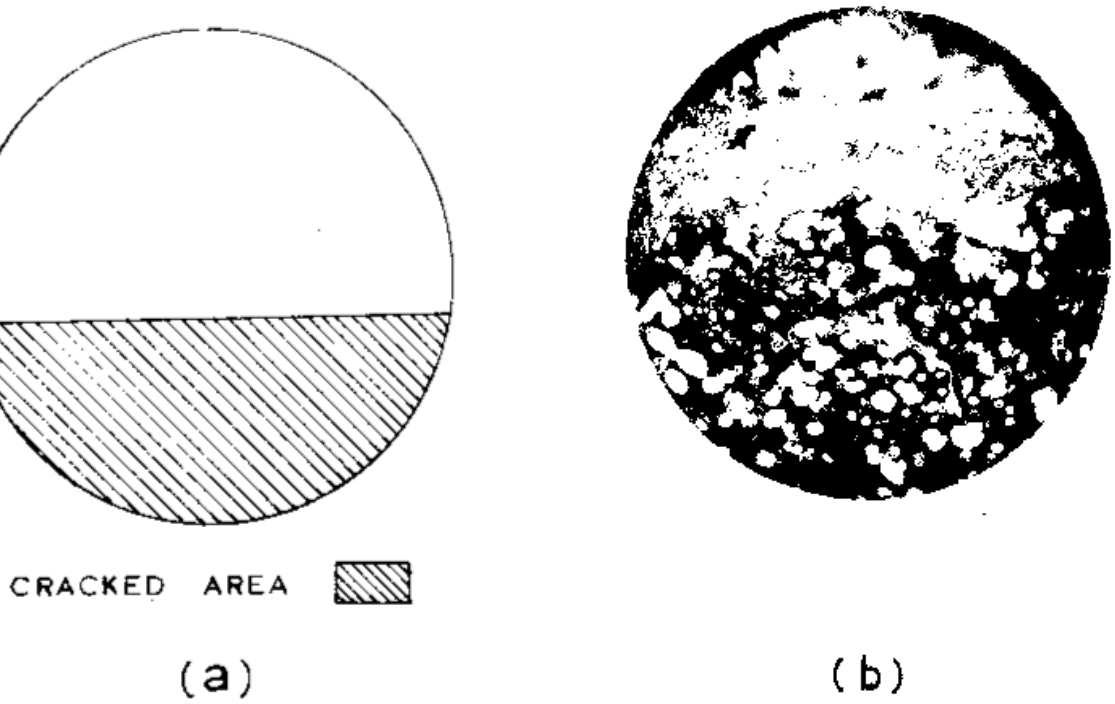

Fig. 3.34 (a) Estimated crack shape – advanced stage of penetration. (b) Actual crack.

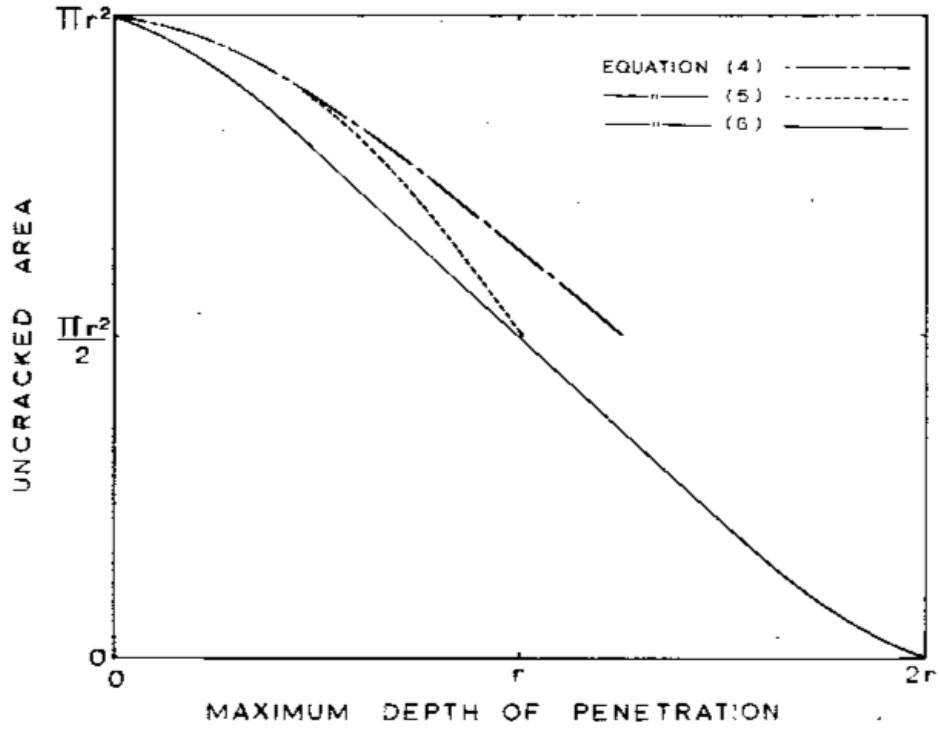

Fig. 3.35 Variation of uncracked area with crack depth for different crack shapes.

When $r < d < 1.7r$, (3) and (7) give

$$d_c = 1.8r - L/(2r(\sigma_p + \sigma_a)) \quad \ldots\ldots\ldots\ldots\ldots\ldots \quad (9)$$

The variation of penetration depth (d) with time (t) may be obtained from the experimental curve shown in Fig. 3.29. A plot of log (d) versus log (t), Fig. 3.36, shows that the variation of crack depth with time, during the open crack initiation stage obeys the relationship

$$d = 0.38\, t^{0.63} \quad \ldots\ldots\ldots\ldots\ldots\ldots\ldots\ldots \quad (10$$

where d is in mm. and t in hours.

From equation (10)

$$t = (d/0.38)^{1.6} \quad \ldots\ldots\ldots\ldots\ldots\ldots \quad (11)$$

Combining equations (8) and (9) with (11), when $d_c < r$, the initiation period t_c is given by

$$t_c = 8.2\,(r^2 - L/\pi(\sigma_p + \sigma_a))^{0.8} \quad \ldots\ldots\ldots\ldots\ldots \quad (12)$$

and when $r < d_c < 1.7r$

$$t_c + 4.7\,(1.8r - L/2r(\sigma_p + \sigma_a))^{1.6} \quad \ldots\ldots\ldots\ldots\ldots \quad (13)$$

In equations (12) and (13), t_c is in hours, r in mm. and σ_p and σ_a are in (mass units) mm $^{-2}$.
In the present work, σ_a was estimated to be the difference between the upper and lower yield stress.

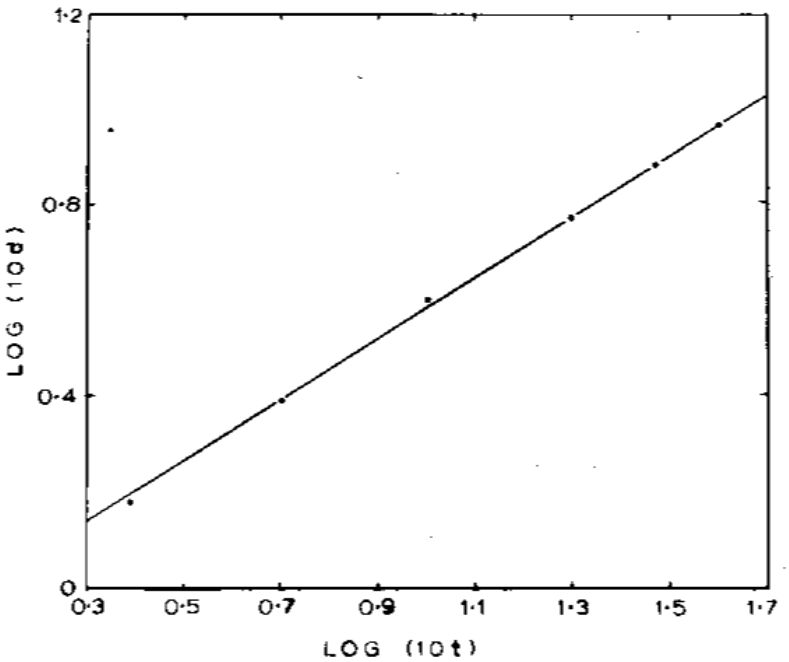

Fig. 3.36 Variation of crack depth (d) with time (t) during the open crack initiation stage.

In the experimental investigation into the effect of prestrain on stress-corrosion cracking, five different prestrains were used and four specimens were tested at each prestrain. The specimens (0.1" diameter) were strained at a rate of 4.8×10^{-4} sec^{-1} and then machined to a diameter of 0.085". The use of specimens of the same diameter meant that the same load could be used in all tests. A preliminary investigation showed that surface machining had no effect on the initiation period for the steel and corrodent used in this investigation. The experimental results and the estimated curve (calculated from equations (12) and (13) for the variation of open crack initiation period are shown in Fig. 3.37. The agreement between the experimental and calculated initiation periods supports the interpretation of the initiation period proposed in this work. The maximum strain used in the experimental study of pre-strain was just less than the U.T.S. strain. The fact that strains greater than the U.T.S. strain further reduce susceptibility to cracking was shown by testing a specimen which had been necked prior to the static stress-corrosion test. The specimen failed by stress-corrosion cracking as shown in Fig. 3.38. Even though the stress at the centre of the neck was twice that in the un-necked region, the stress-corrosion fracture did not occur in the highly deformed neck.

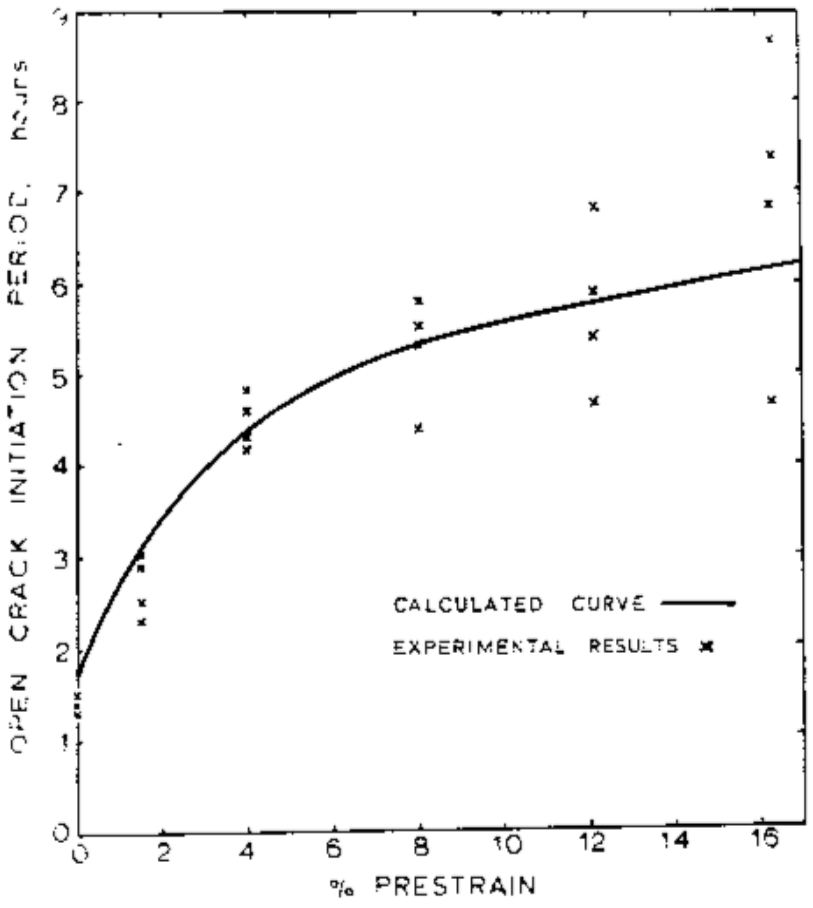

Fig. 3.37 Effect of prestrain on open crack initiation period.

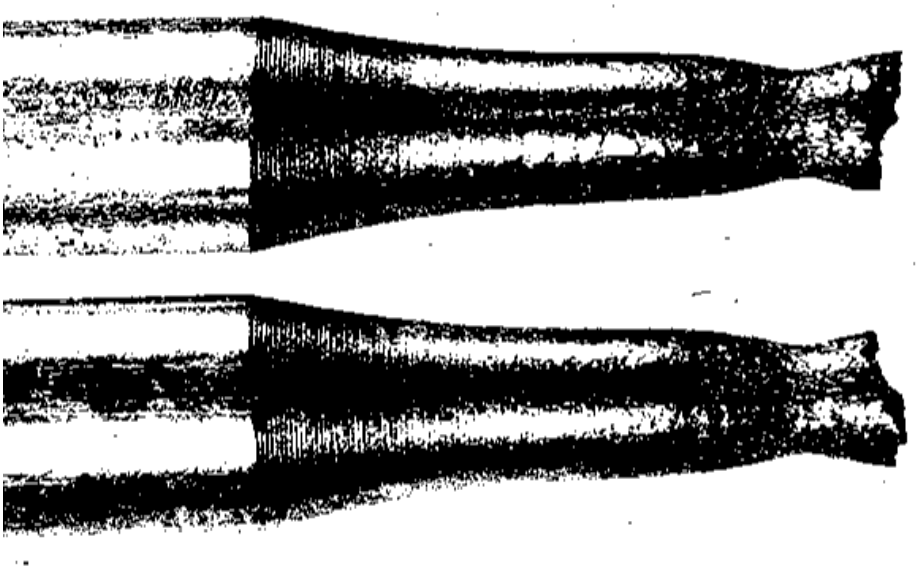

Fig. 3.38 Stress-corrosion fracture in specimen necked prior to the constant strain stress-corrosion test. Specimen photographed on a mirror.

Although plastic deformation did not occur over the entire cross sectional area of a specimen during the open crack initiation period it had not been proven that plastic deformation was not occurring locally at the penetration front. It has frequently been assumed in this and other stress-corrosion systems that plastic deformation is necessary if stress-corrosion cracking is to occur. This assumption is usually based upon the existence of a threshold stress (normally in the region of the yield stress) below which cracking does not occur.

Since the thin film investigation, described earlier in this section, had indicated that intergranular corrosion occurred in the absence of plastic deformation it was decided to investigate the stress corrosion susceptibility of material subjected to applied elastic stresses. The material used was identical to that used previously in this section and had an upper yield stress = 13.2 t.s.i. and a lower yield stress = 10.9 t.s.i. The corrodent used was 8N $Ca(NO_3)_2$ + 500 g NH_4NO_3 / litre. The material was found to fail by stress-corrosion cracking as shown in Table 3.4.

TABLE 3.4
Stress- corrosion cracking with applied elastic stresses.

Applied Stress, t.s.i.	Open crack initiation period, (hours)
8.1	2 ½
5.8	8
2.8	24

Specimens removed from the test before completion of the open crack initiation period were found to contain extensive intergranular penetration. It seemed probable that the stress-corrosion cracking of material subjected to applied elastic stresses was identical to the stress-

corrosion of prestrained material investigated earlier in this section. On this basis the initiation period would be the time required for penetration to decrease the effective cross-sectional area sufficiently for the yield stress to be exceeded in the material beyond the penetration.

The observation that the stress-corrosion cracking readily occurred in specimens stressed to one-fifth of their yield stress, suggested that plastic deformation might not be the dominant factor in the cracking, but it did not prove this since stress concentration at the tip of a corrosion fissure (formed during the open crack initiation period) would be sufficient to cause some local yielding. It is thought however that the following observations show that plastically deformed material is not a prerequisite for the cracking of mild steel in boiling nitrate solutions. Two tensile specimens were immersed in boiling nitrate solution (8N $Ca(NO_3)_2$ + 500 g. NH_4NO_3 per litre) for four hours. Both specimens had been annealed at 1050°C and cooled to room temperature over a period of three days. Prior to immersion in the nitrate solution, one of the specimens was deformed in tension by 15%. After removal from the solution, both specimens were pulled to their U.T.S. before taking longitudinal sections for metallographic examination. Typical sections are shown in Fig. 3.39. Fig. 3.39 (a) shows that intergranular penetration can occur in the absence of applied stress or pre-strain. The fact that the depth of penetration in the deformed material is slightly less than in the fully annealed material is probably due to a greater amount of corrosion on the crack sides in the deformed material than in the annealed material. The greater the amount of corrosion product in the cracks, the more difficult it would be for fresh solution to reach the penetration front. The fact that extensive intergranular penetration can occur in fully annealed material was further demonstrated by anodically polarizing a specimen during its immersion in the nitrate solution. The specimen was maintained at a potential of +400 mV (SCE) for twelve hours with the aid of a potentiostat. The nitrate solution was maintained at 95°C during the immersion. After removal from the solution the specimen was pulled in tension to open up the cracks which are shown in Fig. 3.40.

It was concluded from this study of crack initiation that the only true initiation period was the time taken (only a few seconds) for the removal of any air formed oxide films. The period commonly assumed to be the crack initiation period was in fact the time required to form an open stress-corrosion crack and was actually a stage in the crack propagation. In order that an open crack can form, the material beyond the crack must be plastically deformed and the ease with which this deformation can occur governs the length of the open crack initiation period. The increase in stress that causes this deformation is brought about by the formation of unopened cracks which reduce the cross-sectional area of the specimen while the applied load remains constant. In material which has been prestrained to a stress much higher than the testing stress, the required depth of penetration before an open crack can form, is large and the open crack initiation period is long. In material which has not been pre-stressed beyond the testing stress, the amount of penetration required is small and the initiation period is shorter. It is thought that the open crack initiation stage should be considered as crack propagation rather than initiation since the present work has shown that large (1mm. in depth) cracks can form during this stage when it is difficult to achieve the deformation required for open crack formation (e.g. in highly pre-strained material). If strain-ageing and relaxation of the applied load in the tensile machine could be eliminated then there would, if the present interpretation is correct, be no open crack initiation period. As the latter condition is approached, the depth of penetration required before an open crack can form, may be too small to be detected by metallographic techniques. It is thought that this, has in the past, led to an erroneous distinction between the open crack initiation period and crack propagation.

X 30

(a) Annealed

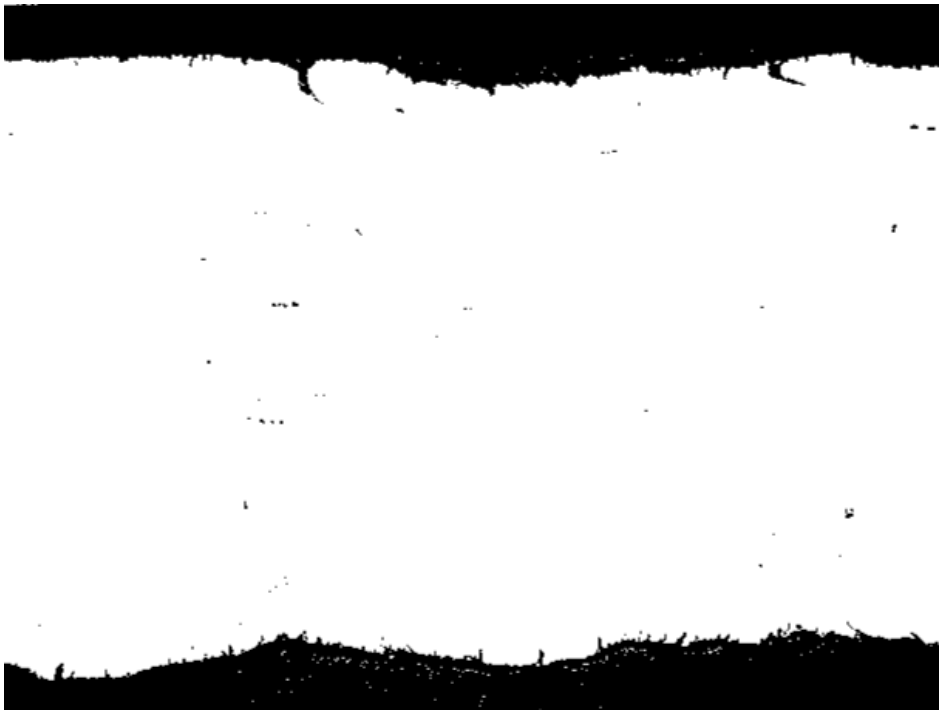

X 30

(b) Prestrained 15%

Fig. 3.39 Intergranular penetration in material immersed in boiling nitrate solution for four hours. Both specimens were pulled in tension after the immersion.penetration

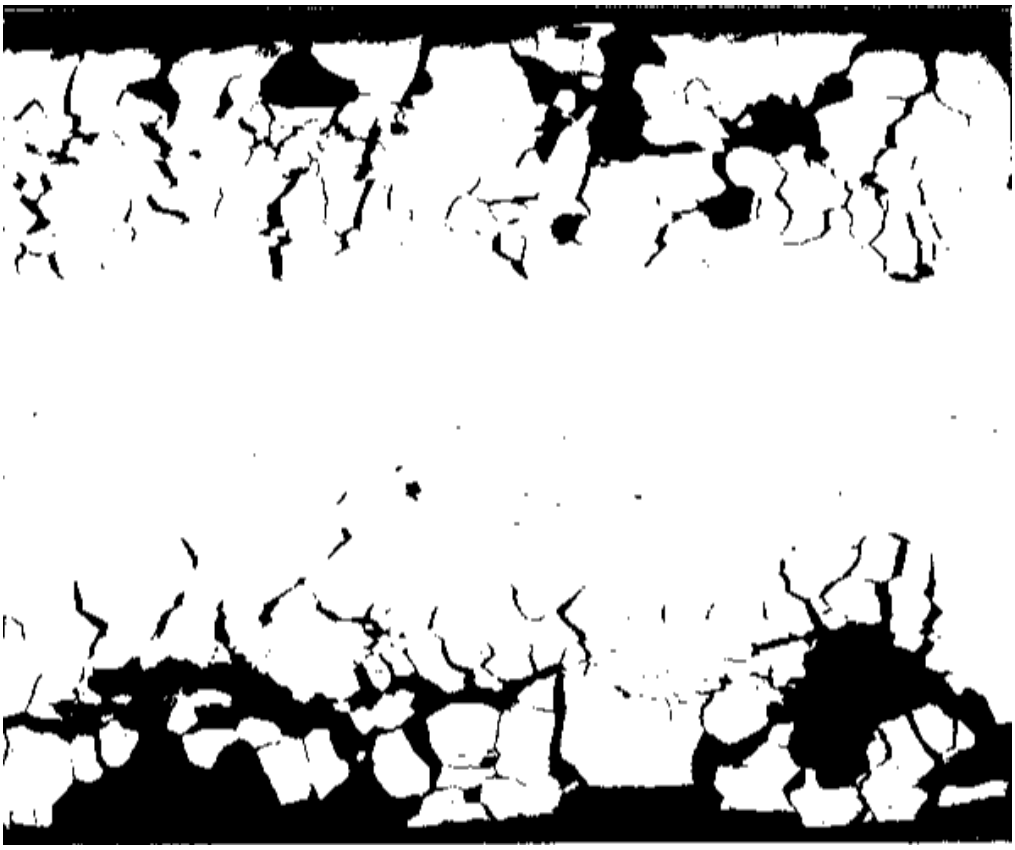

X 35

Fig. 3.40 Intergranular penetration in fully annealed material after anodic polarization in nitrate solution. No stress was applied either before or during the test. After the test the specimen was pulled in tension to open up the cracks.

3.3.2 Crack propagation

The investigation into crack initiation had shown that crack propagation can be divided into two stages. This section deals with the second stage which involves the propagation of open stress-corrosion cracks. The main aim of this part of the work was to investigate the claims of Engell and Baumel (10) and Van Rooyen (11) that cracking is discontinuous. These claims were based upon discontinuous specimen extension and electrode potential during the stress-corrosion test. In view of the lack of experimental details given by these workers (especially Engell and Baumel) it was decided to first confirm, with the aid of constant strain tests in a hardbeam tensometer, that the discontinuities did exist. Material of grain size $l^{-1/2}$ = 4.0 $mm.^{-1/2}$, was used throughout this part of the work. The existence of discontinuities in specimen extension and electrode potential during open crack propagation was confirmed in the present work, although the magnitude of the discontinuities was smaller than that observed by previous workers (10, 11). The latter point is dealt with later in this section. Fig. 3.41 shows a typical load/time trace during a stress-corrosion test. The average time for each step in this trace was four seconds and the average load drop was about 10 lbs. A load drop of 10 lb. represented a specimen extension of about 0.0005". To show that the load drops were an indication of discontinuous extension and were not due to "stick-slip" in the system, a specimen, loaded in oil at 115°C, was unloaded at a continuous rate of 3.8 x 10^{-6} $sec.^{-1}$. Fig. 3.42 shows the

resultant load/time trace to be continuous. Electrode potential deflections were also observed during open crack propagation and the deflections were found to coincide with the load discontinuities shown in Fig. 3.43.

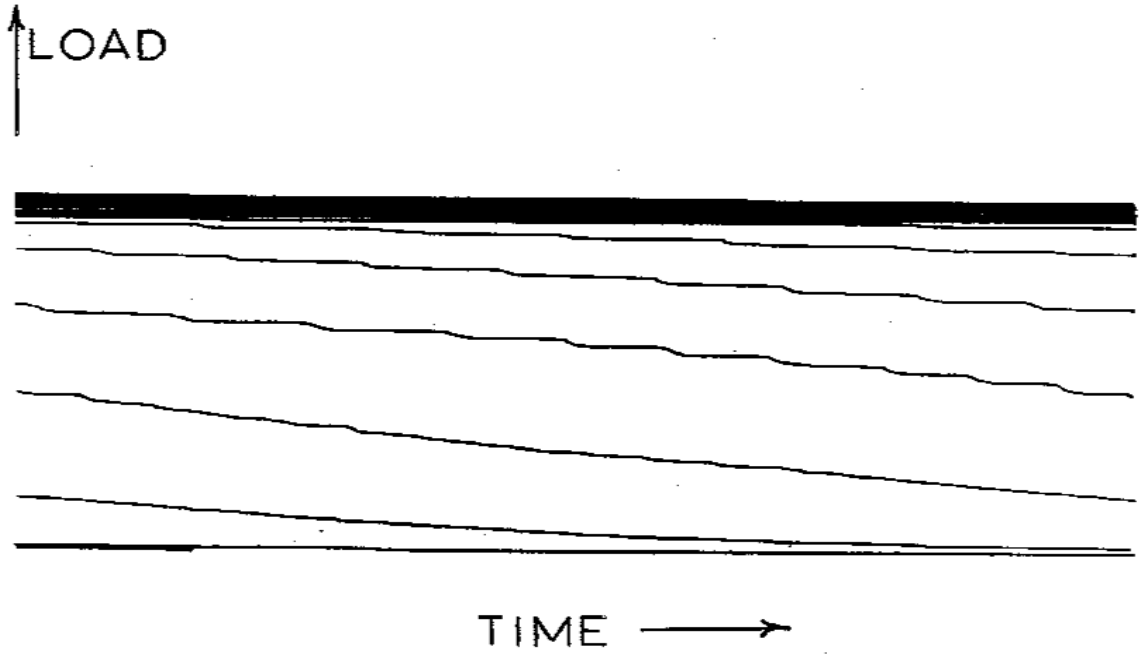

Fig. 3.41 Discontinuous load relaxation (directly proportional to specimen extension) during a stress-corrosion test. Scanning time = 10 minutes.

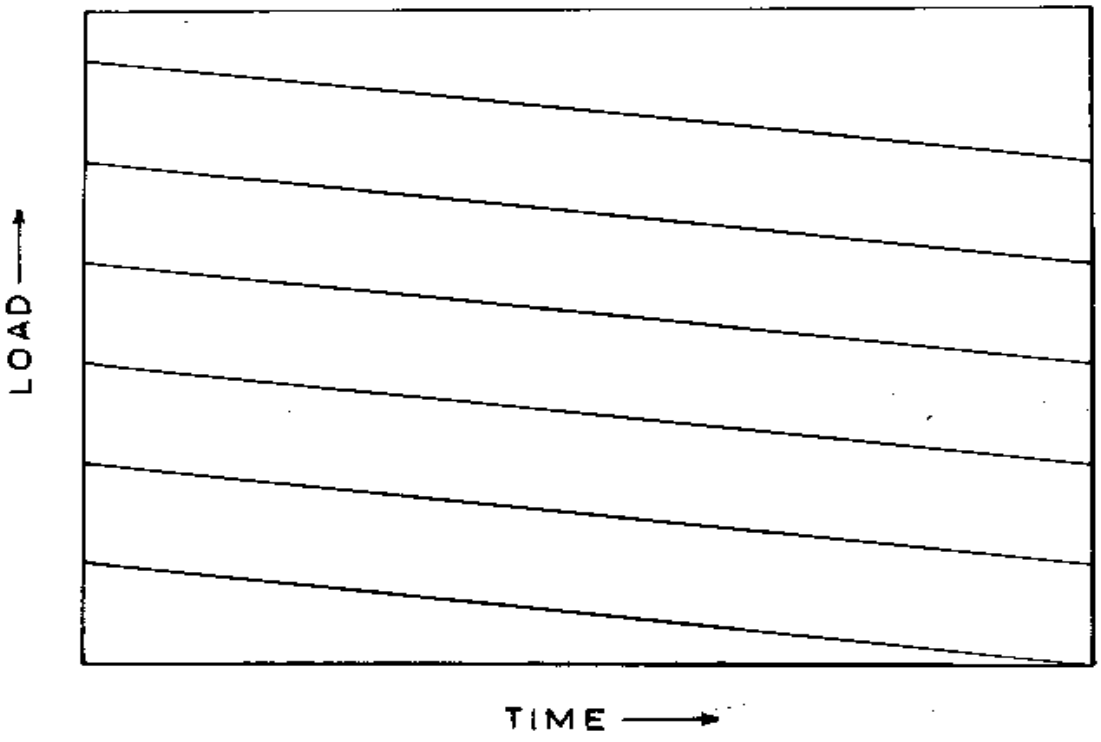

Fig. 3.42 Continuous unloading of specimen in oil at 115°C. Scanning time = 10 mins

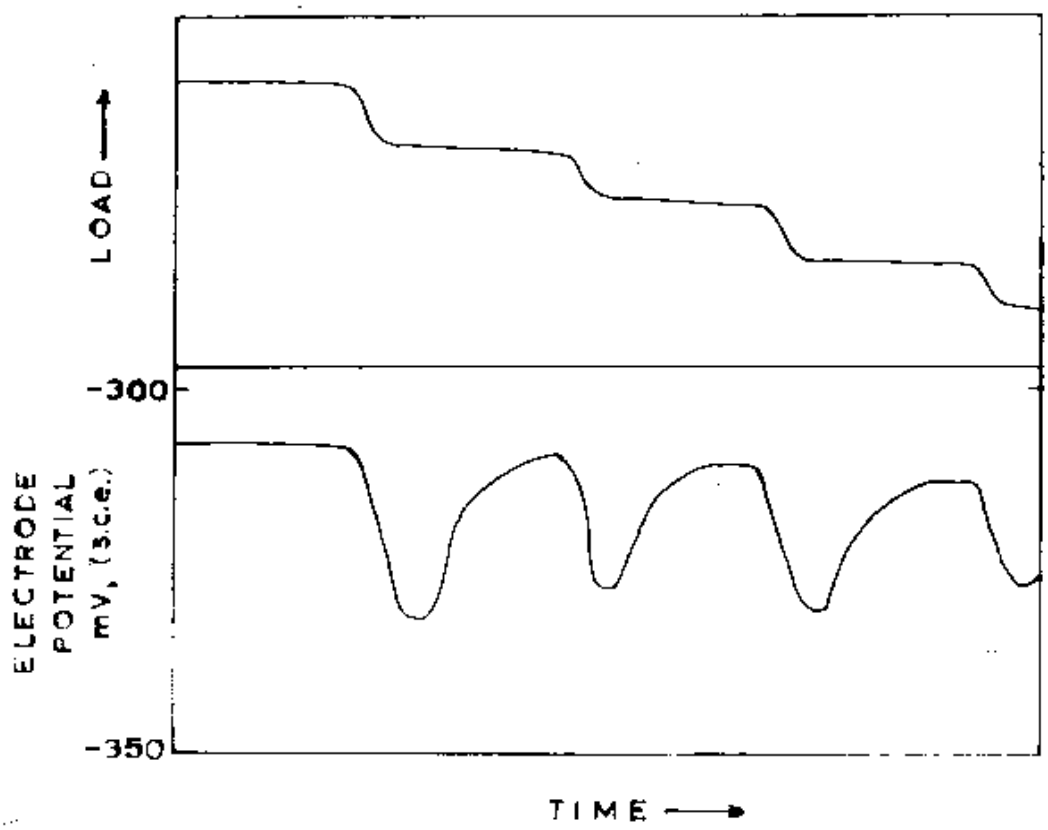

Fig. 3.43 Coincidence of load (proportional to extension) and electrode potential deflections during the open crack propagation stage.

Having verified the existence of discontinuities in specimen extension and electrode potential during crack propagation it was necessary to assess their significance in the cracking mechanism. Previous workers, in this and other stress- corrosion systems have assumed that discontinuous specimen extension is evidence of discontinuous crack propagation as indicated in Fig. 3.44 (a). This assumption is not valid if cracks can penetrate for small distances without opening up, and Fig. 3.44 (b) indicates how continuous crack propagation could produce discontinuous specimen extension. Both mechanisms shown in Fig. 3.44 require plastic deformation of the material beyond a crack if an open crack is to propagate. It is thought that the plastic deformation of the material ahead of a crack accounts for the observed discontinuous extension because at a temperature of 115°C and at the strain rate associated with cracking, the plastic flow is itself discontinuous as shown in Fig. 2.8. This interpretation for discontinuous specimen extension is demonstrated in Fig. 3.45.

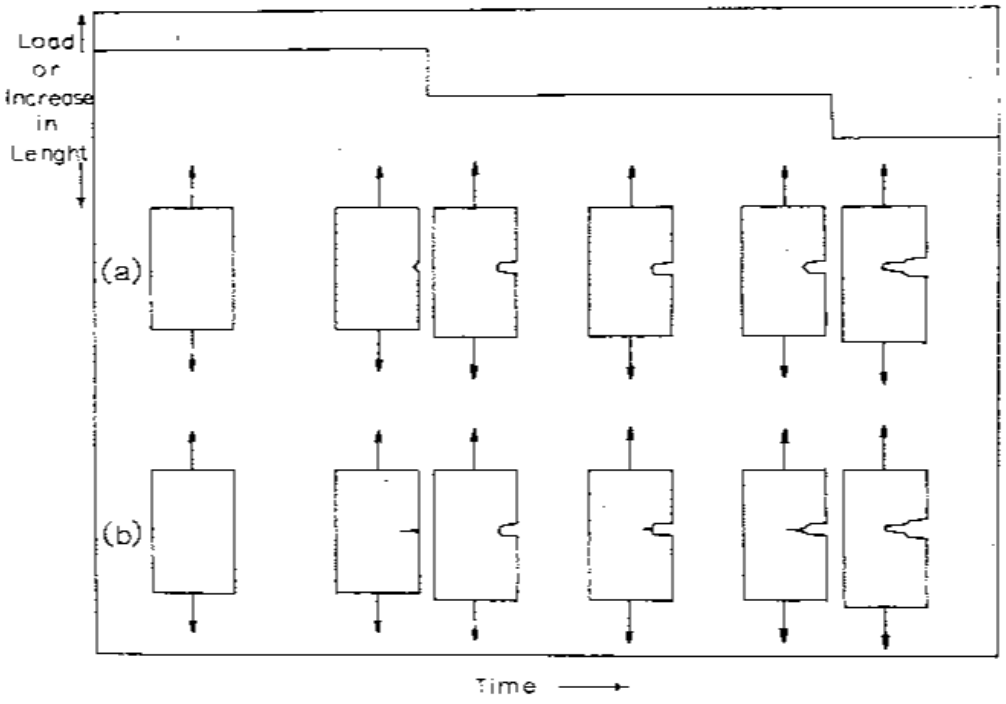

Fig. 3.44 Two interpretations of discontinuous specimen extension during crack propagation.

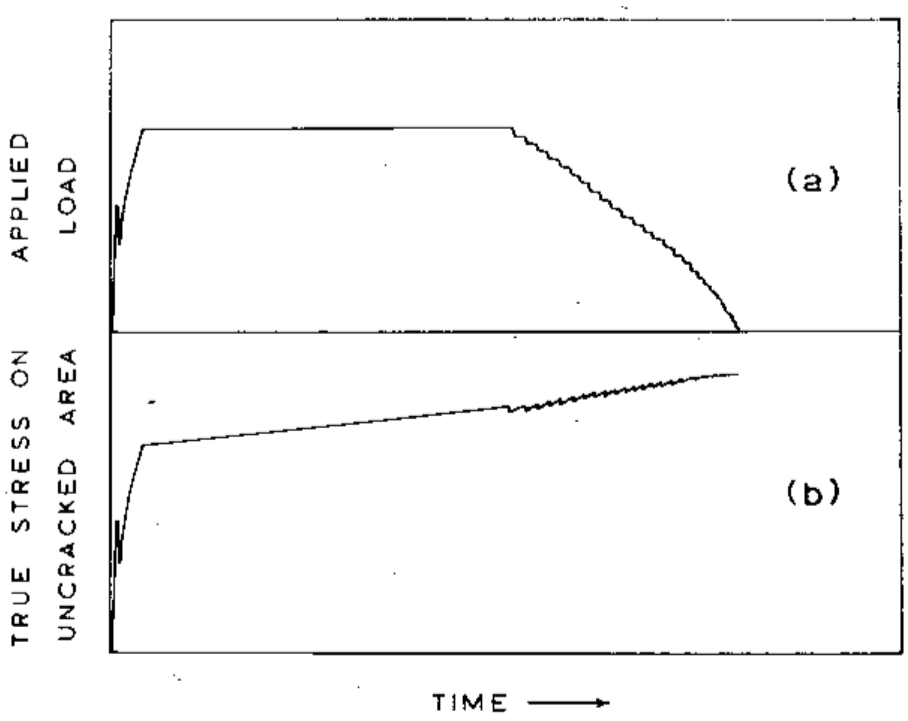

Fig. 3.45 Dependence of specimen extension on plastic deformation of material ahead of a crack during a stress-corrosion test.
(a) Complete history of specimen during stress-corrosion test.
(b) Change in stress on material ahead of a stress-corrosion crack.

To demonstrate that material ahead of a stress-corrosion crack would exhibit discontinuous flow in the same way as a bulk specimen, a specimen was cathodically protected just after open crack propagation had commenced and then pulled to fracture without unloading or removal from the solution. The specimen was cathodically protected potentiostatically with the application of a potential of -700 mV (s.c.e.). The results are shown in Fig. 3.46 and it is clear that jerky flow does occur during a tensile test on a cracked specimen.

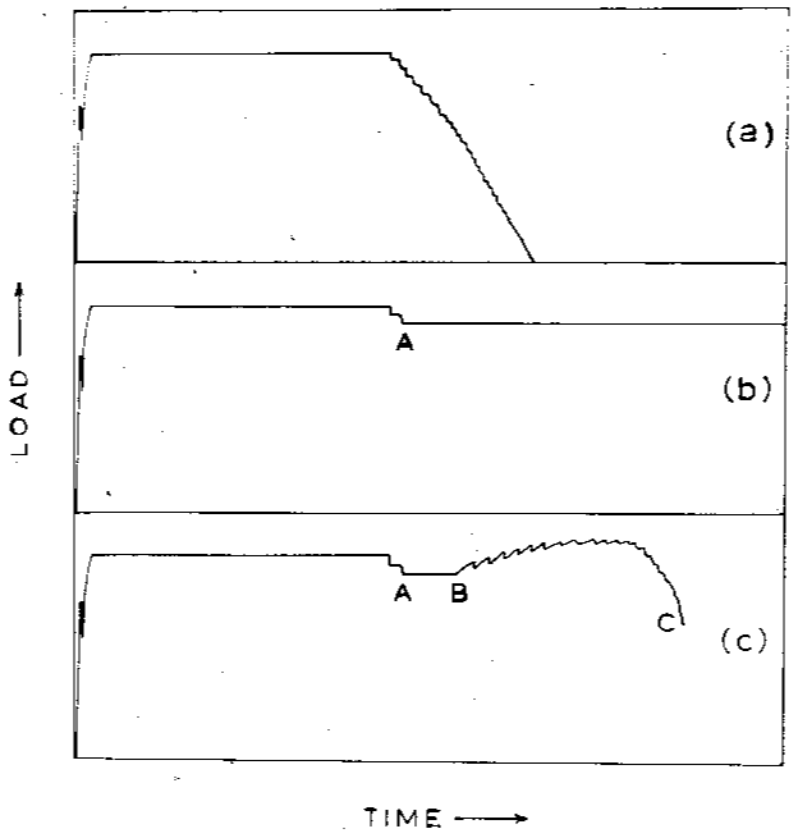

Fig. 3.46 (a) Normal load/time relationship during stress-corrosion test.
(b) Cathodic protection applied at A.
(c) Cathodic protection applied at A the specimen pulled in tension at 1×10^{-5} sec^{-1} during Stage BC.

Fig. 3.47 shows a typical specimen which has undergone the testing sequence in Fig. 3.46 (c) and it can be seen that there is no tendency for a stress-corrosion crack such as A to propagate as an intergranular crack (as was proposed by Engell and Baumel) and final failure occurred by transgranular ductile rupture between two stress-corrosion cracks B and C.

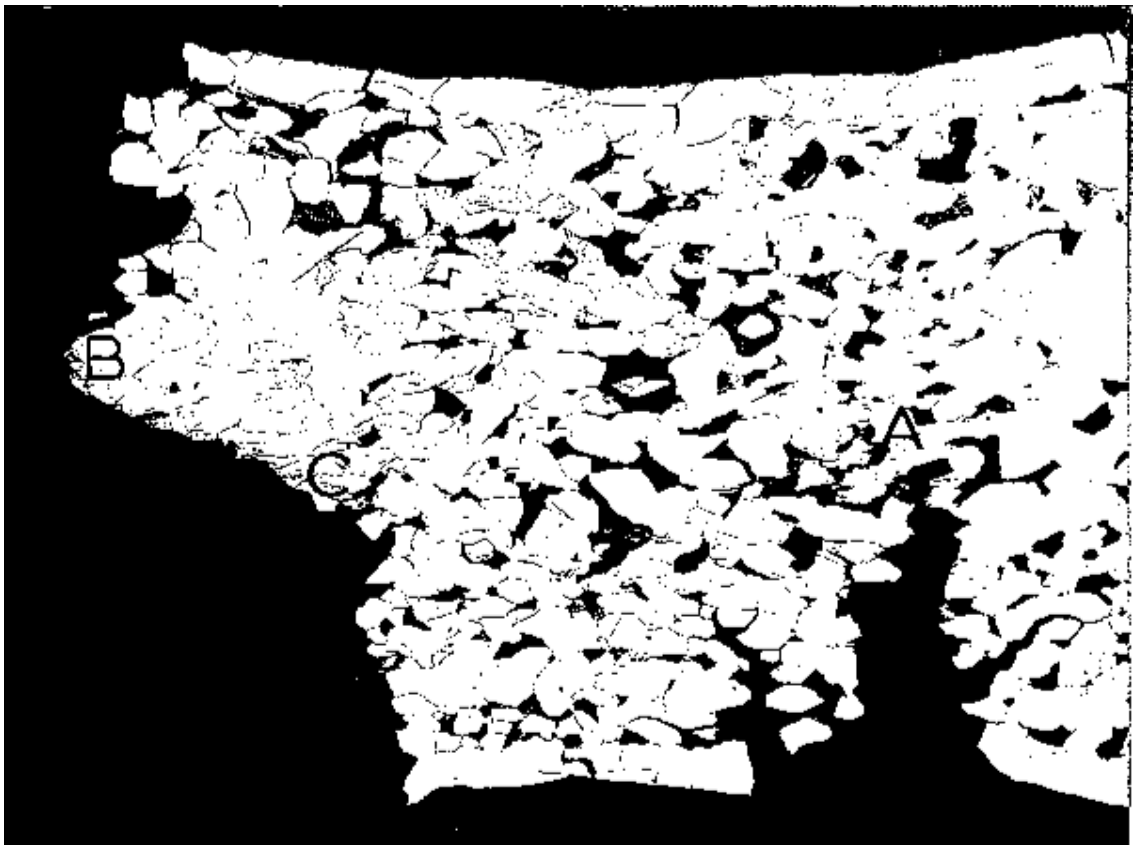

Fig. 3.47 Specimen pulled to fracture in a tensile test at a rate of 1×10^{-5} sec^{-1} after the formation of stress-corrosion cracks in a static stress-corrosion test. Cathodic protection applied during the tensile test. X35

The proposal that discontinuous specimen extension is due to discontinuous plastic flow of the material ahead of a propagating crack is further supported by the following observations:-

(1) The discontinuities in the applied load during stress-corrosion cracking are similar in magnitude and duration to the discontinuities in the plastic portion of a load-time plot during a tensile test in oil at 115°C.
(2) Changes in potential, similar to those that occur during stress-corrosion crack propagation (Fig. 3.43), were found to occur during a continuous tensile test in boiling nitrate solutions. The potential deflections occurred during the early stages of the test, prior to open crack formation, and they coincided with the load drops due to jerky flow as shown in Fig. 3.48.
(3) As crack propagation proceeds the steps decrease in magnitude, just as they do when the U.T.S. is approached during a tensile test.
(4) In a stress-corrosion test with an applied stress just less than the upper yield stress, the first load drop that occurs is larger than the subsequent drops and is similar to the load drop from the upper to the lower yield point in a tensile test.
(5) In a 0.3 C spheroidised carbide steel, which exhibited discontinuous flow to a smaller extent than the other steels in this work, the discontinuous extension during the stress-corrosion test was also less marked, as shown in Fig. 3.49.

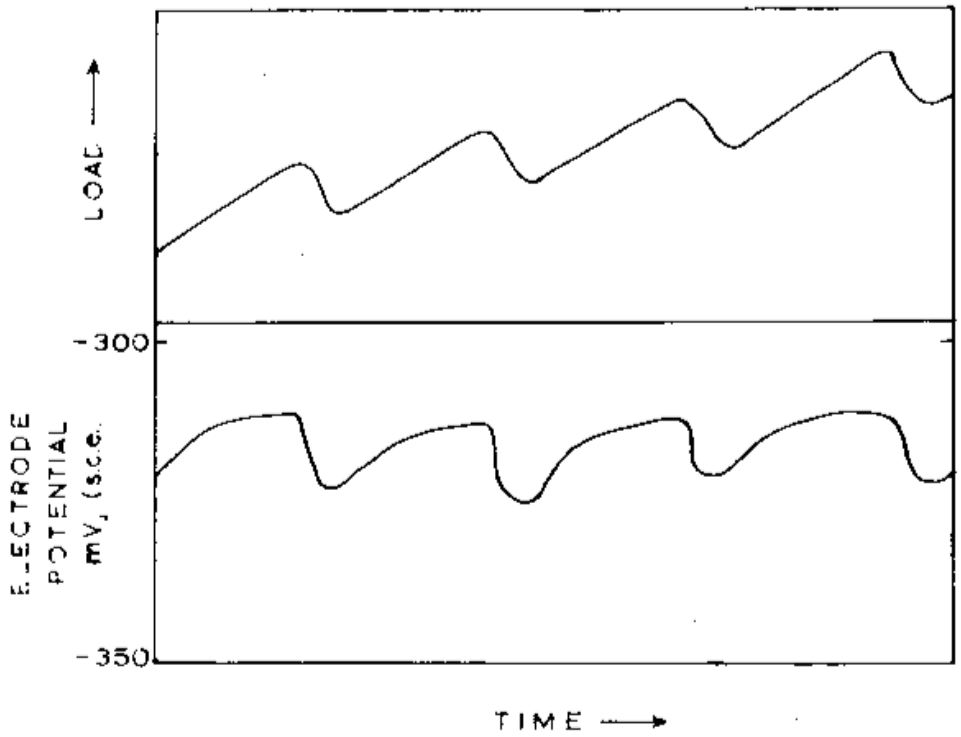

Fig. 3.48 Coincidence between potential deflections and jerky flow during a continuous tensile test in boiling nitrate solution, prior to open crack formation.

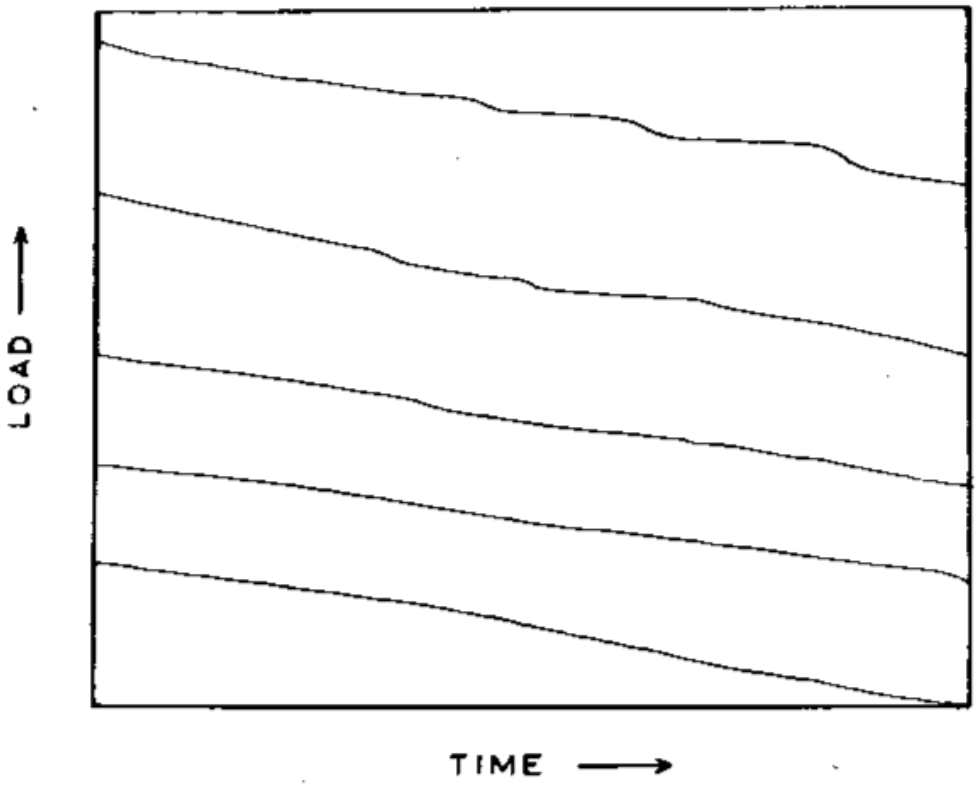

Fig. 3.49 Stress-corrosion crack propagation in 0.3 C spheroidised carbide steel. Scanning time = 10 minutes.

A further fact in favour of the interpretation of discontinuous extension proposed in this work is that it gives a more satisfactory explanation for the potential deflections observed during crack propagation. The potential deflections have previously been attributed to the exposure of fresh metal at a crack tip after a short burst of crack propagation. An objection to the latter interpretation has been that the potential deflections observed are large compared to the small amount of material that would be exposed. In the mechanism suggested in this work each deflection in extension is attributed to a wave of plastic deformation which starts opposite a crack and propagates for a considerable distance along the specimen. This wave of plastic deformation will cause fracture of oxide films on the specimen sides as well as in the crack itself and therefore accounts for the magnitude of the potential deflections. The discontinuities in specimen extension observed in the present work were much smaller (sometimes by a factor of 20x) than those reported by Engell and Baumel. This is thought to be due to one or both of the following possibilities –

(1) The measuring system used by Engell and Baumel may not have been sufficiently accurate to detect each extension discontinuity with the result that each recorded "step" was an aggregate of several smaller ones. In favour of this explanation is the fact that many more discontinuities were observed in the present work.
(2) Engell and Baumel used constant load tests with the result that crack propagation occurred under conditions of increasing stress. This means that the wave of plastic deformation (thought to be the reason for each discontinuity) would have a larger driving force than in a constant strain test. In favour of this explanation was the observation that the electrode potential deflections were also smaller in the present work than those reported by Engell and Baumel, and Van Rooyen (who also used constant load tests).

It was concluded that discontinuities in specimen extension and electrode potential during a stress-corrosion test, can be explained on the basis of discontinuous plastic flow of material beyond a propagating crack, rather than discontinuous crack propagation. Although crack propagation might involve extremely small, purely mechanical stages, external measurements such as specimen extension and electrode potential are of no use in detecting this possibility.

An argument in favour of previous proposals that cracking involves purely mechanical stages is that they explain why rates of crack propagation are high compared to normal corrosion rates. However, it will be shown that the rate of open crack propagation observed in this work is comparable with the rate of intergranular corrosion during the early stages (the first minute) of a test when purely mechanical stages are not feasible. It was shown, on page 57 that the depth of penetration of an unopened crack is given by the relationship

$$d = 0.38\, t^{0.63} \quad \ldots\ldots\ldots\ldots\ldots\ldots\ldots \quad (10)$$

where d is in mm. and t in hours.
This relationship was derived from experimental data and is only true for the material and corrodent used in section 3.3.1. The rate of penetration $d(d)/dt = 0.24\ /t^{0.37}$ decreases with time. This decrease in the rate of penetration as the depth of penetration increased was thought to be due to the difficulty in maintaining a continuous supply of corrodent to the penetration front. However, when an open crack is formed, fresh solution can reach the crack tip more easily and it can be assumed (this assumption is dealt with later) that the rate of further penetration is equal to the rate of penetration at the beginning of the open crack initiation period. It is proposed that the open crack propagates as an unopened crack until the material

ahead of it readily plastically deforms to give one of the short bursts of deformation shown in Fig. 3.41. This model of crack propagation is indicated in Fig. 3.50.

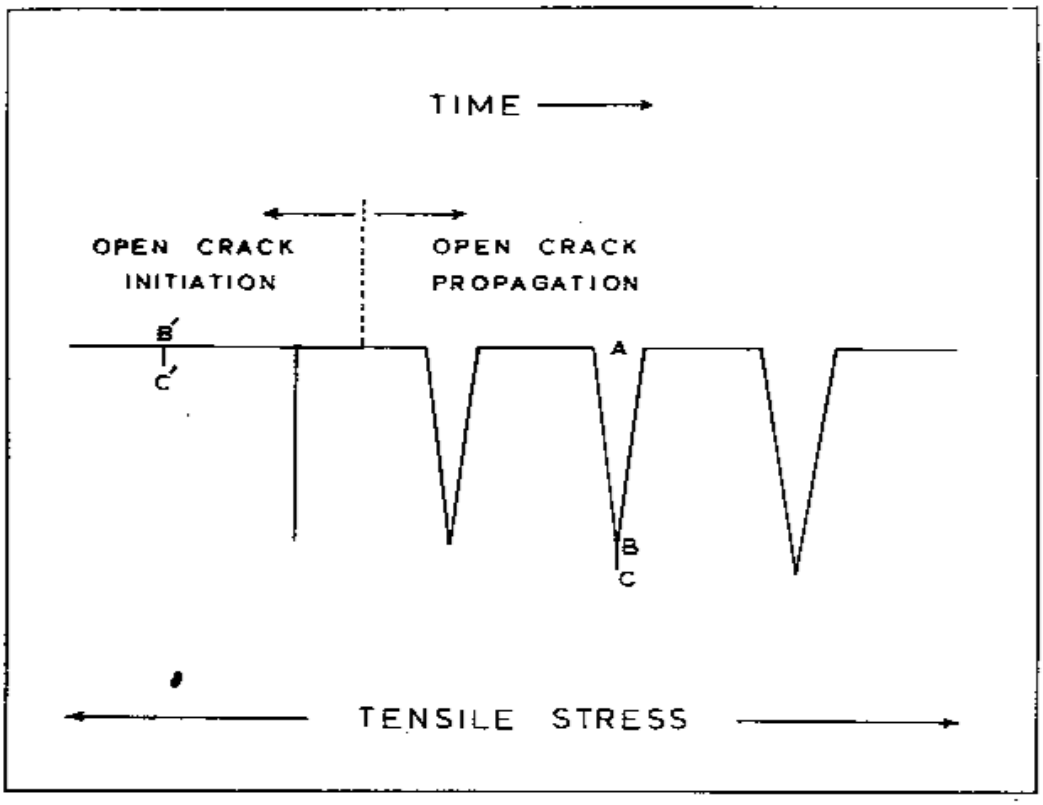

Fig. 3.50 The initiation and propagation of an open stress-corrosion crack.

The average interval between the extension discontinuities (in a specimen that contained only one open stress-corrosion crack) was about 1 minute. Equation (10) gives the depth of penetration during an interval of 1 minute to be 0.03 mm. This means that the possible rate of open crack propagation on a purely electrochemical basis is 1.8 mm/hour. The measured rate of open crack propagation in the material used in section 3.3.1 was about 0.5 mm/hour.

Two assumptions were made in the derivation of this possible rate of purely electrochemical crack propagation:-

(1) Equation (10) is for penetration aided only by elastic deformation of material ahead of the crack whereas the penetration BC (in Fig. 3.50) is aided by some gradual plastic deformation even though the majority of the plastic deformation occurs at intervals of about one minute.
(2) The availability of solution at the tip of an open crack was assumed to be the same as at the specimen surface.

Assumption (1) is quite reasonable in material which exhibits marked strain-ageing and it is acceptable since any error involved has lowered the calculated rate of propagation (i.e., the assumption does not favour the point being made by the calculation). Assumption (2) is more debatable and must be considered when assessing the result. Probably the most satisfactory method of expressing the result of the calculation is to state that open crack propagation may be explained on a basis of purely electrochemical attack, provided the solution at the tip of an open

crack is no more than four times less potent than the solution at the mouth of the crack. It is interesting to note that West (38) using Perspex crack models, found the maximum differences in concentration between the solution at the tip of an open crack and that at the mouth of a crack was only about 4x. The application of the findings of West to the present case does not rule out the possibility that acid concentration at the crack tip is necessary for the electrochemical reaction, because even if acid concentration is required at the crack tip, it is still essential that fresh solution can reach the general vicinity of the crack tip as penetration proceeds. In the model of crack propagation shown in Fig. 3.50 it can be seen that the findings of West will be applicable in the stage AB whereas acid concentration (if it is necessary for the electrochemical reaction) can occur during the stage BC. If acid concentration does precede penetration, then it will have occurred during the stage B'C' (the stage on which the calculation is based) to the same degree as in stage BC. Hence any acid concentration factor has been included in the calculation.

3.4 Proposed mechanism for the stress-corrosion cracking of mild steel in nitrate solutions

A complete understanding of the stress-corrosion cracking of mild steel in nitrate solutions would require the answers to two questions:-

(1) Why are grain boundaries selected for electrochemical attack in nitrate solutions?
(2) What is the role of stress in the cracking?

Since the majority of the present work has been concerned with the latter, it is necessary, if a mechanism is to be proposed, to assess the solution to question (1) on the basis of previous work. Preferential grain boundary attack is attributed to the fact that C and N atoms segregate at the grain boundaries, to leave regions adjacent to the boundaries, which are depleted in interstitial C and N. The difference in potential between the depleted zones and the grain boundary is thought to be the driving force for the electrochemical dissolution of this zone. A correlation between stress-corrosion susceptibility and interstitial segregation has been claimed by Uhlig and Sava (18) but their interpretation of this correlation is not the same as that proposed in the present work. Although it is thought that the heat treatments used by Uhlig and Sava might have had effects additional to the grain boundary segregation of interstitials, this segregation is thought to be the most feasible explanation for preferential grain boundary attack. If this is the case then one would expect preferential attack at interstitial "sinks", other than grain boundaries. Metallographic examination of stress-corrosion cracks also revealed evidence of attack other than grain penetration and Fig. 3.51 shows local areas of chemical attack at intervals of about 3μ along the side of a stress-corrosion crack. The specimen shown in Fig. 3.51 had been strained 5%. The dislocation cell size in material strained 5% is of the order of 2μ and it seems probable that the attack in Fig. 3.51 is sited at dislocation tangles. The fact that the depth of penetration at the dislocation tangles is negligible, compared with that of grain boundaries, is attributed to the probability that for a given depth of penetration the volume of material depleted of interstitials in a tangle of dislocations is greater than that adjacent to a grain boundary. The large volume of corrosion product produced during the attack of a dislocation tangle, makes it difficult for fresh corrodent to continue the attack.

The stress-corrosion cracking of mild steel in nitrate solutions is considered to occur in three stages:-

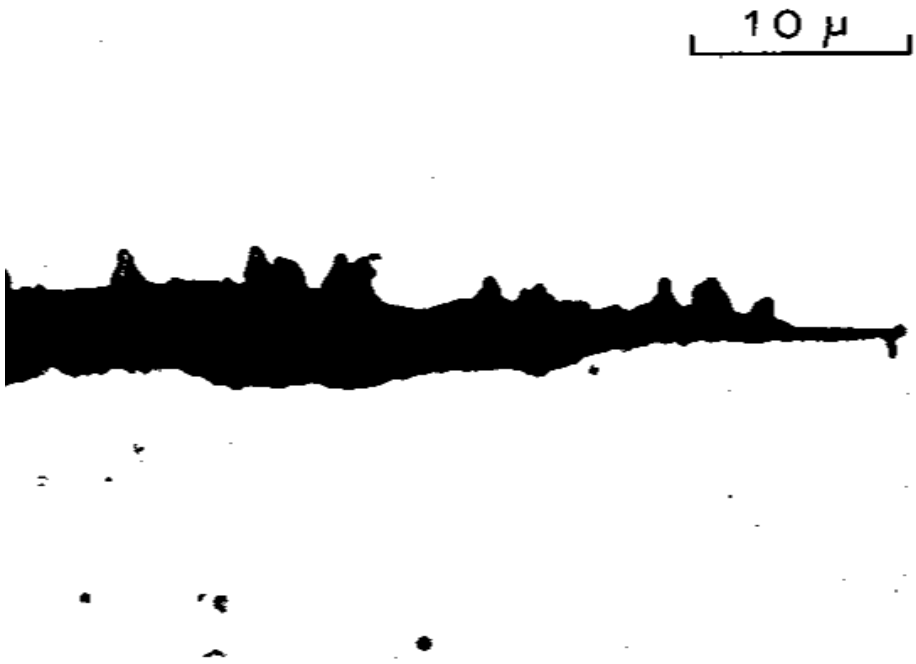

3.51. Secondary attack on stress-corrosion crack sides.

(1) The removal of any air formed oxide film. This stage only required a few seconds in the solutions used during this work. Applied stress is not required during this stage.
(2) The formation of unopened cracks. An unopened crack is defined as a crack which has formed without plastic deformation of material over the entire cross-sectional area of the specimen beyond the crack. Applied stress is not necessary during the early stages of this penetration. In the presence of applied stress, the decrease in cross-sectional area which accompanies the formation of the unopened crack, increases the stress on the uncracked area and elastically strains this material. The elastic strain microscopically opens up the crack and increases the availability of corrodent at the crack tip. Penetration continues until the stress on the uncracked area is sufficient to initiate plastic deformation over the entire area. Before the latter stage (i.e., open crack formation) is reached, some local plastic strain probably does occur at the crack tip, but this opens the crack up to a negligible extent compared with the opening that occurs when plastic deformation is initiated in the entire area beyond the crack.
(3) The propagation of open cracks. Open cracks propagate by a series of stages similar to stage (2). The stages are much shorter (about 1 minute in the present work) than stage (2) itself, because plastic deformation occurs more readily once the initial resistance to deformation (i.e., the upper yield stress) is overcome.

The stage most likely to govern the life of a stress-corrosion specimen is stage (2). The time taken to complete stage (2) will be minimum, for a given corrodent and applied stress, when –

(a) The potential difference between the grain boundaries and the adjacent ferrite is high. This is thought to be when there is a marked grain boundary segregation of interstitials.
(b) The depth of penetration necessary before stage (3) can occur is minimum. This in turn is minimum when the specimen has received no previous deformation and when strain-ageing is minimum.

The intergranular penetration in all three stages of cracking is thought to occur by continuous electrochemical corrosion. The reason for this interpretation has been threefold:-

(1) Facts suggested by previous workers to favour a purely mechanical stage have been explained on an alternative basis. The two most important items in this category have been (a) the explanation of discontinuous specimen extension and electrode potential during a stress-corrosion test, and (b) the demonstration of the feasibility of the observed rate of crack propagation on the basis of continuous electrochemical attack.

(2) The objections (see – Introduction, Page 3) to the role of stress being simply to open up corrosion fissures have been shown to be unjustified. Complete failure has been obtained in specimens stressed to only 1/5 of their yield stress. The marked dependence of susceptibility on the type of steel and its heat treatment, has been shown to be related to the dependence of susceptibility on the deformation behaviour of the material.

(3) In the absence of applied stress, extensive intergranular penetration has been observed in fully annealed material.

It is realized that the bulk of the evidence in favour of a purely electrochemical mechanism is the negative type of evidence cited in (1) and (2) above, but a general lack of positive evidence for an electrochemical mechanism is only to be expected from an investigation which has been mainly concerned with the stress aspects of stress-corrosion cracking.

One factor which might be put forward in favour of a more complicated role for stress than that of opening up corrosion fissures is the lack of marked intergranular corrosion (in the absence of applied stress) when mild steel is immersed in most nitrate solutions. However, the present work, together with that of Engell and Baumel (10), has shown that extensive intergranular penetration can occur if either strong solutions or anodic polarization are employed. This would tend to suggest that intergranular penetration does occur in the less potent nitrate solutions but that the depth of penetration is not sufficient to impair the properties of the material. It is thought that the extent of intergranular penetration will be dependent upon the nature and volume of any solid corrosion product. The role of solid corrosion products is difficult to assess since they may cause opposite effects. They may accelerate cracking by forming a compact layer on the specimen sides so as to make the cathode/anode ratio high or they may oppose cracking by virtue of having sufficient volume to completely isolate the crack tip from the corrodent. It is thought that the stifling of attack in corrosion fissures by solid corrosion product is the reason for the lack of extensive intergranular corrosion (in the absence of stress) of mild steel in the majority of nitrate solutions. In support of this view are the results of an investigation by Szklarska-Smialowska (39) into the effect of electrode potential on the stress-corrosion susceptibility of mild steel in ammonium nitrate solutions. She found that the applied potential that caused maximum susceptibility was that at which there was no visible corrosion product, whereas the conditions that gave the largest time to failure produced an adherent compact layer of oxide. The anodic polarization conditions used in the present work to obtain extensive intergranular penetration in the absence of applied stress (Fig, 3.40) were also those at which no solid corrosion product is formed.

It is thought that the following aspects require further attention in order to obtain a complete understanding of the stress-corrosion of mild steel in nitrate solutions.

(1) Interstitial segregation at grain boundaries:- A systematic investigation into the effect of heat treatment on stress-corrosion susceptibility is required. The accompaniment of

stress-corrosion tests with slow strain rate tensile tests and thin film electron microscopy would help to distinguish between the role of interstitials in the corrosion reaction and in the plastic deformation that accompanies cracking. Ideally a solution which would cause cracking at room temperature should be used to study the effects of low temperature (100°C - 300°C) heat treatments.

(2) Stress-corrosion cracking in material subjected to applied elastic stresses:- Small applied elastic stresses have been found to cause complete failure in a stress-corrosion test but it has not been proved that local plastic deformation at the crack tip is not accelerating the rate of crack propagation. Electron microscopy of thin foils prepared from thin sheet stress-corrosion tensile specimens would give direct evidence of the conditions at the tip of a stress-corrosion crack.

(3) The electrochemical aspects, with particular regard to the nature of solid corrosion products. Solid corrosion products within a corrosion crack are thought to govern the availability of solution at the crack tip. It would be interesting to investigate the permeability of these products to nitrate solutions. The surface tension relationships between the corrosion product and the nitrate solution might also be important in the penetration of nitrate solutions into unopened cracks. It is quite probable that this is the aspect which is dependent upon temperature since the present investigation has suggested that the need for elevated temperatures is not a metallurgical effect.

The mechanism proposed for the stress-corrosion cracking of mild steel in nitrate solutions may be summarized as follows:- Cracking occurs as a result of continuous electrochemical attack of regions depleted of interstitial atoms. The role of applied stress is attributed to that of opening up cracks to admit solution to the crack tip. The extent to which the stress can open up the crack is dependent upon the metallurgical condition of the material beyond the crack. The extent to which the stress must open up the crack to ensure its continuous propagation is dependent upon the corrosion products in the crack. The dependence of the action of stress on the deformation behaviour of the material and of the corrosion products within a crack tends to complicate what is basically a simple action.

Although it is not proposed that this is necessarily the role of stress in other stress-corrosion systems, it is thought that an investigation into other systems along the lines of the present work would be useful in distinguishing between the role of stress in the corrosion mechanism and the role of stress in causing the deformation that accompanies crack propagation. Perhaps one of the most significant points arising from this work has been the relationship between deformation behaviour and susceptibility to stress-corrosion cracking. It is possible that this relationship is the factor that could bring together the purely electrochemical and the alternate chemical/mechanical theories of stress-corrosion cracking. The chief factor in favour of the electrochemical theory has been the lack of evidence for purely mechanical stages, whereas the bulk of the support for the alternate chemical/mechanical theory has come from the marked dependence of susceptibility on metallurgical variables. If the dependence of susceptibility on these variables could be explained by their effect on the deformation necessary for crack propagation, then it might be possible to show that an electrochemical mechanism is possible for all stress-corrosion systems, even though the severe test conditions in a laboratory test may in some cases induce stages of purely mechanical rupture.

4 CONCLUSIONS

1. No evidence has been found to suggest that stress has a function other than to open up corrosion fissures so as to admit fresh corrodent.

2. Available evidence suggests that a continuous purely electrochemical process is capable of causing the cracking.

3. Stress-corrosion cracking involves three stages:-
   (a) The initiation period. During this stage, any air formed oxide films are removed. This stage only required a few seconds in the solutions used in the present work.
   (b) The penetration of fine cracks. As a fine crack propagates. The effective cross-sectional area of the test specimen is decreased. When the resultant stress increase on the uncracked area, is large enough to cause plastic deformation in this area the fine crack is transformed into an open crack.
   (c) The propagation of open cracks. The open cracks propagate by a series of stages similar to stage (b) but of much shorter duration.
   Stage (b) requires the longest period of time but the amount of damage, in terms of actual cracking, may be very slight during this stage.

4. In a material susceptible to nitrate cracking, the extent of cracking is dependent upon the deformation behaviour of the material. The greater the ductility the greater the extent of the stress-corrosion cracking. Strain-ageing hinders crack propagation.

5. Discontinuities in specimen extension and electrode potential during the propagation of a stress corrosion crack are a result of discontinuous plastic flow of the material beyond the propagating crack and are not an indication of discontinuous crack propagation.

6. Susceptibility to cracking decreases as the grain size decreases. The stress σ_{sc} required to form an open stress-corrosion crack during a tensile test varies with grain size in accordance with a Petch-type relationship $\sigma_{sc} = \sigma_o + K_{sc} l^{-1/2}$ where $K_{sc} \sim K_{flow\ stress}$ The Petch relationship does not have its normal significance when applied to stress corrosion fracture. An open stress-corrosion crack forms as a result of continuous penetration during the tensile test. The majority of this penetration occurs after yielding has occurred, with the result that the stress-corrosion fracture stress is the stress on the specimen after a certain period of plastic straining. This is a definition of flow stress and since flow stress obeys a Petch relationship. So does the stress-corrosion cracking stress.

7. Susceptibility to stress-corrosion cracking decreases as the degree of prestrain increases. A quantitative estimate of the extent of this decrease in susceptibility may be derived on the basis of the cracking model proposed in 3) above.

8. Two new forms of stress-corrosion testing have been developed:-

   (a) The slow strain rate stress-corrosion tensile test. It has the following advantages over a static test:-
   - Testing times are relatively short.
   - Results are more reproducible.
   - The test is capable of direct comparison with "corrosion free" behaviour in a normal test.
   - The test is severe and hence it is suitable for detecting stress-corrosion susceptibility in slightly susceptible materials.

   The main limitation of the stress-corrosion tensile test is that great care is necessary to distinguish between time dependent metallurgical behaviour and time dependent corrosion processes.

   (b) Static stress-corrosion tests in a hardbeam tensometer with load recording facilities. [The use of this type of test has recently been reported elsewhere (42)] It provides a simple and accurate means of measuring specimen extension during a static stress-corrosion test. This form of testing is more suitable for crack propagation studies.

REFERENCES

1. E.G. Coleman, D. Weinstein and W. Rostoker, Acta. Met. 9 (1961): p. 491
2. W.D. Robertson and A.S. Tetelman, ASM Seminar - "Strengthening mechanisms in solids", Cleveland (1963): p. 211.
3. R.N. Parkins, "Stress-Corrosion Cracking,",Met. Reviews 9 No. 35 (1964): p. 201.
4. J.T. Waber and H.S. McDonald, "Stress-Corrosion Cracking of Mild Steel," Pittsburgh (Corrosion Publishing Co.) 1947.
5. R.N. Parkins, J. Iron Steel Inst., 172 (1952): p. 149.
6. H.L. Logan, "Physical Metallurgy of Stress-Corrosion Fracture," Ed. T.N. Rhodin. 1959 (New York and London Interscience Publishers) p. 295.
7. J. Flis, J. Miculuch and M. Smialowski, 2nd International Congress on Metallic Corrosion, 1963, New York.
8. R. Usher, "The Stress-Corrosion Cracking of Mild Steel in Aqueous Solutions", Ph.D. Thesis 1957, Kings College, University of Durham.
9. R.N. Parkins and R. Usher, "Ist International Congress on Metallic Corrosion" 1961. London (Butterworth and Co.).
10. H.J. Engell and A. Baumel, "Physical Metallurgy of Stress-Corrosion Fracture" (Ed. By T.N. Rhodin) 1959, New York and London (Interscience Publishers).

11. D. van Rooyen, Corrosion 1960, 16 421t.
12. W. Rutmann, Tech.Mitt.Krupp, 1936, 4, 23.
13. C.E. Stromeyer, J. Iron Steel Inst., 1909, 79, 404.
14. E. Houdrement, H. Bennek and H.W. Wenthrop, Stahl Eisen 1940, 60, 791.
15. E. Herzog, Corrosion et Anticorrosion, 1954, 2 p. 3, 59 and 91.
16. R.N. Parkins and A. Brown, J. Iron Steel Inst., 1959, 193, 45.
17. W. Radeker and H. Grafen, Stahl und Eisen, 1956, 76, 1616.
18. H.H. Uhlig and J.P. Sava, Trans. ASM 1963, 36 361.
19. H.L. Logan, J. Research Nat. Bur. Stand., 1952, 48, 99.
20. H.H. Uhlig, "Physical Metallurgy of Stress-Corrosion Fracture", (Ed. By T.N. Rhodin) 1959, New York and London (Interscience Publishers).
21. M. Smialowski, Z. Szklarska-Smialowska, Corrosion, 1962, 18, 1t.
22. N.J. Petch, J. Iron Steel Inst., 1953, 174, 25.
23. R. Armstrong, I. Codd, R.N. Douthwaite and N.J. Petch, Phil. Mag. 1962, 7, 45.
24. A.H. Cottrell, Trans. Amerc. Inst. Min. (Metall) Engnrs. 212, 192 (1958).
25. A.H. Cottrell, Phil. Mag. 1953, 44, 829.
26. J.W. Edington, T.C. Lindley and R.E. Smallman, Acta. Met. 1964, 12, 1025.
27. D.G. Brandon and J. Nutting, J. Iron Steel Inst., 1960, 196, 160.
28. A.S. Keh, "Direct Observations of Lattice Defects", 1961, New York (Interscience Publishers), p.213.
29. A.S. Keh and S. Weissmann, "Electron Microscopy and Strength of Crystals" (Ed. G. Thomas and J. Washburn), 1963, Interscience Publishers, p.238.
30. K.F. Hale and D. McLean, J. Iron Steel Inst., 1965, 201, 337.
31. W.C. Leslie, Acta. Met., 1961, 9, 1004.
32. A.S. Keh and H.A. Wriedt, Trans. A.I.M.E. 1962, 224, 560.
33. W.C. Leslie and A.S. Keh, J. Iron Steel inst.,1962, 200, 722..
34. G. Lagerberg and Åke Josefsson, Acta. Met., 1955, 3, 236.
35. V.A. Phillips, Acta. Met., 1963, 11, 1139.
36. A.L. Tsou, J. Nutting and J.W. Monter, J. Iron Steel Inst., 1952, 172, 163.
37. H.H. Uhlig and J.P. Sava, Corrosion Science, 1965, 5, 291.
38. J.M. West, Nature, 1960, 185, 92.
39. Z. Szklarska-Smialowska, "2nd International Congress on Metallic Corrosion", (1963), New York.
40. T.P. Hoar and J.G. Hines, J. Iron Steel Inst., 1956, 182, 124.
41. C. Edeleanu, J. Inst. Metals 1952, 80, 187.
42. D. Tromans and J. Nutting, Corrosion 1965, 21, 143.

ACKNOWLEDGEMENTS

The author wishes to thank Dr. R.N. Parkins for his continual interest and advice during the course of this research and Professor N.J. Petch for the research facilities provided in the Department of Metallurgy.

The author is also indebted to Durham Chemicals Limited for the award of the Durham Chemicals Memorial Scholarship.